Functional analysis and therapeutic targeting of AKT isoforms in BRAF mutant melanoma

A thesis submitted by

Siobhan K. McRee

In partial fulfillment of the requirements for the degree of

PhD

in

Genetics

Tufts University

Sackler School of Graduate Biomedical Sciences

August 2018

Advisor: Philip Hinds, PhD

Abstract

Despite recent advances, metastatic melanoma remains the deadliest form of skin cancer, and new therapeutic strategies are urgently needed. The PI3K/AKT pathway is known to promote tumor progression and metastatic dissemination in many cancer types, including melanoma. PI3K/AKT signaling is hyperactivated in many melanomas, often through loss of the negative regulator PTEN, which occurs in 12-20% of cases. PTEN loss cooperates with oncogenic BRAF to induce metastatic melanoma and leads to unrestrained activity of the PI3K effector kinase, AKT. The AKT family of serine/threonine kinases comprises three highly homologous isoforms (AKT1, AKT2, and AKT3) that are major effectors of the PI3K pathway, but despite their unique roles in other cancers, isoform-specific effects in melanoma have yet to be systematically interrogated. We performed shRNA mediated conditional knockdown and CRISPR/Cas9 gene editing of AKTs in a wide variety of human melanoma cell lines, as well as genetic ablation of each isoform in a BRAF-driven mouse model of melanoma. We reveal a role for AKT2 in promoting melanoma cell migration and invasion *in vitro* and find that AKT2 is required for metastatic seeding *in vivo*. Additionally, AKT2 specific depletion delays tumor growth and improves survival of mice with metastatic disease after tumor cell seeding, suggesting that AKT2 supports growth or survival in the metastatic niche. We propose several mechanisms whereby AKT2 may mediate these phenotypes, including via regulation of key epithelial-mesenchymal genes, promoting aerobic glycolysis, and responding to hypoxia. In contrast, we observe that the AKT1 isoform specifically promotes melanoma cell proliferation, and genetic ablation of AKT1 in melanoma prone mice prolongs overall survival. We also reveal that the AKT3 isoform

may be important in UV-initiated melanomagenesis. Lastly, while non-specific pan-AKT inhibitors are used clinically to moderate benefit, their use is hampered by myriad off-target effects. To increase the efficacy of AKT targeting for clinical benefit, we endeavored to identify AKT isoform-specific substrate effectors that may be mediating differential phenotypes, and therefore potential targets for therapy. We also report efforts to use a tumor specific antigen to target a clinically relevant pan-AKT inhibitor to melanoma tumors in the mouse, and additionally test small molecule inhibitors that synergize with existing targeted therapies. In summary, our work moves toward establishing the contribution of AKT isoforms to melanoma, to improve therapeutic strategies and outcome for this devastating disease.

Dedication

To Marion G. Miller, PhD (1956 - 2011).

Influential scientist, dedicated mentor, and the first to suggest I pursue a graduate degree

To my loving family, especially my husband Nate, for helping me achieve this dream.

Acknowledgements

First and foremost, I'd like to thank my advisor Phil Hinds. I knew very early on that I wanted to join his lab, and I can't thank him enough for giving in to my persistent nagging. I have had such a positive experience in my graduate career because of your guidance, willingness to talk science, your wonderful ideas, and fantastic mentorship overall. I know that not all graduate students can say the same, and I'm grateful to have had the opportunities you have provided.

Next, I would like to thank my thesis advisory committee, both present and past. To Dr. Mark Ewen, my first thesis chairperson, thank you for your astute guidance and discerning eye over the years. Thank you as well for helping at every step, even after you no longer had a responsibility to do so. Thank you as well to Drs. Grace Gill and Gavin Schnitzler, both of your invaluable perspectives always gave me food for thought. To Dr. Philip Tsichlis, for being the inspiration behind this project, and present all along the way. To Drs. Karl Munger and Charlotte Kuperwasser, thank you for stepping in when I was in need, and seeing me through to the end. To Karl in particular, you have done an enormous amount of work and provided support on multiple fronts and I appreciate your help more than I can articulate!

To all of my lab mates over the years, but especially Jodie. I always felt that your attention to detail, your scientific rigor and critical eye, as well as your hard work and dedication to science have consistently pushed me to do better. You have guided me every step of the way and shaped me into the scientist I am today. You were always the person I looked up to and turned to for advice throughout my graduate career, a scientific

older sister. You also understood my irrational need to buy yarn and knit, which invariably brought us closer together. Thank you for everything.

To other former labmates. Chi, my first rotation supervisor in the lab. Thank you for setting up the work I now present here and advising me to join the Hinds lab. To Marina, for getting me involved in activities outside of the lab and helping me keep my mental facilities intact. You introduced me to scotch club and I will never be the same.

Thank you to the core facilities and support staff that helped me complete the work outlined here. Steve and Allen, your flow cytometry knowledge is amazing, and I'll never forget your kindness and help. To administrators Di and Anne Marie, you took care of things so seamlessly, and enabled me to be better at my job- Thank you!

To the Bachovchin lab, and especially Dave Sanford and Jack Lai. Thank you for a fruitful collaboration, for synthesizing the compounds used in the experiments herein, and providing technical support. Thank you especially for putting up with my incessant questioning, requests for more compound, and for experimental advice. I learned a lot through your guidance and I have enjoyed the work!

To the neighboring Kuperwasser, Schwob, London, and McNeil labs. No graduate student works in a bubble and being able to depend on nice neighbors for guidance, reagents, late night shenanigans, and everything in between is exactly the kind of collegial atmosphere that every graduate student wants. I was lucky enough to find that in all of you! Not only that, but how many people can say they get a weekly stitch and bitch session with fellow yarn lovers right outside the lab? The wine and snacks were a great bonus too.

I also want to take the time to acknowledge two early scientific mentors in my life who really influenced my decision to make science a full-time career. First, my undergraduate thesis advisor, Dr. Marion G Miller. You were the first person who saw scientific potential in me and encouraged me to experiment in a lab setting. Your dedication to your students was completely inspiring, and I'm so grateful for your help. Next, to Dr. Leona Samson, my first real boss and mentor. Learning from your scientific accomplishment, management, and rigor was a transformational experience that was truly life-changing for me. Your guidance over the years amplified and elevated my progress and showed me how great science was done. You created a truly exceptional environment that nurtured scientific progress and was also full of wonderful people that I am privileged to call friends.

Thank you lastly to my family. First, my husband Nate, who has stood by me through thick and thin. I love coming home to you, even after fourteen short years together (and counting!). You may be the singular reason I made it through graduate school and I thank you from the bottom of my heart for your consistent support, your endurance, your love, and your thoughtful understanding. I'm one lucky gal.

To my mom, dad, and sister. You are so far away yet so close to my heart. You pushed me to follow my dreams and showed me that no matter what, it will all work out. Mom- your consistent love and deeply felt empathy never cease to amaze me, and your creativity in all things has been a constant inspiration. You bring artistry to everything you do and have a gift for storytelling that I have always envied. Papa- your logical nature and DIY enthusiasm are an absolute joy. I love hearing about your project of the day/week/month/year, and I'm always inspired by the way you dive head first into

insanely challenging technical feats with absolute gusto. You help me adjust my pre-conceived notions of what is within the realm of possibility and help remind me never to dismiss something as impossible. Renata- watching you tackle graduate school yourself in addition to dissertation writing, helped me see that it can be done, and kept me from hopelessness. I have watched you grow and seen you overcome a lot, and I love that we can support each other through our different but similar paths in life.

There are so many more people to thank, and as I take the next step in my career, it's that much more rewarding and enjoyable knowing I have all of you behind me in support. Thanks to everyone, including all those I didn't get a chance to write down here, who have played a role in helping me find the joy in scientific discovery. I'm excited to be moving on, and I feel so grateful!

Table of Contents

List of Tables

List of Figures

List of Copyrighted Materials

Shain AH, Bastian BC. 2016. From melanocytes to melanomas. Nature Reviews Cancer 16(6):345-358.

Luke JJ, Flaherty KT, Ribas A, Long GV. 2017. Targeted agents and immunotherapies: optimizing outcomes in melanoma. Nature Reviews Clinical Oncology 14(8):463-482.

Hayward NK, Wilmott JS, Waddell N, Johansson PA, Field MA, Nones K, Patch A-MM, Kakavand H, Alexandrov LB, Burke H et al. 2017. Whole-genome landscapes of major melanoma subtypes. Nature. 545(7653):175-180.

Rehan Akbani, Kadir C. Akdemir, B. Arman Aksoy, Monique Albert, Adrian Ally, Samirkumar B. Amin, Harindra Arachchi, Arshi Arora, J. Todd Auman, Brenda Ayala,J ulien Baboud, Miruna Balasundaram, Saianand Balu, Nandita Barnabas, John Bartlett, Pam Bartlett et al. 2015. Genomic Classification of Cutaneous Melanoma. Cell.161(7):1681-96.

Fecher LA, Cummings SD, Keefe MJ, Alani RM. 2007. Toward a molecular classification of melanoma. Journal of Clinical Oncology: official journal of the American Society of Clinical Oncology 25(12):1606-1620.

Manning BD, Toker A. 2017. AKT/PKB Signaling: Navigating the Network. Cell 169(3):381-405.

Schroeder A, Heller DA, Winslow MM, Dahlman JE, Pratt GW, Langer R, Jacks T, Anderson DG. 2011. Treating metastatic cancer with nanotechnology. Nature Reviews Cancer 12(1):39-50.

Kalluri R, Weinberg RA. 2009. The basics of epithelial-mesenchymal transition. The Journal of clinical investigation 119(6):1420-1428.

Gray-Schopfer V, Wellbrock C, Marais R. 2007. Melanoma biology and new targeted therapy. Nature 445(7130):851-857.

Toker A, Marmiroli S. 2014. Signaling specificity in the Akt pathway in biology and disease. Advances in Biological Regulation 55:28-38.

List of Abbreviations

2D – 2-dimensional
ABCA1 – ATP binding cassette subfamily a member 1
ACLY – ATP citrate lyase
ACRBP – Acrosin binding protein
ALP – Alkylphospholipid
αMSH – alpha Melanocyte stimulating hormone
AMPK – AMP-activated protein kinase
ARF – Alternate reading frame
ARI – Arisaph
ASK1 – Apoptosis signal regulating protein 1
ATP – Adenosine triphosphate
ATP5O - ATP synthase, h+ transporting, mitochondrial f1 complex, o subunit
BAD – Bcl-associated death promoter
BRAF – Raf murine sarcoma viral oncogene homolog B
BrDU – Bromodeoxyuridine/5-bromo-2'-deoxyuridine
BW – Body weight
CAF – Cancer-associated fibroblast
CAMK2D – Calcium/calmodulin dependent protein kinase ii delta
cAMP – cyclic adenosine monophosphate
CARD14 – Caspase recruitment domain family member 14
CCDC138 – Coiled coil domain containing protein 130
CDK – Cyclin dependent kinase
CDKN2A – Cyclin dependent kinase inhibitor 2A
c-FOS – BJ murine osteosarcoma viral oncogene homolog
CHK1 – Checkpoint kinase 1
C-KIT – KIT proto-oncogene receptor tyrosine kinase
c-MYC – cellular myelocytomatosis viral oncogene
CREB – cAMP-response element binding protein
CRISPR – Clustered regularly interspaced short palindromic repeats
CSC – Cancer stem cell
CSD – Chronically sun damaged
CST – Cell Signaling Technology
CTLA-4 – Cluster of differentiation 154
DAPI – 4',6-diamidino-2-phenylindole
DASH – Dipeptidyl peptidase-4 activity and/or structure homolog
DCT – Dopachrome tautomerase
DKO – Double knockout
DMEM – Dulbecco’s modified eagle medium
DMSO – Dimethyl sulfoxide
DNA – Deoxyribonucleic acid
DOX – Doxycycline
DS-MKP – Dual specificity mapk phosphatases
ECM – Extracellular matrix
EDTA – Ethylene di-amine tetra-acetic acid

EGFR – Epidermal growth factor receptor
EMT – Epithelial-Mesenchymal transition
eNOS - Endothelial nitric oxide synthase
ERK – Extracellular signal-regulated kinase
ETS – E26 transformation-specific
EVMM – Extravascular migratory metastasis
FACS – Fluorescence activated cell sorting
FAK – Focal adhesion associated kinase
FAP – Fibroblast activation protein
FBS – Fetal bovine serum
FDA – Food and drug administration
FGFR - Fibroblast growth factor receptor
FITC – Fluorescein isothiocyanate
FLT-3 – Fms-related tyrosine kinase-3
FOXO – Forkhead box-O
GeCKO – Genome-scale CRISPR knockout
GEMM – Genetically engineered mouse model
GFR – Growth factor reduced
GI – Gastrointestinal
GLUT1 – Glucose Transporter 1/ solute carrier family 2 member 1
GLUT4 – Glucose Transporter 4/ solute carrier family 2 member 4
GLYR1 – Glyoxylate reductase 1 homolog
GO – Gene ontology
GPNMB - Glycoprotein non-metastatic melanoma protein B
GRB2 – Growth Factor Receptor Bound Protein 2
GSK – Glycogen synthase kinase
GTP – Guanosine triphosphate
GTP – Guanosine triphosphate
HIF – Hypoxia inducible factor
HM – Hydrophobic motif
HMGA2 – High Mobility Group AT-Hook 2
HRAS – transforming protein 21
HRP – Horseradish peroxidase
IgG – Immunoglobulin G
IKK – IkB kinase
IP – Immunoprecipitation
ITPR2 – Inositol 1,4,5-trisphosphate receptor type 2
KD – Knockdown
KIAA1217 - Sickle tail protein homolog
KO – Knockout
KRAS – Kirsten rat sarcoma virus
MAPK – Mitogen activated protein kinase
MARS2 – Methionyl-tRNA synthetase 2, mitochondrial
MCR1 – Melanocortin 1 Receptor
MDM2 – Mouse double minute 2 homolog
MEK – Mitogen activated protein kinase kinase, or MAPK/ERK kinase

MERIT40 – Mediator of RAP80 interactions and targeting subunit of 40 kDa
MITF – Microthalmia-associated transcription factor
mTOR – Mechanistic target of rapamycin
mTORC – Mechanistic target of rapamycin complex 2
MYH – Myosin heavy chain
NCKAP5L – Nck associated protein 5 like
NDRG1 – N-myc downstream regulated 1
NF1 – Neurofibromatosis type 1
NFIB – Nuclear factor 1B
NMR – Nuclear magnetic resonance
NOD/SCID – Non-obese diabetic severe combined immune deficiency
NRAS – Neuroblastoma RAS viral oncogene homolog
NPM1 – Nucleophosmin 1
NT – Non-targeting
OIS – Oncogene-induced senescence
PARP – Poly (ADP-ribose) polymerase
PAX3 – Paired box gene 3
PBS – Phosphate buffered saline
PCM1 – Pericentriolar material 1
PD-1 – Programmed cell death protein 1
PDE3B – Phosphodiesterase 3
PDK1 – Phosphoinositide-dependent kinase 1
PDX – Patient-derived xenograft
PER – Proton efflux rate
PFKFB2 - 6-Phosphofructo-2-Kinase, or fructose-2,6-biphosphatase 2
PGC1 – PPARG coactivator 1 alpha
PH – Pleckstrin homology
PHLPP – PH domain and leucine-rich repeat protein phosphatases 1 or 2
PI3K – Phosphoinositide 3-kinase
PIP2 – Phosphatidylinositol (4,5)-bisphosphate
PIP3 – Phosphatidylinositol (3,4,5)-trisphosphate
PKB/AKT – Protein kinase B
PLEC – Plectin-1
PND – Post-natal day
PP2A – Protein phosphatase 2
PRAS40 – Proline-Rich AKT Substrate 40
PRSS1 – Protease serine 1
PTEN – Phosphatase and tensin homolog
PVDF – Polyvinylidene fluoride
RAF – Rabidly accelerating fibrosarcoma
RAS – Rat sarcoma
RB – Retinoblastoma
RNA – Ribonucleic Acid
ROS – Reactive oxygen species
RP1L1 – Retinitis pigmentosa 1-like 1 protein
RPMI – Roswell Park Memorial Institute medium

RTK – Receptor tyrosine kinase
SA-βGal – Senescence-associated beta galactosidase
SDS-PAGE – Sodium dodecyl sulfate polyacrylamide gel electrophoresis
sgRNA – single guide RNA
SHC – Src homology 2 domain-containing
shRNA – short hairpin RNA
SLAIN2 – SLAIN motif-containing protein 2
SLUG – slug homolog, zinc finger protein, SNAI2
SNAI2 – Snail family transcriptional repressor 2, SLUG
SNL – Sentinel lymph node
SOS – Son of Sevenless
SOX10 – Sex determining region Y-box 10
SSFA2 – Sperm specific antigen 2
STAT – Signal transducer and activator of transcription
SVIL – Supervillin
SWI/SNF – SWItch/Sucrose Non-Fermentable
TBC1D4 – TBC1 domain family member 4
TCOF1 – Treacher collins syndrome 1
TDRD5 – Tudor domain containing protein
TEAD – TEA domain family member
TERT – Telomerase reverse transcriptase
TF – Transcription factor
TM – Turn motif
TP53 – Tumor protein p53
TSC – Tuburous sclerosis complex
TTN – Titin
TTC28 - Tetratricopeptide repeat protein 28
TUMM – Tufts University mouse melanoma
TWIST – Twist family bHLH transcription factor 1
TYR – Tyrosinase
UDP – Uridine diphosphate
UV – Ultraviolet
VEGFR – Vascular endothelial growth factor receptor
WNK1 – Lysine deficient protein kinase 1
WT – Wild type
ZC3HAV1 – Zinc finger CCCH-type antiviral protein 1
ZEB1 – zinc finger E-box binding homeobox 1
ZEB2 – zinc finger E-box binding homeobox 2

Chapter 1. Introduction

1.1 Melanoma Skin Cancer

1.1.1 Cancer Statistics

Melanoma is a deadly skin cancer arising from transformed melanocytes, pigment producing cells within the skin. Cutaneous melanoma was the 5th and 6th most diagnosed cancer among men and women, respectively, and collectively responsible for an estimated 9,730 deaths in 2017 (Siegel et al., 2017). It is the rarest form of skin cancer, but disproportionally (>75%) accounts for skin cancer mortality (ACS, 2017), due to its high propensity for metastasis. Indeed, patients with localized disease have on average a 98% 5-year survival rate, compared with a dismal 18% in the case of distant malignancy (Siegel et al., 2017). Melanoma incidence has also been rising for the past four decades in both men and women, while mortality has remained relatively steady (Siegel et al., 2017); this is largely attributed to successful public awareness campaigns that have increased both diagnoses and early resection (Schadendorf et al., 2015), the latter correlating with positive outcome.

Disease incidence and survival can vary significantly by gender, by race/ethnicity, and with socioeconomic status. Men have a 60% higher incidence and more than twice the death rate of women, and men are generally diagnosed at an older age, with unfavorable prognostic indicators such as increased melanoma thickness and the presence of ulceration, which may contribute to increased mortality compared to women. Men are also more often diagnosed with melanomas on the trunk, compared to the arms and legs, which are the common sites of diagnosis in women. However, women have more favorable survival independent of clincopathologies, even for patients with advanced

disease (Siegel et al., 2017). In addition to gender, melanoma skin cancer incidence can vary by race/ethnicity and is also affected by socioeconomic status. Caucasian populations, with fewer pigmented melanocytes, are more susceptible than others to melanoma development, while populations with higher pigmentation often develop acral or mucosal melanomas (Schadendorf et al., 2015). However, African American populations diagnosed with melanoma skin cancer have lower 5 year relative survival compared to Caucasians at all stages of disease, and are diagnosed at later stages of disease development (Siegel et al., 2017). Unequal access to health care, including early detection, are thought to play a large role in the racial disparity observed in melanoma outcomes (Siegel et al., 2017).

Melanomas typically present in individuals between the ages of 40 and 60 years, with a median diagnosis of 57 years (Schadendorf et al., 2015). However, melanoma is also the most common cancer diagnosed in young adults between the ages of 20-29 years (Schadendorf et al., 2015). This divergence can best be understood by highlighting the relative risks factors associated with the development of both age-related and young-adult melanomas.

1.1.2 Risk Factors and Disease Development

Risk factors for melanoma development fall in to two broad categories: genetic and environmental. A family history, previous melanomas, and atypical nevi, are the strongest overall risk factors for disease development, but specific genetic factors such as light skin, red hair, and polymorphisms in the Melanocortin 1 Receptor (MCR1) can also pre-dispose to disease (Miller and Mihm, 2006). The strongest and most well-known environmental risk factor is ultraviolet (UV) irradiation exposure, commonly from

sunlight or indoor tanning beds. UV radiation can be divided into three categories based on wavelength: UVA (400–320 nm), UVB (320–290 nm), and UVC (290–200 nm). UVB radiation is considered most responsible for cutaneous melanoma development, for its ability to penetrate the skin and induce DNA damage (Garibyan and Fisher, 2010). Intermittent UV exposure, such as severe sunburns during childhood, confer the highest epidemiological risk for melanoma later in life. In addition, artificial tanning has a dose-dependent risk association (Lo and Fisher, 2014) and this route of exposure disproportionally affects young people. Thankfully, rapid rises in melanoma incidence among younger age groups is slowing, due to increased public awareness regarding the cancer-initiating potential of tanning bed irradiation (Schadendorf et al., 2015).

Melanoma is the most highly mutated cancer, and the spectrum of mutations that arise underscore the importance of UV exposure to disease development. Compared to other human cancers, melanoma has the highest frequency of somatic mutation, overwhelmingly characterized by C→T substitution mutations, which occur when UV radiation-induced covalent bonds in adjacent DNA pyrimidines are incorrectly repaired (Lawrence et al., 2013). Not surprisingly, melanomas arising on chronically sun-damaged (CSD) skin have higher mutational burdens than those with only intermittent sun damage (non-CSD). Non-CSD melanomas are not devoid of mutations, rather both are characterized by mutations in different oncogenic drivers (Shain and Bastian, 2016) and contribute to both disease progression and further classification.

1.1.3 Melanocyte Transformation and Melanoma Classification

Melanocytes, the melanoma cell of origin, largely reside in the basal epidermis of the skin, where they secrete the pigment melanin to neighboring keratinocytes. These

melanocytes give rise to the cutaneous melanoma subtype that is the subject of the studies described therein, but melanocytes are also found throughout the body, such as in the hair follicle, the eye, mucosal epithelia, and the meninges, to name a few (Miller and Mihm, 2006). Melanocytes arise from neural crest progenitor cells that migrate from the central nervous system and distribute to form the dermal and epidermal layers.

Within the skin, early models of melanoma progression emphasized a linear, stepwise transition from melanocytic nevi (a benign proliferation of melanocytes), through the transformation processes of dysplasia, hyperplasia, invasion, and metastasis. This sequential process is known as the Clark Model (Miller and Mihm, 2006), but more recent models favor a variety of paths to progression, with intermediate phenotypes not wholly represented by the Clark Model (Shain and Bastian, 2016). A summary of key stages is represented in Figure 1.1**,** showing that melanomas are initiated from melanocytic nevi (top row, second panel from the left). Nevi enter a "senescence-like" state, in which they display limited proliferation and rarely progress to dysplasia or change size for many years. However, oncogenic events, such as mutation from UV irradiation-induced DNA damage, can facilitate melanocytic transformation. these events can lead to the formation of melanomas *in situ*. This term refers to an irregular growth of melanocytes still contained within the epidermal layer (Figure 1.1, second column from the right). Melanomas *in situ* are precursors to invasive melanomas; cells no longer limited to the epidermis enter the dermal layer, and increasing depth of invasion is correlated with elevated metastatic disease risk (Figure 1.1, far right column) (Shain and Bastian, 2016).

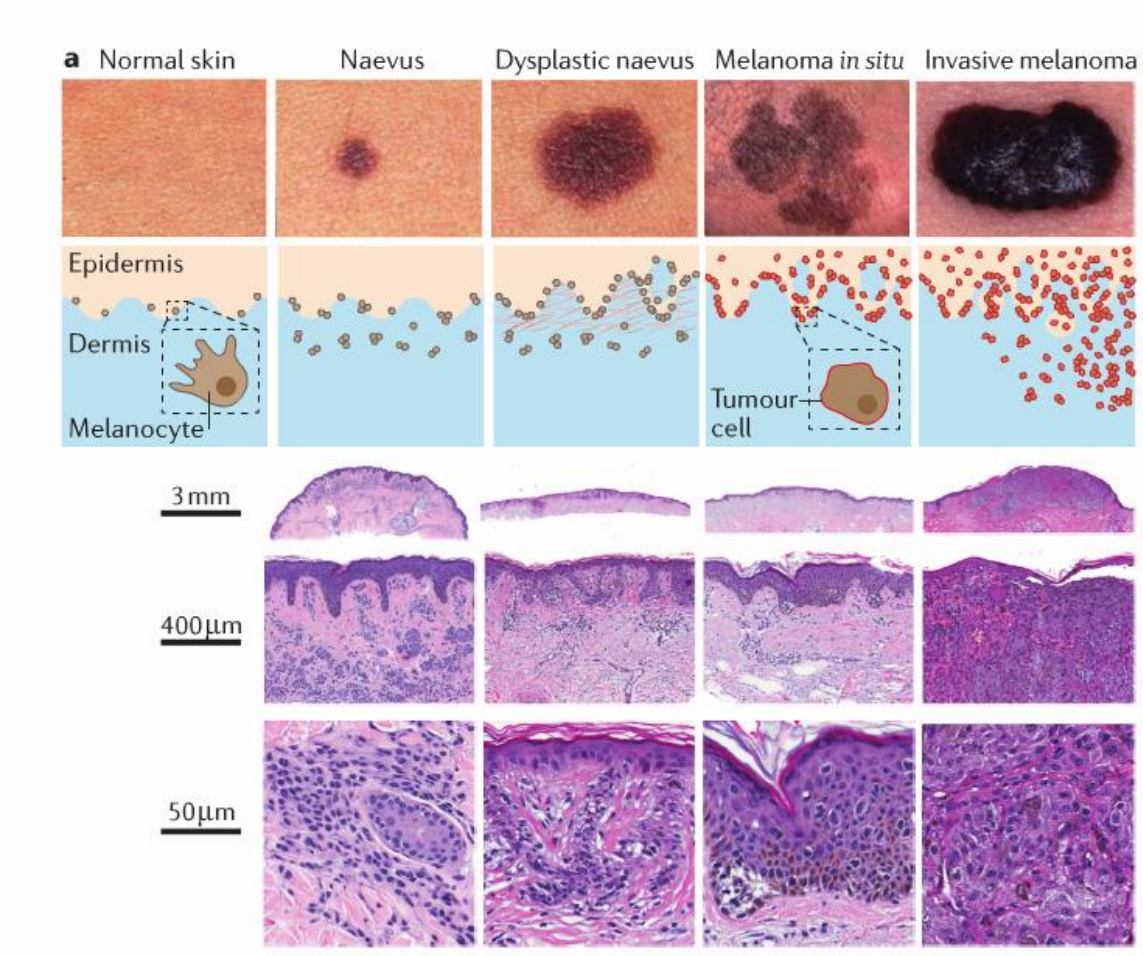

Figure 1.1. Morphological progression of melanocytic neoplasms. Top row: clinical images showing a free-standing naevus, a dysplastic naevus, melanoma in situ and an invasive melanoma. Second row: schematics illustrating the architectural features for each type of lesion. Rows 3–5: photomicrographs illustrating the representative histopathological features of each type of lesion. Reprinted with permission from (Shain and Bastian, 2016).

1.1.4 Common Genetic Alterations

The evolution from a benign lesion to a metastatic tumor occurs by acquisition and accumulation of genetic changes that lead to unrestrained cellular proliferation (Shain et al., 2015). In melanoma, many recurrent, oncogenic mutations occur, and understanding how these alterations affect disease progression can aid in therapeutic design. Hyperactivating the MAPK kinase pathway, which controls cell growth and survival (to be discussed further at length), is a major means toward disease progression, and the vast majority of oncogenic alterations in melanoma result in activation of this pathway (Figure 1.2B). The most common oncogenic mutation in melanoma is a valine (V) to glutamic acid (E) substitution mutation in the Ras effector kinase BRAF at codon 600 ($BRAF^{V600E}$) (Davies et al., 2002; Pollock et al., 2003). This mutation causes constitutive activation of the kinase domain, hyperactivating downstream MAPK signaling. This is an early mutational event, found in 80% of benign nevi and over 66% of metastatic melanomas (Ibrahim and Haluska, 2009).

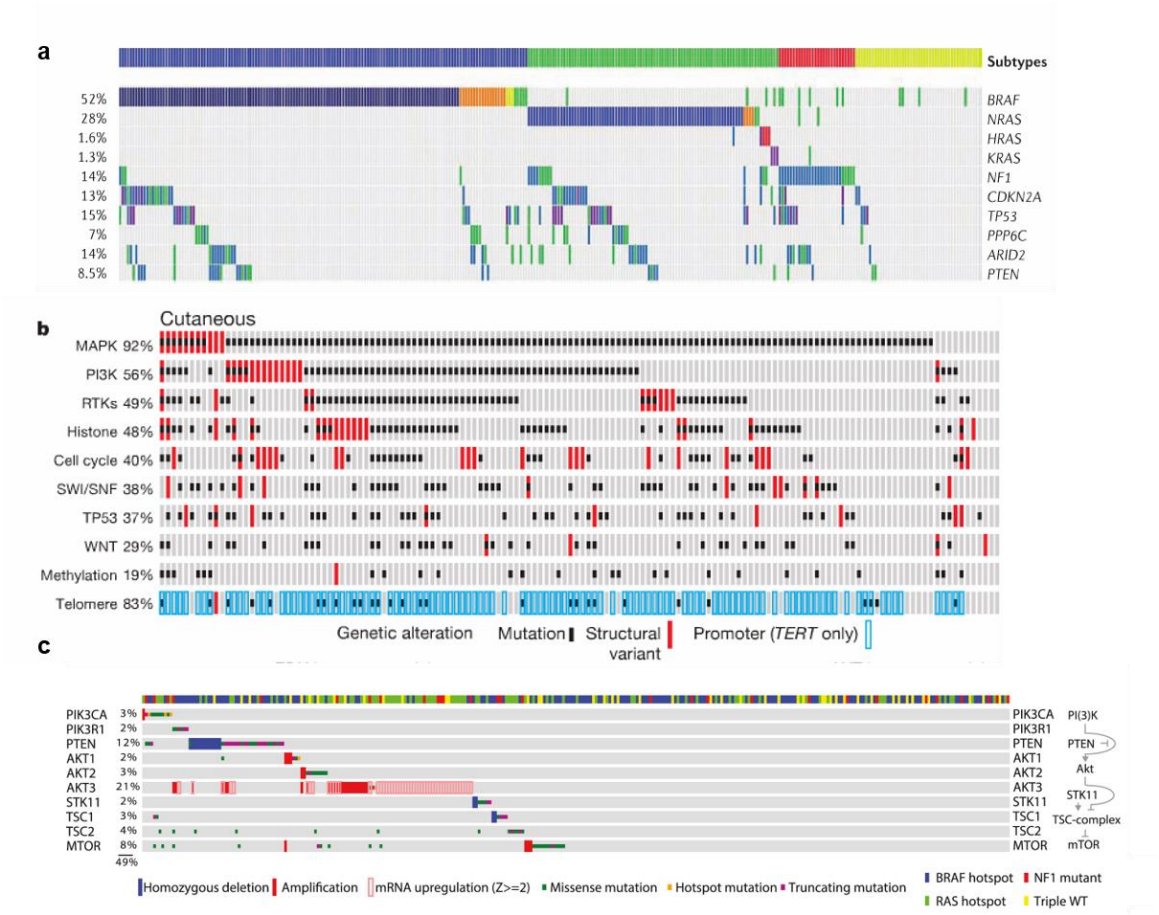

Figure 1.2. Genetic alterations in melanoma. A) The frequency and overlap of oncogenic alterations in melanoma by molecular subtype. Blue=BRAF mutant, Green=NRAS mutant, Red=NF1 mutant, Yellow=Triple WT (Luke et al., 2017). B) Frequency of alteration of common signaling pathways and genetic variant observed (mutation, structural, or TERT promoter) (Hayward et al., 2017) C) Alterations in PI3K/AKT signaling pathway components, color-coded by subtype. Reprinted with permission from (Akbani et al., 2015).

Activating mutations in another MAPK effector, NRAS, occur in roughly 15-28% of melanomas and mutually exclusive to BRAF mutations (Miller and Mihm, 2006). NRAS is also commonly mutated at a "hotspot," in which the majority of mutations are Q → R/K transition mutations at codon 61 (Hayward et al., 2017). Mutations in other RAS family members, such as HRAS and KRAS also occur, but with less frequency than NRAS (Akbani et al., 2015). Loss of function mutations or inactivation of NF1, a negative regulator of RAS, also occur in 14% of samples, and serve to functionally downregulate MAPK signaling (Akbani et al., 2015).

Together, these recurrent alterations stratify melanomas into four broad subtypes: BRAF mutant, NRAS mutant, NF1 mutant, and those lacking these common oncogenic driver mutations, known as Triple WT **(**Figure 1.2).While BRAF and NRAS alterations drive MAPK activation, they are early mutational events (Shain et al., 2015), and alone are insufficient for full malignant transformation. Additional alterations must occur for benign lesions to progress.

Alterations in cell cycle regulators are common in melanoma and associated with lesion progression. The tumor suppressor locus encoding CDKN2A (Cyclin-dependent kinase inhibitor 2A), is alternatively spliced to yield two cell cycle regulatory proteins $p16^{INK4a}$ and $p14^{ARF}$ (Quelle et al., 1995). Deletion of this locus results in functional loss of the $p16^{INK4a}$ protein, a failure to bind CDK4/6 and initiate the G1/S checkpoint, and subsequent loss of cell cycle control. Inactivating mutations, promoter silencing by methylation, and genetic deletion, all occur in melanoma (Ibrahim and Haluska, 2009). Loss of the Retinoblastoma protein (RB), a key gatekeeper of S-phase entry, leads to premature cell cycle progression and is frequently observed in melanoma (Hayward et al.,

2017). Taken together, alterations in cell cycle genes may be present in up to 90% of all melanomas by some estimates (Schadendorf et al., 2015). Other alterations associated with progression are mutations in the TERT promoter. TERT mutations create a *de novo* ETS binding site that increases transcription 2-4 fold (Huang et al., 2013).

Some alterations occur predominately in later stage or invasive melanomas. Mutations in SWI/SNF complex members such as ARID proteins occur primarily at later stages, as do TP53 mutations (Shain and Bastian, 2016; Shain et al., 2015). Late stage melanomas also have increasing mutational burdens, and mutational load correlates with cumulative sun exposure (Shain et al., 2015). As previously mentioned, UV exposure is a risk factor in melanoma, and incorrect repair of UV-induced lesions is associated with specific alterations. Sequence analysis of cutaneous melanoma samples show that greater than 90% of tumors harbor UV signature mutations (Hayward et al., 2017; Lawrence et al., 2013). Accordingly, CSD melanomas have a greater diversity of genetic alterations, including changes in BRAF other than the hotspot V600E mutation (Shain and Bastian, 2016). Interestingly, the $BRAF^{V600E}$ mutation is not induced by classical UV irradiation-induced mutation pathways, as it results form a T→A transversion. Additionally, its presence in non-CSD melanomas (and other non-UV exposed tumor types such as colon cancer), suggested to some that it was not a UV-associated mutation (Lo and Fisher, 2014). However, T→A transversions causing $BRAF^{V600E}$ mutations are a rare and minor byproduct of UV irradiation, and error-prone DNA polymerases may also introduce this change during DNA repair, indicating that the $BRAF^{V600E}$ mutation may indeed relate to UV-exposure after all (Shain and Bastian, 2016). Additionally, indirect effects of UV irradiation such as reactive oxygen species (ROS) generation are increasingly appreciated

mutational drivers. Recent analysis of early nevi harboring $BRAF^{V600E}$ mutations also demonstrate that they are fully clonal, further supporting that the acquisition of this mutation is an early, initiating, oncogenic event (Shain and Bastian, 2016).

Despite debate regarding the origin of the $BRAF^{V600E}$ mutation, its presence may play a role in later genetic alterations, such as loss of the tumor suppressor PTEN (Shain et al., 2015). PTEN negatively regulates the PI3K/AKT pathway (to be discussed later at length), which is important for cell growth and the second most frequently altered pathway in melanoma (Figure 1.2B). PTEN loss occurs in up to 20% of melanomas (Akbani et al., 2015) and combined with PTEN mutations, PTEN is altered in as many as 40% of all melanomas (Hodis et al., 2012; Schadendorf et al., 2015) Additionally, PTEN loss is significantly more frequent in the BRAF mutant melanoma subtype, compared to other subtypes (Figure 1.2C) (Akbani et al., 2015; Haluska et al., 2006). Studies also show that PTEN loss cooperates with BRAF mutations to increase metastatic penetrance (Dankort et al., 2009), and AKT phosphorylation, a marker for PI3K pathway activation, is highest in melanomas with MAPK pathway alterations in addition to PI3K alterations (Hayward et al., 2017). Mutations or gene amplification may also occur in other PI3K effectors to enhance downstream signaling (Figure 1.2C). Activating mutations and gene amplification in AKT1 and AKT2 are found in all melanoma subtypes (Akbani et al., 2015), while AKT3 mRNA and gene amplification are more common in the NRAS, NF1, and Triple WT subtypes (Figure 1.2C). The substitution mutation E17K, which hyperactivates AKT signaling, has been found in both AKT1 and AKT3 in clinical samples and cell lines (Davies et al., 2008; Lassen et al., 2014). Additionally, a novel mutation was identified in AKT1, Q79K, which increases AKT1 association with the

plasma membrane, and was identified in a patient with metastatic melanoma that had relapsed after BRAF inhibitor therapy, suggesting AKT signaling promotes adaptive resistance (Shi et al., 2014). Despite reports that PI3K pathway alterations like PTEN loss are associated with increased invasiveness, there are very few studies that have investigated how alterations in AKT or its effectors contribute to melanoma progression or metastasis.

1.1.5 Modeling Melanoma in vivo

To strengthen our understanding regarding the molecular basis of melanoma, models of progression have helped define the sufficiency or requirement for various observed genetic alterations. *In vivo* models can allow studies that combine genetic, microenvironmental, and environmental risk factors in ways that *in vitro* systems cannot. The earliest mutation seen to occur in melanoma, as discussed above, is the V600E substitution mutation in the BRAF kinase. Accordingly, it was thought to be an initiating oncogenic driver, but widespread expression of $BRAF^{V600E}$ in development was lethal (Mercer et al., 2005). Three research groups targeted expression of $BRAF^{V600E}$ to murine melanocytes via different mechanisms. Goel et al expressed human transgenic $BRAF^{V600E}$ constitutively in murine melanocytes using the Tyrosinase promoter and enhancer (Goel et al., 2009). Two groups, Dankort et al and Dhomen et al instead combined $BRAF^{V600E}$ with a conditional $CreER^{T2}$ transgene, also driven by Tyrosinase, in which topical application of tamoxifen activates Cre-recombinase and expression of $BRAF^{V600E}$ in melanocytes (Dankort et al., 2009; Dhomen et al., 2009). Each group found that mice harboring expression of targeted $BRAF^{V600E}$ in melanocytes developed only benign hyperplasia physiologically similar to human nevi, without penetrant melanoma.

Only upon combination with tumor suppressor loss, was metastatic melanoma apparent; loss of PTEN (Dankort et al., 2009), $p16^{INK4A}$ (Dhomen et al., 2009), CDKN2A, or p53 (Goel et al., 2009) was sufficient to induce melanoma, with metastases to both lungs and lymph nodes. This is consistent with previous observations that loss of $p16^{INK4a}$ (in the CDKN2A locus) predisposed mice to tumorigenesis, including melanoma (Sharpless et al., 2001).

There are many additional genetically engineered mouse models (GEMM) that have taken similar approaches to study the combined effect of genetic alterations on melanoma incidence (Pérez-Guijarro et al., 2017), and a few have combined genetic pre-disposition with environmental risk factors, to additionally model melanoma development. Epidemiological data showing that early childhood sunburn carries significant risk of melanoma development later in life were modeled *in vivo*, in which UV irradiation of neonatal but not adult mice potentiated tumor development (Noonan et al., 2001). GEMM models have also shed light on the molecular basis of the addictive tanning response, a major route of exposure and largest predictor of melanoma in young people (Fell et al., 2014). Further, our lab has also shown that neonatal UVB irradiation can synergize with genetic loss of ARF to enhance $BRAF^{V600E}$ melanoma penetrance with decreased latency (Luo et al., 2013).

Induced tumor models are frequently employed to model melanoma development, and recently, Patient-derived xenograft (PDX) models are increasingly common. PDXs are generated by implanting human tumor tissue directly into immunocompromised mice and perpetuating them *in vivo*, circumventing the need for 2D culture on plastic. PDXs more accurately model tumor heterogeneity and predict therapeutic response than

cultured cell models, or even cell line based xenograft models (Einarsdottir et al., 2014). Additionally, PDX establishment requires very few melanoma cells, and a recent tissue banking effort created a collection of 459 melanoma PDXs that span a spectrum of genetic alterations and recapitulate the dynamics of clinical presentation (Krepler et al., 2017).

In addition to murine-based models, a cost-effective alternative is the zebrafish model. An early model expressing $BRAF^{V600E}$ in melanocytes using the Microthalmia-associated transcription factor (MITF) promoter showed that nevi developed similar to human disease, and further conditional knockout of p53 could promote invasive malignancy (Patton et al., 2005). Zebrafish are easily propagated and especially well-suited to drug-dosing studies and chemical screens, making them an attractive model for drug discovery (Colanesi et al., 2012; Idilli et al., 2017). A conditional temperature sensitive zebrafish mutant helped elucidate the complex role of the melanocyte-specific lineage gene MITF in melanomas; hypomorphic MITF is oncogenic when combined with $BRAF^{V600E}$ at low levels, but loss of MITF causes melanoma regression (Lister et al., 2014). Furthermore, because zebrafish are also transparent, visualization of fluorescent proteins is straightforward; Zon and colleagues labelled individual neural crest progenitor cells, visualized developing melanomas, and identified a neural de-differentiation program is characteristic of melanoma-initiating cells (Kaufman et al., 2016).

Each of the aforementioned models share commonalities that shed light on the basic molecular origins of melanoma. First, $BRAF^{V600E}$ is oncogenic, but insufficient for malignant disease. Additional genetic alterations synergize with $BRAF^{V600E}$ to drive melanoma, and alterations commonly found in later stage lesions, such as PTEN or p53

loss increase melanoma invasiveness. Finally, melanocyte neural crest identity plays an important and somewhat surprising role in disease development.

However, a more detailed molecular understanding of biochemical pathways involved in these aspects of melanomagenesis and which may be mediating the observed pathologies is warranted, as well as being a crucial step in the development of molecularly targeted therapies.

1.2 The MAPK Pathway

1.2.1 Activation and downstream signaling

The MAPK pathway transduces extracellular signals from receptor tyrosine kinases (RTKs) at the cell surface to induce a downstream phosphorylation cascade resulting in transcription of genes involved in cell proliferation and survival (Figure 1.3). There are many RTKs that can activate RAS, but a few well-known examples are epidermal growth factor receptor (EGFR), c-KIT, platelet-derived growth factor receptor (PDGF), vascular endothelial growth factor (VEGFR) receptor, fibroblast growth factor receptor (FGFR), and fms-related tyrosine kinase-3 (FLT-3) (Fecher et al., 2008). RAS is a membrane-bound GTPase, and activation occurs when GTP-bound. Once activated, RAS can bind and signal to a number of effectors, but perhaps the best characterized are RAF and PI3K. There are three RAF serine/threonine kinase family members, A-RAF, B-RAF, and C-RAF, all of which have unique phosphorylation targets (Fecher et al., 2007) and homodimerize to activate downstream effectors (Acosta and Kadkol, 2016). Activated RAF proteins phosphorylate MEK 1/2 which in turn phosphorylates ERK, which signals to a variety of targets involved in proliferation, survival, and cytoskeletal regulation (Fecher et al., 2007). Importantly, ERK phosphorylation can induce cell cycle

progression through a series of steps, including transcriptional upregulation of cyclin D1, degradation of cyclin dependent kinase (CDK) inhibitor p27, as well as activation of the p90RSK complex (Figure 1.3).

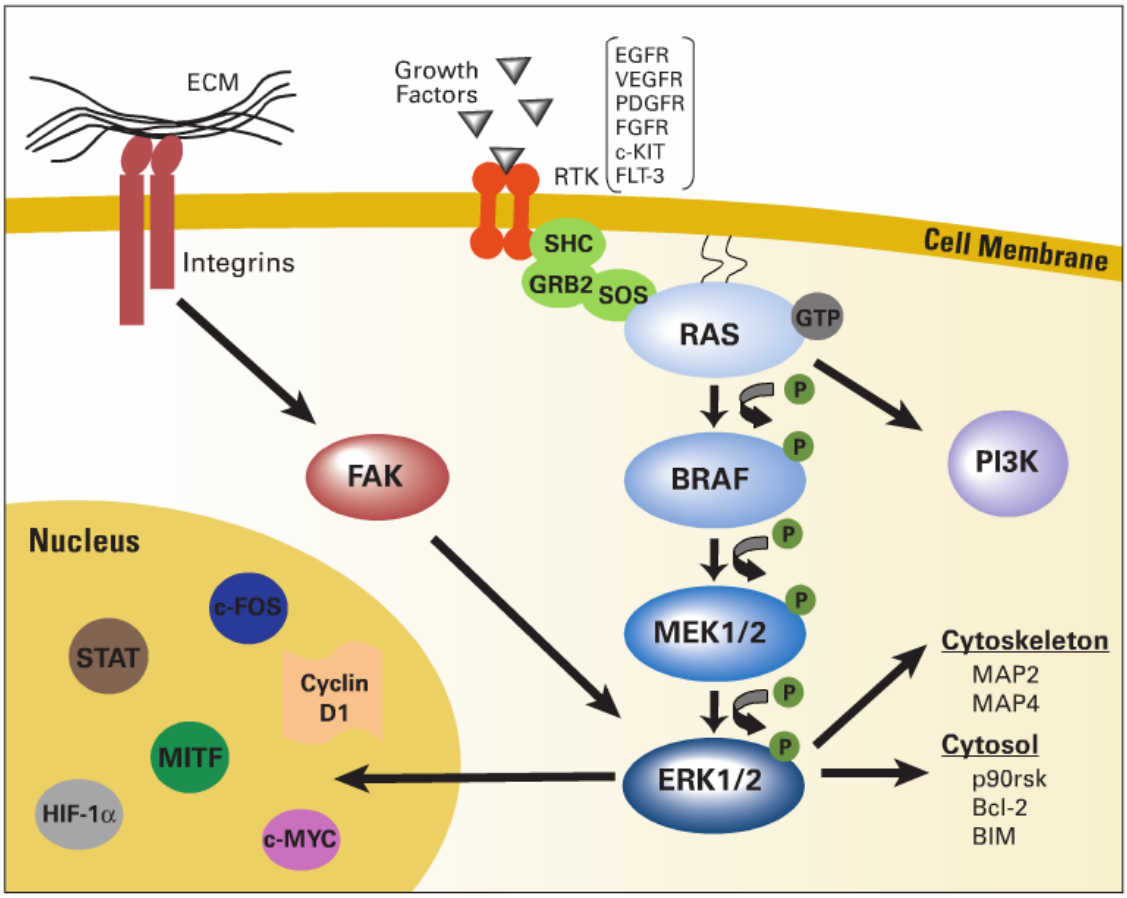

Figure 1.3. A simplified illustration of the MAPK signaling pathway**.** Receptor tyrosine kinases interact with growth factors at the plasma membrane, signaling to Ras, which can signal to downstream effector Raf. There are three Raf isoforms A-RAF, B-RAF, and C-RAF, capable of signaling to MEK, which in turn phosphorylates ERK. Pathway activation leads to transcription of genes involved in cell proliferation, survival, and angiogenesis. Reprinted with permission from (Fecher et al., 2007).

This stepwise signaling cascade resulting from RTK activation is the classical MAPK pathway, but modified signaling can result from other cellular triggers such as hypoxia, DNA damage, osmolarity, and inflammation to name a few, in which downstream events differ from those described above, and are beyond the scope of these studies, but reviewed in (Acosta and Kadkol, 2016).

As discussed previously, mutations in MAPK pathway effectors are tumor promoting. There are three isoforms of RAS (H-RAS, K-RAS, and N-RAS), and mutations in all three isoforms are found in melanoma to varying degrees. Mutations in NRAS are overwhelmingly common, occurring in as many as 28% of tumors, while HRAS and KRAS mutations occur less than 1% of the time (Hayward et al., 2017). Similarly, mutations in BRAF are prodigious compared to mutations in A-RAF or C-RAF. Mutations in NRAS or BRAF rarely occur within the same tumor, most likely because the net effect in both cases is pathway activation (Fecher et al., 2007). BRAF is thought to be the most commonly mutated of the RAF isoforms because only one phosphorylation event is needed to activate its kinase domain (Acosta and Kadkol, 2016). BRAF functions as a homodimer, but can also form heterodimers with other RAF isoforms (Rajakulendran et al., 2009; Weber et al., 2001). Additionally, aberrant splicing of $BRAF^{V600E}$ may create shorter variants with enhanced dimerization ability and these dimers are resistant to V600E specific inhibition by RAS inhibitors (Poulikakos et al., 2011).

However, there are also negative feedback loops that downregulate MAPK pathway activation. Dual specificity MAPK phosphatases (DS-MKPs) can inactivate MAPKs by dephosphorylating the threonine or tyrosine residues within their activation

domain. DS-MKPs may de-phosphorylate either the active threonine or tyrosine residue on MAPKs, or both, hence their dual-specificity (Farooq and Zhou, 2004). Additionally, DS-MKPs are induced by active MAPK signaling both transcriptionally and translationally (Acosta and Kadkol, 2016). The sprouty family of proteins also function to attenuate both MAPK and PI3K signaling through inhibition of downstream effector signaling. They are induced by RTK signaling that allows them to translocate to the plasma membrane and disrupt RAS and RAF activation (Neben et al., 2017). Another negative feedback loop of particular importance in melanoma involves NF1. NF1 is a GTPase activating protein that stimulates GTP hydrolysis of RAS, to convert RAS to its inactive GDP-bound state (Acosta and Kadkol, 2016). Because NF1 favors RAS inactivation, it is lost in roughly 15% of melanomas (Larribère and Utikal, 2016), which comprise the NF1 subtype (Akbani et al., 2015). NF1 is regulated by the RTK C-KIT, which is also overexpressed in melanoma, although primarily in tumors without other alterations in BRAF, NRAS, or NF1 (Akbani et al., 2015).

1.2.2 Oncogene Induced Senescence (OIS)

While myriad alterations within the MAPK pathway serve to amplify its signaling and promote tumor growth, singular alterations, such as the common $BRAF^{V600E}$ mutation, are insufficient for tumor progression, in part due to suppressive mechanisms such as oncogene-induced senescence (OIS). In melanocytes, the acquisition of an oncogenic BRAF mutation may initially stimulate a nevus to grow, but it will cease proliferating almost completely, and in some cases for decades (Michaloglou et al., 2005). This cell-cycle arrest is associated with increased levels of $p16^{INK4A}$ and the presence of senescence-associated β-galactosidase (SA-βGal) activity in the absence of

telomere attrition (Michaloglou et al., 2005). Senescence is a process of cell-cycle arrest associated with proliferative exhaustion, and a major barrier to cancer development (Hanahan and Weinberg, 2000). Tumor cells must overcome senescence, often through inactivation of $p16^{INK4A}$ and pRB cell cycle regulatory genes, lengthening of critically short telomeres by upregulating telomerase activity, and resistance to apoptosis (Mooi and Peeper, 2006).

In addition, the PI3K pathway may play a role in overcoming BRAF-induced OIS. Specifically, Peeper and colleagues showed that PTEN depletion could abrogate $BRAF^{V600E}$ induced senescence, and AKT3 overexpression enhanced subsequent tumorigenesis (Vredeveld et al., 2012). Subsequent studies will be necessary to fully elucidate the mechanistic role of PI3K/AKT members in overcoming OIS.

1.2.3 The MAPK pathway and MITF regulation

The MAPK pathway also plays a role in regulating melanocyte specific genes, such as the lineage-specific melanocyte master regulator, MITF. When αMelanocyte stimulating hormone (αMSH) binds the Melanocortin 1 receptor (MCR1), adenyl cyclase is induced, which stimulates the second messenger cyclic adenosine monophosphate (cAMP). cAMP-response element binding protein (CREB), in addition to neural crest lineage genes SOX10 and PAX3, cooperate to induce MITF transcription (Levy et al., 2006). MITF can then be dually phosphorylated by the MAPK pathway, which simultaneously increases MITF activation and targets it for ubiquitin-mediated degradation. The net consequence of these two phosphorylation events is downregulation of MITF (Molina et al., 2005; Wu et al., 2000). Consistent with this, elevated expression of MITF counteracts BRAF-mediated melanoma cell proliferation, and MITF is

suppressed in melanomas with oncogenic BRAF (Wellbrock and Marais, 2005). In apparent opposition to this, MITF is amplified in roughly 10% of melanomas (Hayward et al., 2017), and has been shown to cooperate with $BRAF^{V600E}$ to favor malignant transformation (Garraway et al., 2005). While hyperactivation of MAPK signaling should cause increased MITF degradation, MITF levels are maintained in melanomas at mostly low levels, unless amplified. It has been suggested that melanoma cells counteract MITF degradation via WNT/β-catenin signaling, which can induce MITF (Gray-Schopfer et al., 2007), since stabilized β-catenin expressed in melanocytes can cooperate with NRAS to induce melanoma in a mouse model (Delmas et al., 2007). While this careful balance of MITF levels will be discussed further in more detail, it is generally acknowledged that individual melanoma cells can maintain differential dependencies on MITF and acclimatize to preferred MITF levels, becoming stably $MITF^{hi}$ or $MITF^{lo}$ (Arozarena and Wellbrock, 2017). This intrinsic difference in MITF levels stipulates differential MITF-mediated downstream signaling within these varied molecular contexts and makes targeting MITF in melanoma an especially challenging proposition.

Interestingly, MAPK regulation of MITF has consequences during BRAF inhibitor therapy. In $BRAF^{V600E}$ melanoma cells treated with BRAF or MEK inhibitors, MITF and target genes are drastically induced, leading to cellular perturbations in metabolism (Haq et al., 2013) and disabled feedback inhibition (Pratilas et al., 2009) that may ultimately drive adaptive resistance to targeted therapy (Haq et al., 2014; Konieczkowski et al., 2014). In summary, MAPK signaling modulates MITF levels, and melanoma cells maintain MITF within a critical window to best support oncogenic transformation or overcome drug inhibition.

1.3 The PI3K/AKT Pathway

1.3.1 Pathway Activation and Downstream Signaling

The PI3K/AKT signaling pathway is the second most frequently altered pathway in melanoma, and yet the mechanisms associated with tumor progression and metastasis promotion are not well understood. The PI3K/AKT signaling pathway is a complicated hub that orchestrates signals critical for cell growth, cell metabolism, and overall survival. Signaling through RAS, other RTKs, or GPCRs activates phosphoinositide 3-kinase (PI3K), which catalyzes the phosphorylation of phosphatidylinositol (4,5)-bisphosphate (PIP2) to phosphatidylinositol (3,4,5)-trisphosphate (PIP3) and recruits the protein kinase effector AKT to the plasma membrane (Figure 1.4) (Fruman et al., 2017). Signaling is terminated by de-phosphorylation of PIP3 back to PIP2 by the phosphatase and tensin homolog (PTEN) (Manning and Toker, 2017). AKT activation occurs via phosphorylation at two critical activating residues. Phosphoinositide-dependent kinase-1 (PDK-1) phosphorylates AKT1 on the residue Threonine 308 (T308) within its kinase domain, which is both necessary and sufficient for AKT activation (Fruman et al., 2017). Additional phosphorylation at Serine 473 (S473) by mechanistic target of rapamycin (mTOR) complex 2 (mTORC2) on AKT1 fully activates the kinase and stabilizes T308 phosphorylation (Manning and Toker, 2017). Active AKT can translocate to the nucleus or cytosol to act on a wide variety of substrates (Figure 1.4), specifically phosphorylating those with the consensus site R-X-R-X-X-S/T, and potentially R-X-X-S/T (Manning and Cantley, 2007).

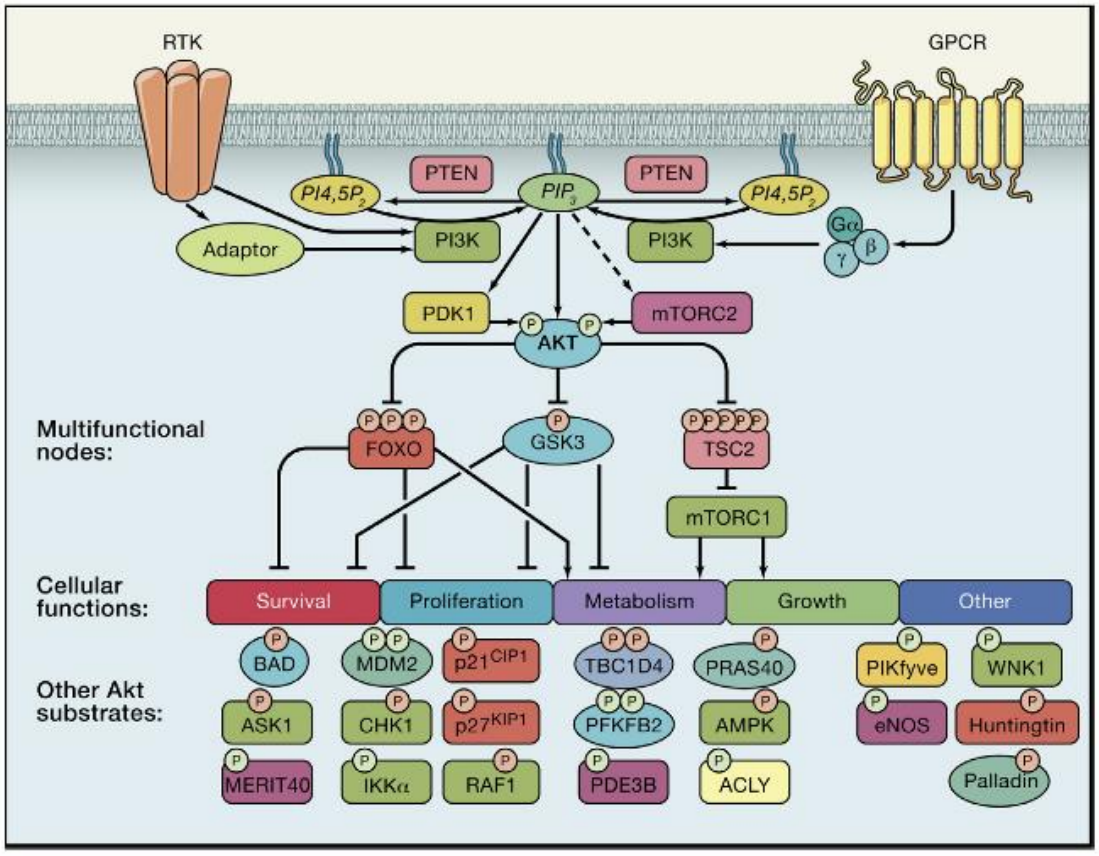

Figure 1.4. The PI3K/AKT Signaling Pathway. RTKs or GPCRs activate PI3K, catalyzing the conversion of $PI4,5P_2$ to PIP_3. PIP_3 then facilitates activation of AKT through PDK1-mediated phosphorylation at T308 or mTORC2-mediated phosphorylation at S473. Active AKT then mediates a wide variety of cellular functions involved in cell survival, growth and proliferation, metabolism, others. Reprinted with permission from (Manning and Toker, 2017).

Negative regulation of AKT signaling is performed by protein phosphatases. Protein phosphatase 2 (PP2A) de-phosphorylates the T308 residue, while the PH domain and leucine-rich repeat protein phosphatases 1 or 2 (PHLPP) de-phosphorylate the S473 residue (Toker and Marmiroli, 2014).

1.3.2 The AKT isoforms and isoform specificity

There are three isoforms of AKT encoded on separate chromosomes, known as AKT1 (or PKBα), AKT2 (PKBβ), and AKT3 (PKBγ) (Manning and Cantley, 2007). They share 80% homology and similar protein structures, but have many non-redundant functions, mediated in part by differential subcellular localization, tissue-restricted expression, and substrate specificity (Toker and Marmiroli, 2014). AKT isoform specificity has been partially elucidated by phenotypic characterization of isoform-specific and double knockout (DKO) mice. For example, AKT1-null mice show increased perinatal mortality and reduced body weight (Cho et al., 2001b), while AKT2-deficient mice develop normally but exhibit diabetes-like symptoms, including elevated fasting plasma glucose and peripheral insulin resistance (Cho et al., 2001a). AKT3-null mice exhibit reduced brain size but no other physiological abnormalities (Dummler et al., 2006). AKT1/AKT2 DKO mice die shortly after birth, while AKT1/AKT3 DKO mutants die at embryonic day 12. AKT2/AKT3 DKO mice have reduced body size and develop insulin and glucose resistance later in life but are otherwise normal (Dummler et al., 2006). Additionally, AKT-isoform specificity also occurs during negative regulation. For example, protein phosphatase PHLPP1 de-phosphorylates AKT2 and AKT3, while PHLPP2 showed preference for de-phosphorylating AKT1 and AKT3 (Brognard et al., 2007). Because PHLPP is also subject to AKT-mediated phosphorylation and

degradation (Toker and Marmiroli, 2014), this feedback loop could further influence downstream AKT-isoform specificity.

Efforts to elucidate isoform-specific substrates have uncovered phosphorylation preferences between AKT isoforms. A phospho-proteomic screen performed by Sanidas et al in mouse lung fibroblasts analyzed AKT-specific substrates and compared phosphorylation in cells expressing a single AKT isoform, showing that isoform-specific signaling can regulate RNA processing (Sanidas et al., 2014). Many additional studies have implicated specific AKT isoforms in the regulation of downstream targets, many of which are important for tumor growth and progression, but in general, no comprehensive understanding regarding the functional significance or mechanistic regulation of AKT-specific substrates is available, and this remains an active area of investigation.

1.3.3 AKT isoform specificity in cancer

AKT-isoform specificity also occurs in cancer. Studies performed in breast cancer models have elucidated that AKT1 accelerates tumor growth, while AKT2 primarily promotes metastasis (Dillon and Muller, 2010). The isoforms may perform antagonistic functions, such that AKT1 promotes, while AKT2 inhibits mammary tumor formation (Maroulakou et al., 2007) and AKT1 may limit, while AKT2 promotes breast cancer cell invasion (Chin and Toker, 2009). AKT3, in contrast, was shown to be important in the triple-negative subtype of breast cancer, while the other isoforms were dispensable (Chin et al., 2014a). AKT isoforms also differentially contribute to tumorigenesis in glioblastoma, colon, and prostate cancer (Gonzalez and McGraw, 2009).

In melanoma, there is emerging evidence for AKT isoform specificity. AKT3 is selectively amplified in 20% of melanomas that lack BRAF mutations (NRAS, NF1, and

Triple WT subtypes) while AKT1 and AKT2 activating mutations or gene amplification are found in BRAF mutant melanomas (Akbani et al., 2015). A novel AKT1 mutation (Q79K) was discovered in a patient with metastatic melanoma that relapsed after BRAF inhibitor therapy (Shi et al., 2014), and AKT1 activation reportedly increased metastasis in murine $BRAF^{V600E}$ melanomas to a greater degree than PTEN deletion alone (Cho et al., 2015). A specific role for AKT2 had not been described when the current studies were initiated, however, during the writing of this thesis, the AKT2 isoform was implicated in the progression of melanoma metastasis (Yu et al., 2018).

1.3.4 The AKT pathway in metastatic melanoma

There is myriad evidence that implicates the PI3K/AKT pathway in metastatic progression in many tumor types, and specifically in melanoma. Increased AKT phosphorylation (P-AKT), a marker for PI3K pathway activation, is elevated in metastatic tumor samples compared with benign or localized lesions (Dai et al., 2005). Concordantly, overexpression or hyperactivation of AKT can drive radially spreading melanomas to become vertically invasive, and increased incidence of metastasis in mouse models (Cho et al., 2015; Dankort et al., 2009; Govindarajan et al., 2007). Important regulatory proteins downstream of AKT, such as β-catenin, have also been shown to promote metastatic melanoma *in vivo* (Damsky et al., 2011).

Melanoma also has one of the highest rates of lethal brain metastases of any cancer, consistent with the extremely poor prognostic outcomes associated with disseminated disease (Westphal et al., 2017). Brain metastases were found to have the highest P-AKT levels compared to lung or liver metastases (Davies et al., 2009). Similarly, molecular profiling of patient matched cranial and extracranial metastases

found increased PI3K pathway activation specifically in cranial metastases (Chen et al., 2014), and in accordance with this, PI3K inhibition effectively reduced brain metastases in a mouse melanoma model (Niessner et al., 2016). There is also some evidence to suggest that AKT activation is influenced by brain-specific microenvironmental factors, since astrocyte-conditioned melanoma cells showed enhanced P-AKT and increased invasiveness (Niessner et al., 2013). Given that the PI3K/AKT pathway is also important in the early stages of tumor promotion in melanoma, dissecting specific effects on metastasis has proved difficult (Damsky et al., 2014). Understanding the unique paradigms associated with metastasis-specific programs and the specific roles for PI3K pathway effectors within the metastatic process will prove critical for future therapeutics.

1.4 Metastasis: a complex, multi-step process

1.4.1 The Epithelial-Mesenchymal Transition (EMT)

Tumor cells must acquire distinct traits that enable successful departure from the primary tumor through migration, invasion, dissemination, survival, and finally, growth at a secondary site (Figure 1.5). The EMT program is a biologic process in which epithelial cells de-differentiate to acquire a mesenchymal phenotype that allows enhanced migration and resistance to apoptosis. EMT occurs during normal development and wound healing (Nakamura and Tokura, 2011), but plays an important role in pathological processes, and is thought to be a crucial component of early metastatic dissemination in nearly all tumor types (Lambert et al., 2017). Activation of multiple transcription factors (TFs), cytoskeletal reorganization, extracellular matrix degradation, and changes in cell surface protein expression are all components of a successful EMT program (Kalluri and

Weinberg, 2009), but there are no hard and fast rules governing the requirements for various EMT components in different tissue or tumor types (Lambert et al., 2017).

In epithelial cancers, there are key markers whose expression determines the cellular phenotype, and a change in expression of these factors governs the cellular phenotype (Figure 1.6). Loss of E-cadherin is an early characteristic feature of EMT, and cells downregulating E-cadherin are detected at the invasive front of many tumors (Li et al., 2015). E-cadherin expression is regulated by transcription factor binding to its promoter, and important repressors are SNAI2 (also known as SLUG), ZEB1, ZEB2, and TWIST. These factors are all highly upregulated during EMT, resulting in E-cadherin downregulation (Figure 1.6). Activation of the MAPK signaling pathway strongly activates SLUG to repress E-cadherin expression (Li et al., 2015).

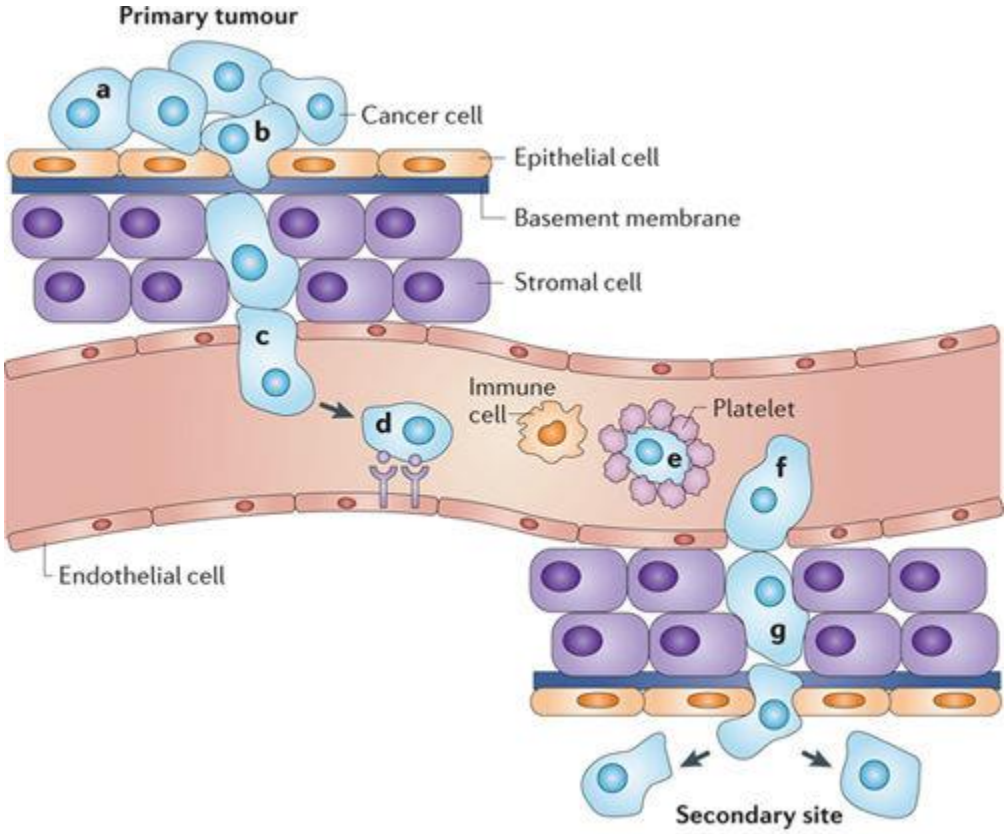

Figure 1.5. The steps of metastasis. First, metastatic cells must break free from the primary tumor (a) and migrate into the surrounding stroma (b). Next, intravasation (c) into the bloodstream may be required, where cancer cells may bind to metastasis-supporting sites (d) or to platelets (e), which protect the cancer cells from the immune system. After reaching the secondary site, cancer cells can extravasate (f-g) to a secondary site. Reprinted with permission from (Schroeder et al., 2011).

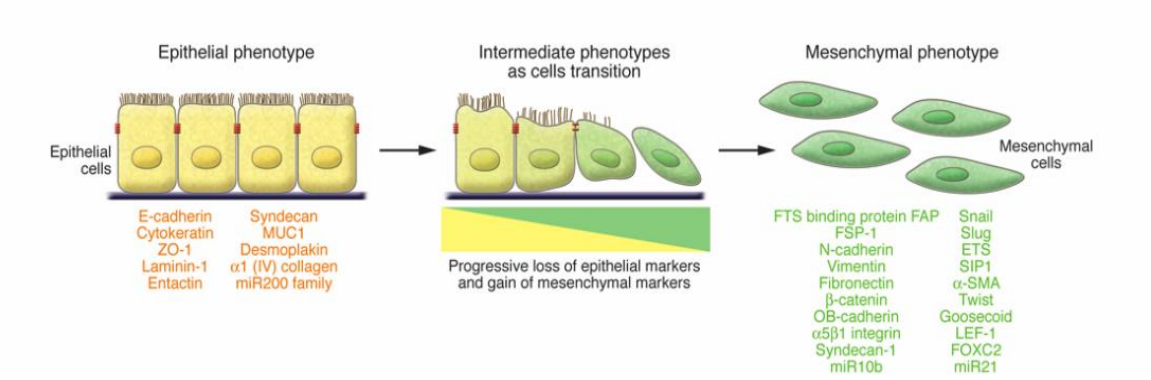

Figure 1.6. The process of EMT. Molecular transition of polarized epithelial cells to motile mesenchymal cells involves changes in expression of EMT-associated transcription factors and proteins. Reprinted with permission from (Kalluri and Weinberg, 2009).

In melanoma, there is some evidence that classical EMT factors play a role in disease progression. Increased N-Cadherin expression, an EMT-associated marker, was shown to correlate with poorer prognosis in melanoma patients bearing primary tumors or lymph node metastases (Murtas et al., 2017). Additionally, gene expression profiling of primary versus metastatic tumor samples identified an EMT signature upregulated in metastatic samples (Alonso et al., 2007). While not all melanoma patients display classical cadherin switching, aberrant E-cadherin expression with increased N-cadherin was associated with worse clinical prognosis (Yan et al., 2016). The PI3K/AKT pathway, de-regulated in the majority of melanomas, is strongly implicated in regulating EMT in multiple cancers (Chin and Toker, 2009; Qiao et al., 2008), and may also play a role in melanoma. β-catenin, an AKT target, regulated an EMT-like process in melanoma cells through modulation of the tumor microenvironment (Zhou et al., 2017). Furthermore, the EMT-TF SLUG was found to be a target of AKT in melanoma cells (Fenouille et al., 2012) and activation of mTORC1 downstream of AKT was shown to induce EMT (Pearlman et al., 2017). In addition, aberrant PI3K/AKT signaling is thought to mediate an EMT switch in many cancers (Song et al., 2009; Wang et al., 2007) including melanoma (Fenouille et al., 2012; Schlegel et al., 2015), and emergent evidence points to BRAF inhibition as inducing an EMT-like phenotype upon PTEN loss (Fedorenko et al., 2015), suggesting that BRAF inhibition in the context of PI3K/AKT perturbations may promote a more invasive and refractory cancer.

Despite the observation of EMT-like processes in malignant melanomas described above, melanocytes are derived from neural crest cells, and so by definition, melanomas are not epithelial cancers and do not undergo a classical EMT. Furthermore, EMT is not a

simple switch; cells may adopt partial epithelial or mesenchymal phenotypes that are also reversible (Lambert et al., 2017). Melanoma cells undergo an EMT-like process in which cells express combinations of EMT TFs that broadly define two reversible phenotypes-differentiation and invasion. Cells may "switch" between states, termed phenotype switching (Vandamme and Berx, 2014), and both states may simultaneously exist within a tumor mass. This plasticity drives heterogeneity (Vandamme and Berx, 2014), which aids in adaptive tumor responses that contribute to the refractory nature of melanoma tumors to treatment (Li et al., 2015). A differentiation-like state is associated with high levels of the TFs ZEB2 and Slug, while an invasive phenotype is characterized by increased expression of TFs ZEB-1 and TWIST (Adler et al., 2017; Caramel et al., 2013). However, in addition to the expression of classical EMT factors, there are melanocyte-specific TF's that are also thought to contribute to EMT-like processes in melanoma.

Microphthalmia-associated transcription factor (MITF) is a master regulator of melanocytes, controlling cellular programs such as pigmentation, proliferation and metabolism, as well as cellular invasion, and melanoma EMT (Hsiao and Fisher, 2014). Its role in melanoma is controversial (Vandamme and Berx, 2014), since it can be both a tumor promoting oncogene amplified in melanomas (Garraway et al., 2005) but low levels of MITF are associated with worse prognosis, suggesting a pro-differentiation phenotype may be less aggressive (Haluska et al., 2006). MITF is also subjected to extensive regulation, both transcriptionally and post-translationally (Hsiao and Fisher, 2014), and aberrantly by $BRAF^{V600E}$ (Reddy et al., 2017). EMT genes ZEB1 and ZEB2 transcriptionally regulate MITF to control normal melanocyte homeostasis, regulating MITF expression during neural crest migration (Denecker et al., 2014). This

developmental program may explain their involvement in melanoma differentiation and phenotype switching. In fact, it has been proposed that MITF levels function as a "rheostat" mediating cellular plasticity and phenotype switching, in part through ZEB1/2 expression. MITF depletion reportedly induces G1-arrested but highly invasive cells, while MITF amplification is proliferative and increases a differentiated, poorly invasive phenotype (Vandamme and Berx, 2014).

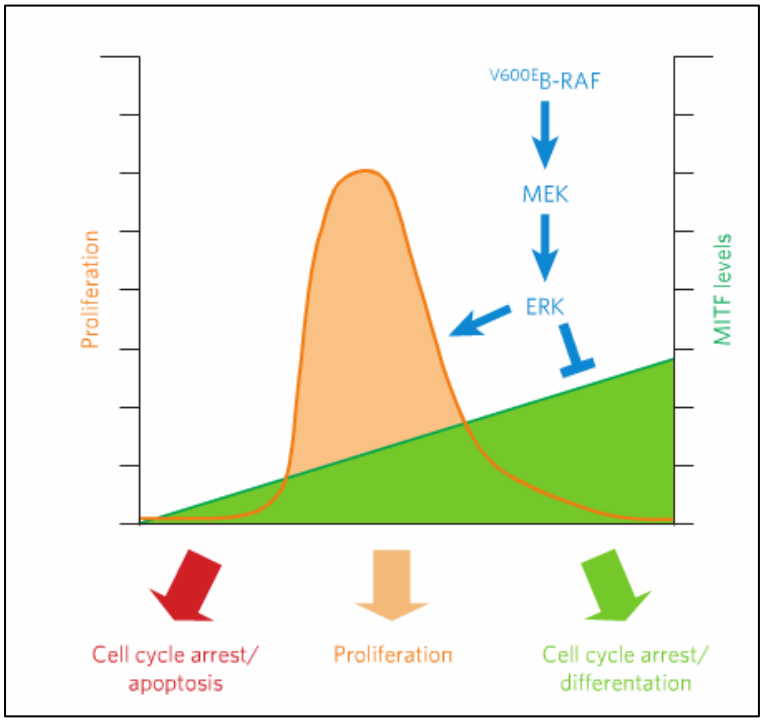

Figure 1.7. A model of MITF regulation in melanoma. MITF levels must be maintained within an optimal window that supports cell proliferation. Reprinted with permission from (Gray-Schopfer et al., 2007).

However, other studies suggest the role of MITF in this rheostat modulation model is less straightforward. Melanoma cells display differential dependencies on MITF; in cells where MITF is amplified or readily expressed, MITF depletion enhances melanoma cell invasion, but in cells that have low levels of MITF, further reduction suppresses an invasive phenotype (Arozarena and Wellbrock, 2017). The possibility that MITF may be either anti- or pro-invasive is supported by data showing that MITF can both induce and suppress gene sets involved in cell migration (Arozarena and Wellbrock, 2017). In fact, conflicting data regarding the role of EMT-associated genes and MITF in melanoma suggest that a complex network of positive and negative feedback loops regulates reversible reprogramming (Vandamme and Berx, 2014), and is far from fully understood.

In summary, EMT in melanoma cells is not a simple step-wise hierarchical progression, but rather a rheostat model involving phenotype switching and cellular heterogeneity. However, classical EMT-associated transcription factors do play a role in regulating melanocyte homeostasis and melanoma cell invasion through MITF regulation, but a full understanding of MITF in melanoma progression is still being elucidated.

1.4.2 Metastatic dissemination of melanoma cells

The most commonly discussed route of metastatic dissemination is via the vasculature, in which tumor cells intravasate into the circulation (Figure 1.5C). Melanoma cells may utilize melanocyte-specific programs to modify the local microenvironment and enable successful intravasation. A recent study found that melanosomes, organelles used by melanocytes for pigment trafficking, are utilized by

melanoma cells to transport a microRNA cargo that modifies the dermal niche, triggers fibroblast re-programming, and promotes invasion (Dror et al., 2016). For example, the microRNA mir-211 was the identified in melanosome cargo of melanoma cells but not normal melanocytes, and induced cancer-associated fibroblast (CAF) formation via MAPK upregulation (Dror et al., 2016). Neighboring keratinocytes reportedly support dermal invasion as well; keratinocytes can secrete growth factors that downregulate E-Cadherin expression and increase matrix metalloproteinases that breakdown the basement membrane. (Arozarena and Wellbrock, 2017). In addition, de-repression of the microRNAs mir-221/222 can enhance the invasive ability of melanoma cells, once triggered by Notch signaling from distal keratinocytes to melanocytes (Golan et al., 2015).

In addition to vascular intravasation as illustrated in Figure 1.5, a second means of metastatic dissemination is via the lymphatics. This is closely related to the process of angiotropism, whereby melanoma cells migrate along the external surface of blood vessels without intravasating (Van Es et al., 2008). Lymph node biopsies to detect metastatic spread are sometimes used for clinical staging and lymph node invasion is correlated with unfavorable outcome in many cancer types, but detection of lymphatic invasion in clinical samples has been challenging by histology due to artifacts introduced by tissue processing (Moy et al., 2017). Tumor cells have long been observed in close association with blood vessels, “cuffing” the external surface, and were thought to be in the process of intravasating. However, this pericyte-like behavior is now recognized as extravascular migratory metastasis (EVMM), the histopathological correlate to angiotropism, and increasingly appreciated as an important mechanism of metastatic

spread in melanoma (Moy et al., 2017). Recent studies investigating how UV-irradiation affects melanoma metastasis implicated angiotropism as the primary mechanism, through neutrophilic inflammation that promoted pericyte mimicry leading to angiotropism (Bald et al., 2014). Subsequently, a separate study identified angiotropism in 70% of primary cutaneous melanoma lesions and 35% of their respective brain metastases (Moy et al., 2017). Furthermore, this pericyte-like migration without intravasation is reminiscent of early neural crest melanoblast migration in development (Lugassy and Barnhill, 2007). Supporting this notion, gene expression profiling of angiotrophic primary melanomas identified neural crest genes as significantly associated with the process of angiotropism and EVMM (Lugassy, 2011). However, while EVMM is classically denoted as an alternate pathway to dissemination independent of intravasation, it may also aid in melanoma cell intravasation (Landsberg et al., 2016).

There are several models of melanoma dissemination, involving either the lymph, the vasculature, or a combination. It has been hypothesized that lymphogenous spread occurs prior to intravasation and subsequent hematogenous spread, and this is known as the stepwise-spread model (Adler et al., 2017). The evidence for this model is largely based on patient studies that show a majority of patients with metastatic disease first present with regional lymph node metastases (Adler et al., 2017). A second model is known as the simultaneous-spread model, in which both lymphatic and direct intravasation into the circulation can occur. This model is best supported by evidence that sentinel lymph node (SNL) removal upon detection of regional metastases has no survival benefit for patients (Medalie and Ackerman, 2004), and argues against the stepwise-spread model. However, up to 30% of patients that do undergo lymph node

dissection do not experience further disease progression or relapse with disseminated disease (Adler et al., 2017). A third model attempts to reconcile these disparate progression patterns, known as the differential-spread model. This model states that there are multiple pathways to dissemination, and some melanomas may not possess the capacity to metastasize at all (Adler et al., 2017). Further, metastatic sites may be re-seeded, or the primary tumor may resolve, while metastases persist. In all, the pathways to dissemination are myriad and complex, and depend both on the microenvironment as well as intrinsic tumor heterogeneity (Shain and Bastian, 2016).

1.4.3 Growth in the metastatic site

Once melanoma cells leave the primary tumor and disseminate, they must also be capable of growth at a secondary site. Tumor initiating cells, sometimes called cancer stem cells, are described as having unique properties that allow them to survive the cellular stresses associated with dissemination and favorably modify the pre-metastatic niche. However, no cellular hierarchy of cancer stem cells (CSCs) is present in melanoma, in part due to the lack of reliable CSC markers (Quintana et al., 2010; Schadendorf et al., 2015), but also due to the high plasticity and heterogeneity of melanoma itself (Meacham and Morrison, 2013).

In melanoma, there is evidence that distinct subpopulations of slow-cycling cells are required for consistent tumor growth, but markers for these cells are transient, and non-hierarchical (Roesch et al., 2010). Furthermore, depending on the mouse model in which the studies were done, the tumor-initiating capacity of melanoma cells drastically differs, with as few as a single melanoma cell capable of tumor-initiating capacity in severely immune-compromised mice (Quintana et al., 2008). These results suggest that

melanoma cells have a high degree of plasticity that alters their ability to form tumors and may therefore affect their ability to grow efficiently at secondary metastatic sites.

Metabolic reprogramming, both of melanoma cells and the surrounding microenvironment, also play important roles in supporting tumor growth in the metastatic niche. Often, the tumor microenvironment is not well vascularized, meaning tumor cells must adapt to low availability of oxygen and nutrients (Ratnikov et al., 2017). One mechanism by which tumor cells support continued growth in hypoxic, or low oxygen conditions, is through the process of glycolysis. While all cells perform glycolysis to convert glucose to pyruvate, non-malignant cells prefer utilizing pyruvate for oxidative phosphorylation via the TCA cycle, while cancer cells preferentially convert pyruvate to lactate in aerobic glycolysis even when abundant oxygen is available. This preference is known as the "Warburg Effect" (Fischer et al., 2017). Glycolytic genes are strongly upregulated during low oxygen, in part through hypoxia-inducible factors (HIFs), which induce a transcriptional program of >70 genes involved in glycolytic metabolism, but also angiogenesis and metastasis (Majmundar et al., 2010). The HIF1α subunit, normally targeted for ubiquitin-mediated degradation in normoxia, is stabilized under low oxygen conditions and free to dimerize with HIF1β to induce hypoxia-responsive genes (Land and Tee, 2007). PI3K/AKT signaling promotes HIF1α stabilization through mTOR (Land and Tee, 2007), and MAPK signaling can also aberrantly increase HIF1α transcription and stabilization (Fischer et al., 2017). The MAPK pathway also promotes glycolysis through a melanocyte specific mechanism; $BRAF^{V600E}$ suppresses melanocyte lineage factor MITF, which directly regulates PGC1α, a critical instigator of oxidative phosphorylation (Haq et al., 2013). By this mechanism, melanoma cells may switch to

oxidative phosphorylation in cases of MAPK pathway inhibition, such as during targeted therapy to promote adaptive resistance (Haq et al., 2014).

Glucose transport, necessary for both glycolysis and oxidative phosphorylation, is enhanced and aberrantly regulated in melanoma. GLUT4 is the primary insulin-responsive glucose transporter in muscle and adipose, while GLUT1 is ubiquitously expressed (von der Crone et al., 2000). Both transporters depend on PI3K/AKT signaling for their translocation to the plasma membrane, and the AKT2 isoform specifically regulates glucose availability and insulin response by controlling GLUT1 and GLUT2 (Cho et al., 2001a; Jensen et al., 2010). GLUT1 upregulation, but not GLUT4, occurs during glucose deprivation and hypoxia (Ratnikov et al., 2017; von der Crone et al., 2000). GLUT1 is expressed at low levels in non-malignant cells, but is drastically upregulated in cancer, including melanomas, where it enhances murine metastasis, and correlates with poor prognosis in melanoma patients (Koch et al., 2015). Studies investigating the regulation of GLUT1 and GLUT4 have shown differential sensitivity to insulin, mediated by AKT2 phosphorylation status; AKT2 phosphorylation at site S474 is required for GLUT1 plasma membrane incorporation, while only T309 phosphorylation is needed for GLUT4 incorporation in murine adipocytes (Beg et al., 2017). Furthermore, this regulation was preserved in hyperproliferative lung cancer cells (Beg et al., 2017), but to date, no studies have examined AKT2 regulation of GLUT1 in melanoma.

In summary, metastatic dissemination of melanoma is supported through a variety of diverse mechanisms involving multiple pathways, including the hypoxia response, metabolism, and phenotypic plasticity. Each of these pathways collaborate to support a

highly metastatic and treatment refractory cancer, necessitating the development of new therapies to prevent dissemination and growth of melanomas at metastatic sites.

1.5 Clinical targeting of melanoma

1.5.1 Targeted Therapy

Before 2011, the standard of care for unresectable metastatic melanoma was chemotherapy, commonly the DNA methylation agent dacarbazine, and the median overall survival was a dismal ~9 months (Luke et al., 2017). In the years since, that there has been a dramatic increase in the number of FDA-approved targeted therapies, as a direct result of understanding molecular disease drivers. When mutations in the BRAF gene were first described as not only common, but frequently a single substitution mutation at codon 600 (Davies et al., 2002), selective inhibitors were developed to target the mutant form, leaving WT BRAF unaffected (Joseph et al., 2010; Tsai et al., 2008). These studies led to the development of the $BRAF^{V600E}$ targeted inhibitor known as Vemurafenib which greatly outperformed dacarbazine in phase 3 trials, and was approved in 2011 as monotherapy for metastatic melanoma (Chapman et al., 2011). A few years later, a second $BRAF^{V600}$ inhibitor, dabrafenib, was approved by the FDA (Hauschild et al., 2012). However, it became clear that targeted inhibition of BRAF was easily circumvented downstream, and targeted inhibition of MEK became a clinical imperative. The MEK inhibitor trametinib was approved first as a monotherapy in 2013, and later as a combination therapy with dabrafenib in 2014, now the standard of care for patients with $BRAF^{V600}$ melanoma (Long et al., 2015). Soon after, the MEK inhibitor Cobimetinib was approved for use in combination with Vemurafenib, after it was found to be superior to Vemurafenib alone (Ascierto et al., 2016). Recently, the novel BRAF inhibitor

Encorafenib has been developed, and is currently in Phase 3 clinical trials (Koelblinger et al., 2018).

While targeted inhibition is superior to conventional chemotherapy, adaptive resistance is nearly guaranteed and limits long term efficacy (Haarberg and Smalley, 2014). Patients receiving vemurafenib often experience substantial regression initially, but develop recurrent aggressive disease, often in the form of refractory brain metastases (Niessner et al., 2013). Further, a majority of patients present with BRAF mutations, but for those with Triple WT tumors lacking definable driver mutations, there are very few therapeutic options. In this case, the use of alterative therapeutic modalities is a necessary supplement to targeted inhibition in the treatment of melanoma.

1.5.2 Immunotherapy

Immunotherapy is a therapeutic option that is not reliant on the presence of defined molecular alterations. The immune system is considered a major barrier to the development of cancer, and avoiding immune destruction is necessary for malignant progression (Hanahan and Weinberg, 2011). Immune checkpoint blockade, the mechanism of approved immunotherapies available today, has achieved unprecedented and durable clinical responses across a spectrum of cancers, and especially in melanoma (Jenkins et al., 2018). Checkpoint inhibitors work by disrupting tumor-associated antigen presentation to T-cells, which would normally inhibit T-cell function and illicit self-tolerance (Pardoll, 2012). Without this T-cell recognition, a tumor can be recognized and destroyed by an amplified immune response.

There are two predominant checkpoint inhibitors approved for use clinically, which regulate different levels of the immune response by different mechanisms (Pardoll,

2012). The first type of checkpoint inhibitor is a PD-1 blocking antibody, of which there are two approved therapies, Pembrolizumab and Nivolumab. Both are antibodies that block the interaction between PD-1, expressed on activated T-cells, and its ligand PDL-1, which can be expressed by tumor cells and inhibits T-cell action when interacting with PD-1 (Pardoll, 2012). Only about 33% of melanoma patients treated with pembrolizumab respond to therapy, but a startling 80% of responders show durable response and disease control for 5-10 years (Jenkins et al., 2018). The other type of checkpoint inhibitor in clinical use are CTLA-4 receptor blocking antibodies. CTL4-4 binding counteracts the stimulatory binding of other receptors, which would otherwise amplify a T-cell response. By blocking CTLA-4, T-cells are stimulated, activated, and amplified in response to a tumor-associated antigen (Pardoll, 2012). Ipilimumab is a CTLA-4 antibody approved for use in melanoma patients as a monotherapy, or in combination with the nivolumab anti-PD-1 antibody. Patients receiving the combination treatment of both PD-1 and CTLA-4 blocking antibodies experience improved outcomes but suffer severe immune-related toxicities.

The complexity of the immune system is not fully understood, but there are many mechanisms of resistance to immune therapies that have been identified. These may include but are not limited to insufficient T-cell generation, restrained T-cell function, and impaired T-cell memory (Jenkins et al., 2018). A deeper understanding of immune cell function, an expanded arsenal of immune stimulating compounds, and novel combinations of targeted and immunomodulatory drugs, may greatly improve response rates and treatment options for melanoma patients.

1.5.3 Targeting the PI3K/AKT Pathway

Inhibitors targeting various effectors in the PI3K/AKT pathway have been developed in the last several years and progressed through clinical trials for the treatment of multiple tumor types, including melanoma. Inhibitors of PI3K and its isoforms, AKT (not isoform-specific), mTORC1, and dual mTORC1/2 inhibitors have all been tested in clinical trials with mixed outcomes (Kwong and Davies, 2013). But to date, the FDA has only approved a handful of compounds, and single agent inhibition has largely been unsuccessful (Jansen et al., 2016). Pathway blockade frequently induces cytostatic effects on tumor cell growth without apoptosis, which suppresses but does not eliminate tumor growth, necessitating additional inhibitors (Okkenhaug et al., 2016).

AKT inhibitors fall into three broad classes: ATP-competitive inhibitors, allosteric inhibitors, and irreversible inhibitors. ATP-competitive inhibitors, as the name suggests, target the ATP-binding pocket to compete for ATP binding necessary for kinase activation, rendering the kinase inactive. However, ATP-binding pockets are similar between kinases and also between AKT isoforms (Figure 1.8), so these drugs tend to have poor selectivity. One notable inhibitor in this class is AZD5363, which progressed into Phase I and II clinical trials (Nitulescu et al., 2015). A second class of AKT inhibitor are the allosteric inhibitors, which target the PH domain. Active AKT undergoes a conformational change that requires the PH domain, and allosteric inhibitors "lock" AKT into the inactive conformation (Wu et al., 2010). As previously mentioned, ATP-binding catalytic domains within many kinases are remarkably similar, therefore allosteric inhibitors, which instead target the PH domain, often purport to be AKT-isoform-specific (Lindsley et al., 2005; Wu et al., 2010). Isoform-specificity is more easily achieved

between AKT1/2 and AKT3 than between AKT1 and AKT2 (See Figure 1.8 for sequence homology), and there are currently no inhibitors that target AKT1 or AKT2 with any specificity that is relevant at doses necessary for kinase inhibition *in vivo*. One well-known and frequently used inhibitor in this class is the Merck compound MK-2206, which progressed to Phase I and II clinical trials, and is currently active in a number of clinical trials for various tumor types including melanoma, both alone or in combination therapies (ClinicalTrials.gov). Other allosteric inhibitors of note are Alkylphospholipids (ALPs). These compounds have long hydrocarbon chains which make them unique in structure to the common multi-ringed compounds characteristic of most allosteric or ATP-competitive inhibitors. These long-chain compounds easily accumulate in cell membranes, and prevent plasma membrane recruitment of the PH domain of AKT, in addition to displacing the natural ligands within the PH domain of AKT (Nitulescu et al., 2015). One such ALP is Ilmofosine, which progressed to Phase I trials but failed due to high off-target gastrointestinal toxicity (Giantonio et al., 2004). The last class of AKT inhibitors are irreversible, inactivating AKT by forming covalent bonds with critical cysteine residues within the PH domain (Weisner et al., 2015).

Thus far, the potential for clinical utility of AKT inhibition has not been realized, for multiple reasons. First, patients have had to discontinue use of AKT inhibitors due to significant toxicities, including skin rashes and hyperglycemia (Jansen et al., 2016). Second, off-target effects due to structural homology with other non-AKT kinase inhibitors is a limitation that has also hampered drug design (Nitulescu et al., 2015). Lastly, feedback inhibition or activation through compensatory signaling mechanisms leads to unwanted effects (Kwong and Davies, 2013). For example, a common

shortcoming of PI3K inhibition is the frequent upregulation of RTKs that activate AKT signaling independent of PI3K (Kwong and Davies, 2013). Currently, there are no approved PI3K/AKT inhibitors for the treatment of melanoma, despite evidence that this approach would by therapeutically beneficial. A more complete understanding of the molecular crosstalk involved, or the isoform-specific effects of AKT in melanoma, may facilitate the development of improved therapeutic strategies targeting this pathway.

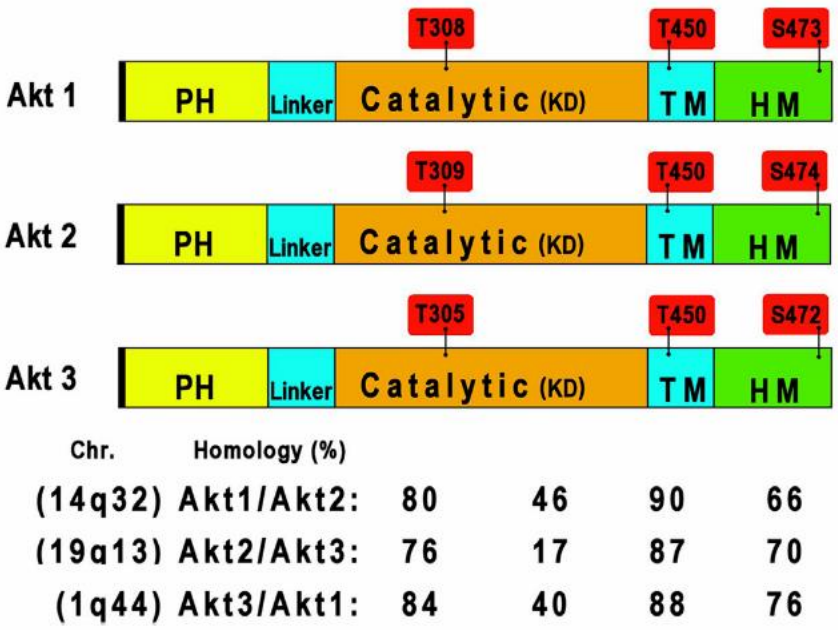

Figure 1.8. AKT isoform structural domains, major phosphorylation sites, and relative sequence homology**.** AKT isoforms are located on different chromosomes but share up to 84% sequence homology. PH=pleckstrin homology, KD= kinase domain, TM=turn motif, HM= hydrophobic motif. Reprinted with permission from (Toker and Marmiroli, 2014).

1.5.4 Co-Targeting the MAPK and AKT pathways in melanoma

Combined pan-AKT/BRAF inhibition has shown demonstrated efficacy in murine melanoma models (Kwong and Davies, 2013). Multiple groups have demonstrated that activation of the PI3K/AKT pathway is an adaptive response to overcome MAPK targeted therapy (Hugo et al., 2015; Perna et al., 2015; Shi et al., 2013). PTEN loss concurrent with oncogenic RAS or $BRAF^{V600E}$ abrogates the effectiveness of MAPK inhibitors (Paraiso et al., 2011; Xing et al., 2011) and consistent with this, co-targeting the MAPK and AKT Pathways delays the onset of drug resistance both *in vitro* and *in vivo* (Deuker et al., 2015; Hugo et al., 2015; Lassen et al., 2014). It has been suggested that isoform-specific targeting of either PI3K or AKT could enhance effective tumor targeting while limiting clinical adverse events (Okkenhaug et al., 2016), but isoform-specific inhibition has not thus far been tested in combination with MAPK inhibition. Further, AKT pathway alterations such as PTEN loss and AKT1/2 mutations occur preferentially in BRAF mutant tumors (Akbani et al., 2015; Haluska et al., 2006; Shain et al., 2015), but this association is not fully understood and has not been exploited therapeutically. Therefore, understanding differential isoform-specific roles of AKT in melanoma is a critical unmet need which may help realize the potential of combined MAPK/AKT inhibition in melanoma.

1.6 Project Rationale

Differential roles for AKT isoforms have been unequivocally demonstrated in other tumor types, but to date, few studies have investigated AKT isoform-specific functions in melanoma. Additionally, the difficulty of targeting AKT for reasons mentioned above highlights the need for identification of new targets and approaches.

The proposed studies sought to characterize how AKT isoforms (AKT1, AKT2, and AKT3) may differentially contribute to distinct stages associated with melanoma transformation, including initiation, progression, and metastasis. In addition, the lack of selective AKT inhibitors, as well as the previous success of immune therapies in melanoma, motivated the testing of novel immune-stimulating small molecules and tumor-targeted AKT inhibitors that have the potential to synergize with existing MAPK inhibitors. I used shRNA knockdown and CRISPR/Cas9 gene editing to deplete each AKT isoform in a variety of human melanoma cell lines and show that the AKT2 isoform is implicated in melanoma cell seeding of the metastatic niche *in vivo* (Chapter 3) and additionally explore possible mechanisms whereby AKT2 may support metastatic tumor growth. Additionally, I show that AKT1 supports cell proliferation and tumor growth *in vitro*, and in collaboration with others, genetically ablated the AKT isoforms in a murine model of melanoma, further supporting the hypothesis that AKT1, but not AKT2, is important for tumor initiation (Chapter 4). Lastly, I test several novel anti-cancer agents that may synergize with MAPK inhibition, using an adapted autochthonous murine melanoma model (Chapter 5). I explore the ability of immune-stimulating small molecules to reduce tumor growth and test a tumor targeted pan-AKT inhibitor. Overall, these studies provide support for the use of AKT inhibition as anti-melanoma therapy,

especially in $BRAF^{V600E}$ positive, metastatic disease. Further investigation into the mechanistic pathways mediating isoform-specific effects will help hone the effectiveness and enhance therapeutic options for this devastating disease.

Chapter 2. Materials and Methods

2.1 In Vitro

2.1.1 Cell Lines/Tissue Culture

SM1 cells were a generous gift of Antoni Ribas (UCLA) and TUMM cell lines were generated as described below (see tumor cell isolation methods). Human melanoma cell lines were generous gifts of Frank Haluska (Tufts Medical Center), and routinely validated for melanocytic identity by RNA or protein expression of MITF-M and pigment enzymes TYR and DCT. Human cells were maintained in DMEM (Invitrogen) with 10% FBS (Atlanta Biologicals) and 1% penicillin/streptomycin (Invitrogen). SM1 and TUMM murine cell lines were cultured in RPMI1640 with 10% FBS and 1% PSF (penicillin/streptomycin/fungizone). Knockdown experiments utilized doxycycline (Sigma) at concentrations of 0.5-1 µg/mL.

2.1.2 Lentiviral Generation of Stable Cell Lines

Validated doxycycline inducible shRNA hairpins in the pLKO tet-on backbone were a generous gift from Alex Toker and Rebecca Chin (Beth Israel Deaconess Medical Center, BIDMC) See (Chin et al., 2014a) for hairpin sequences. A non-targeting hairpin scramble sequence (Sigma) was cloned into the Tet-pLKO-puro backbone, a gift of Dmitri Wiederschain (Wiederschain et al., 2009) as Addgene plasmid #21915. 293T cells were transfected with shRNA constructs and packaging plasmids (psPAX2 and VSV-G) using PEI (polyethylenimine MW25,000, Polysciences). Viral supernatants were collected at 48h and 72h post-transfection and mixed. Stably transduced cell lines were generated by infection overnight in the presence of 8 µg/ml polybrene and selected with 1

µg/mL Puromycin (Gibco) for three days. Cells infected with pLENTI-Luciferase-expressing virus (generous gift of Charlotte Kuperwasser, Tufts University) were selected with neomycin (G418, 500µg/mL, Gibco) for 2-3 weeks.

2.1.3 CRISPR/Cas9 Generation of Stable Cell Lines

AKT sgRNAs were generated using sgRNA Designer (Broad Institute, https://portals.broadinstitute.org/gpp/public/analysis-tools/sgrna-design) or CRISPR Design (Zhang Lab, MIT, http://crispr.mit.edu/) and cloned into the LentiCRISPRV2 expression plasmid (Generous gift of Charlotte Kuperwasser, Tufts University). NT sgRNA sequences are from the GeCKO sgRNA library (Shalem et al., 2014). Virus was produced in 293T cells as described above, and human melanoma cell lines were infected and selected with 1 µg/mL Puromycin (Gibco) for three days. Cells were validated for successful knockout by immunoblotting. See Table 2.1 for sgRNA sequences.

2.1.4 Immunoblot Analysis

Protein pellets were lysed in RIPA buffer (150mM NaCl, 50mM Tris pH 7.4, 1% NP-40, 0.1% SDS, 5mM EDTA, 0.1% sodium deoxycholate, 1mM DTT) supplemented with protease and phosphatase inhibitors (Roche), and then cleared by centrifugation at 4 degrees. Protein concentrations were determined using the DC Protein Assay (BioRad). Equivalent masses of protein were boiled for 5 minutes in 1X Laemmli Buffer prior to resolving using SDS-PAGE. Proteins were transferred onto 0.2µM PVDF membranes (BioRad) for immunoblotting with indicated antibodies (see Table 2.2). Membranes were washed and subsequently incubated with the appropriate horseradish peroxidase-conjugated secondary antibody and visualized using enhanced chemiluminescence (Pierce).

Table 2.1. Guide RNA sequences used for CRISPR/Cas9 cell line generation

Name	**Forward (5'→3')**	**Reverse (5'→3')**
AKT1 (1.2)	CACCGGGCCAAGCCCAAGCACCGCG	AAACCGCGGTGCTTGGGCTTGGCCC
AKT1 (1.4)	CACCGCTGAGACGCCCGGTACATGT	AAACACATGTACCGGGCGTCTCAGC
AKT1 (1.5)	CACCGTGTGCCGCAAAAGGTCTTCA	AAACTGAAGACCTTTTGCGGCACAC
AKT2 (2.5)	CACCGGCCAGCTGATGAAGACCGAG	AAACCTCGGTCTTCATCAGCTGGCC
AKT3 (3.5)	CACCGTAAGGTAAATCCACATCTTG	AAACCAAGATGTGGATTTACCTTAC
AKT3 (3.6)	CACCGAGAATGGACAGAAGCTATCC	AAACGGATAGCTTCTGTCCATTCTC
NT1	CACCGGCGATCGGAGTGCCACGATA	AAACTATCGTGGCACTCCGATCGCC
NT2	CACCGGGGACGCGAAAGAAACCAGT	AAACACTGGTTTCTTTCGCGTCCCC

Table 2.2. Primary antibodies used for immunoblotting, unless an application is otherwise specified

Antibody (Application)	**Cat.No/Company**	**Dilution**
AKT1	2938/Cell Signaling	1:1000
AKT2	5239/Cell Signaling	1:1000
AKT3	8018/Cell Signaling	1:1000
AKT3 (IP)	14293/Cell Signaling	1:50
P-AKT, S473	4060/Cell Signaling	1:2000
P-AKT, T308	13038/Cell Signaling	1:1000
P-AKT1	9018/Cell Signaling	1:1000
P-AKT2	8599/Cell Signaling	1:1000
βACTIN	A-5441/Sigma	1:10,000
HIF1α	610958/BD Biosciences	1:250
PARP	9542/Cell Signaling	1:1000
MITF-M	MS771/Thermo Scientific	1:400
PTEN	9552/Cell Signaling	1:1000
Phospho-Ser/Thr Akt Substrate (IP)	9611/Cell Signaling	1:50
DCT/TRP2	Ab74073/Abcam	1:1000
αTubulin	3873/Cell Signaling	1:5000

2.1.5 Immunoprecipitation

Samples were lysed in RIPA as described, or in CST lysis buffer (Cell Signaling Technologies) and sonicated twice on ice for 15s before protein determination was performed as above. Protein concentrations of lysates were normalized to 1mg/ml and precleared for 1 hour at 4°C with Protein A-conjugated magnetic beads (Pierce). The appropriate antibody or equivalent control IgG was added to the pre-cleared lysate and incubated overnight at 4°C with rotation. After incubation with Protein A beads for 60-90 minutes, antibody/bead complexes were washed 3x prior to elution by boiling in 1X Laemmli buffer. Immunoprecipitated samples were resolved by SDS-PAGE followed by immunoblotting as described above.

2.1.6 Wound Healing/Scratch Assay

Human melanoma cells were passaged into 6-well plates and grown until 80% confluency, and pre-incubated with DMSO- or DOX-containing media for 24h before wounding. Using a ruler as a guide, a wound was made vertically across the growth area using a P1000 pipette tip. The cells were then washed with PBS, and the culture media was replaced with DMEM/0.5%FBS/1% Pen/Strep containing appropriate concentrations of DMSO or DOX as needed. The cells were immediately imaged using an inverted scope at 10x magnification, aligned to a horizontally draw guide perpendicular to the wound, to ensure consistency of wound imaging. 16 hours later, the plates were imaged again, aligning the horizontal guide to the same field of view as the initial image, and visualized again at 10x magnification. Scratch distances were quantified using ImageJ and expressed as percent wound closure relative to DMSO-treated wells.

2.1.7 Migration/Invasion Assays

Cells were pre-incubated with Doxycycline (DOX, 1µg/mL) or DMSO containing media for 24hrs prior to assessment of migration or invasion. For migration, 25,000 cells were seeded in the upper chamber of uncoated porous transwells (8 µm pores, Corning) in serum-free DMEM supplemented with the appropriate concentration of DOX or DMSO. The lower chamber contained media supplemented with 10% FBS as a chemoattractant. After 16h, inserts were washed with PBS and non-migratory cells removed from the upper chamber by scrubbing. Inserts were fixed in ice-cold methanol prior to staining with DAPI. Migration was assessed in triplicate by quantitation of nuclei using fluorescence microscopy. Images were obtained at 20x (6 images per transwell, 3 transwells per condition) and the average number of cells per field was determined using ImageJ software. Invasion assays were performed as described above, substituting GFR Matrigel coated transwells (Corning) and incubated for 36h.

2.1.8 Cell Proliferation Assays

Human melanoma cells were plated in triplicate in 12-well plates (30,000 cells per well) with media containing Doxycycline (1µg/mL) or an equivalent concentration of DMSO, which were refreshed at 48h. Adherent and floating cells were collected, washed in PBS, and stained with 0.4% Trypan blue prior to counting using a TC10 automated Cell Counter (Bio-Rad).

2.1.9 BrdU Incorporation and Flow Cytometry

BrdU (5µg/mL final concentration) was added to cells 1 hour prior to collection. Cells were trypsinized, washed, and fixed with ice-cold 70% ethanol. After fixing, cells

were washed, permeabilized, and stained with FITC anti-BrdU (BD Biosciences) and propidium iodide. Flow cytometric analysis was performed on a FACS Calibur (BD), and data was analyzed using Summit software.

2.1.10 Clonogenicity Assay

Human melanoma cells were trypsinized, counted, and 100-200 cells per well were plated in 6-well plates containing the required amount of media. Once macroscopic colonies developed, cells were washed 1x with PBS, fixed with ice-cold methanol, and stained overnight with 0.05% Crystal Violet (dissolved in PBS). Plates were washed with PBS 3x to remove excess stain, allowed to dry, and colonies were counted by hand.

2.1.11 Anchorage Independent Growth (Soft Agar) Assay

Sterile low melting agarose (SeaPlaque, Lonza) was prepared at 5% stock concentration by dissolving slowly by microwaving and then autoclaving. Next, 6-well plates were coated with 1.5mL of 1% final concentration by diluting in appropriate cell culture medium and allowed to solidify at room temperature for 30 minutes. Next, cells were trypsinized, counted, and 10,000 cells per well were prepared at a final concentration of 0.5% agarose, and allowed to solidify on top of the first layer containing 1% agarose for 30 minutes at room temperature. Next, 0.5mL of media containing 0.5µg/mL of DMSO or Doxycycline is added, and plates are allowed to incubate at 37 degrees for 2-3 weeks, or until macroscopic colonies are visible. Media is refreshed every 2-3 days. Plates were then fixed with 10% neutral buffered formalin and washed 1x with PBS. Colonies were then stained with 0.05% crystal violet overnight and washed with PBS until clear. Images were taken at 10x magnification and quantified using ImageJ.

2.1.12 Metabolite Extraction and Metabolomics

WM1799 cells expressing shNT or shAKT2 hairpins were plated in 10cm dishes at a density of 750,000 cells per dish. The next day, 1µg/mL of doxycycline or equivalent concentration of DMSO was added to existing media. At indicated time points, cells were collected by first washing with PBS, adding 1.5mL ice cold 80% methanol directly to plate, and scraping the cells using a cell scraper in the presence of Chelex-100 beads. Cells and methanol were transferred to a 2mL tube (first extraction), and then the process was repeated for a second extraction, collected in a new tube. Samples were then centrifuged for 1 minute at 14,000rpm using a microcentrifuge and dried using a Speed Vac or stored at -80C. Once dry, first and second extractions were dissolved in 50mM phosphate buffer pH 7.0 with 500µM DSS-6 NMR standard and transferred to glass NMR tubes for analysis by NMR. NMR and subsequent data analysis were performed by Jim Baleja, PhD, at the Tufts University Biological NMR Center.

2.1.13 Seahorse Glycolytic Rate Assay

WM1799 cells were pre-incubated with DMSO/DOX for 48hrs, and 21,000 cells were seeded into microtiter plates (Agilent) one day prior to assay. One hour prior to assay, cells were washed and incubated with RPMI at pH 7.4 (Agilent) and placed in a non-CO_2 incubator. Assays were performed using a Seahorse XFe96 Analyzer and standard GRA assay settings, including recommended concentrations of drug as supplied by the GRA Flux Pack (mini). Analysis was performed using Excel macros supplied by Wave Software 2.4.0.

2.1.14 Simulation of Hypoxia

Cobalt Chloride (Sigma) was prepared as a 25mM stock dH2O and sterile filtered using a 0.22µM syringe. Human melanoma cells at 50% confluence were treated at a final concentration of 100µM for 4, 8, or 24 hours. Residual culture media containing floating cells in addition to cellular protein was then collected for immunoblotting.

2.1.15 Quantitative RT-PCR

Cells were lysed in TRIzol (Invitrogen) and RNA isolated by phenol-chloroform extraction with lithium chloride precipitation. cDNA synthesis was performed using SMARTScribe™ Reverse Transcriptase (Takara, Inc) and qPCR was performed on a CFX96 real-time thermal cycler (Bio-Rad). See Table 2.3 for primer sequences.

Table 2.3. Primer Sequences used for RT-qPCR

Name	**Forward (5'→3')**	**Reverse (5'→3')**
CDH1	GAACGCATTGCCACATACAC	GAATTCGGGCTTGTTGTCAT
MITF-M	CATTGTTATGCTGGAAATGCTAGAA	GGCTTGCTGTATGTGGTACTTGG
MMP2	CCGTCGCCCATCATCAAGTT	CTGTCTGGGGCAGTCCAAAG
NFIB	CTCTGCATCTCCACAGGATTC	GATAGCTTGTGTTGGAAATGGC
SNAIL	CACTATGCCGCGCTCTTT	GGTCGTAGGGCTGCTGGAA
TEAD2	CTCACTCCGTAGAAGCCACC	TGCCTTCTTCCTGGTCAAGT
TEAD3	GCACCTTCTTCCGAGCTAGA	TACGGCCGAATGAGTTGATT
TYR	ATTCCATATTGGGACTGGCGGGAT	TCGGCTACAGACAATCTGCCAAGA
TRP1	CCAGTCACCAACACAGAAATG	GTGCAACCAGTAACAAAGCG

TRP2	CCAATGATCCCATTTTTGTG	AGGCATCTGCAGGAGGATTA
TBP	GAGCCAAGAGTGAAGAACAGTC	GCTCCCCACCATATTCTGAATCT
ZEB1	GCACCTGAAGAGGACCAGAG	TGCATCTGGTGTTCCATTTT

2.1.16 Statistical Analysis

Statistics were performed using GraphPad Prism 5.02, utilizing Student's unpaired T-Test or One Way-ANOVA with Tukey post-test, as indicated. Significant p-values are listed, or noted as *P<0.05, **P<0.01, or ***P<0.001. Error bars represent standard error means, and P-values <0.05 were considered significant.

2.2 In Vivo

2.2.1 Mouse Strains

All mice were maintained in a heat- and humidity-controlled, AAALAC-accredited vivarium operating under a standard light-dark cycle. All protocols have been approved by the Institutional Care and Use Committee (IUCUC) at Tufts University School of Medicine, where mice were housed, and experiments were conducted. $BRAF^{V600E}$; $Arf^{-/-}$, $BRAF^{V600E}$; $Arf^{-/-}$; $Akt1^{-/-}$, $BRAF^{V600E}$; $Arf^{-/-}$; $Akt2^{-/-}$, $BRAF^{V600E}$;$Arf^{-/-}$ $Akt3^{-/-}$, C57BL6/H, and $Rag2^{-/-}$ mice were bred in house. NOD/SCID and C57Bl6/J mice were purchased from the Jackson Laboratory (Bar Harbor, ME). Primers used for genotyping purposes are listed in Table 2.4.

2.2.2 Tumor Cell Isolation and Tissue Preparation

Tumors were minced and digested with 3 mg/ml collagenase and 250 U/ml hyaluronidase for 2-4 hours at 37°C. Contaminating red blood cells were lysed with RBC Lysis Buffer (Sigma), and organoids were triturated using an 18G syringe needle, incubated in 0.05% Trypsin/0.53mM EDTA, and passed through a 40µm cell strainer. Cells were maintained in RPMI1640/10% FBS/1% penicillin/streptomycin/fungizone, and cell line genotypes are listed in Table 2.5.

2.2.3 UV Irradiation

Pups were collected at PND 3.5 and placed individually in sterilized 6-well plates at a standardized distance under a UV-B lamp. Mice were then irradiated in the presence of a dosimeter until a dose of 750mJ/cm^2 was administered, approximately 10-15 minutes of irradiation. Pups were then returned to their home cage and observed for the presence of tumors within 2-3 months.

2.2.4 Allografts

Allograft studies utilized C57BL6/J mice were maintained with approval of the Tufts University Institutional Animal Care and Use Committee. Mouse melanoma cells ($2x10^6$) were injected subcutaneously into the hind flank of 6-10-week-old male mice. Once tumors were palpable, tumor growth was measured with digital calipers every 2-3 days and tumor volume was calculated using the following formula: $[(\pi/6)*L*W^2)]/2$. Mice were sacrificed when tumor volume reached 1.5cm^3 or tumors measured 2cm in any single direction.

Table 2.4. Murine genotyping primer sequences

Primer Name	**Sequence (5'→3')**
Rag2 A	GGGAGGACACTCACTTGCCAG
Rag2 B	AGTCAGGAGTCTCCATCTCAC
Rag2 NEO	CGGCCGGAGAACCTGCGTGCAA
BRAF RTU1 F	GTGGATGGCACCAGAAGTC
BRAF RTL1 R	GAAACCAGCCCGATTCAAGGA
AKT1 flox 1	CCTGTGGCCTTCTCTTTCACC
AKT1 flox 2	GCTGTTGGCTAACTTGGAGGAAGC
AKT2 1	TACACTTCATTCTCAGTATTGTTTTGC
AKT2 2	TGGACAATCTGTCTTCATGCCAC
AKT2 3	ACCAACCCCCTTTCAGCACTTG
ARF 1	ACCACACTGCTCGACATTGGG
ARF 2	AGTACAGCAGCGGGAGCATGG
ARF 3	TTGAGGAGGACCGTGAAGCCG

Table 2.5. Murine cell lines with known genetic alterations

Cell Line	$BRAF^{V600E}$	INK4A	ARF	Notes
SM1	+	WT	WT	Generous gift From Toni Ribas
SM1-750	+	WT	WT	SM1 cells passaged in BL6 mice and infected with pLENTI-luciferase
TUMM4218	+	-/-	-/-	
TUMM4228	+	WT	-/-	
TUMM4246	+	WT	-/-	
TUMM8253	+	WT	-/-	Mouse received UV irradiation at PND 3.5

2.2.5 Xenografts

Male NOD/SCID mice (Jackson Labs, 6-10 weeks old) were injected subcutaneously with 2 million human melanoma cells according to approved protocols. Once palpable, tumors were measured 3x weekly using calipers and volume was calculated using the formula $[(\pi/6)*L*W^2)]/2$ until a limit of $1500mm^3$ or 2cm in any single direction was reached. Doxycycline chow (200mg/kg, Teklad) was introduced when tumors were palpable.

2.2.6 Luciferase Imaging

Mice were anaesthetized with isofluorane and injected intraperitoneally 10µl/g body weight of Luciferin (Fisher/GoldBio) 5 minutes prior to imaging. Imaging was performed using an IVIS SpectrumCT in vivo imaging system using Living Image® Software.

2.2.7 Metastasis Assays

Human ($1x10^6$) or mouse melanoma cells ($0.5x10^6$) were injected into the tail vein of NOD/SCID or C57Bl6/J mice, respectively, using a 27G 1cc luer-lock syringe. Mice were maintained on regular or doxycycline chow (200mg/kg, Teklad) and imaged weekly until euthanasia.

2.2.8 Immunohistochemistry

Formalin-fixed paraffin embedded tissue sections were deparaffinized and hydrated prior to staining with hematoxylin and eosin according to standard procedures.

2.2.9 Drug Dosing

Vemurafenib (Selleck Chemicals) was resuspended in DMSO to 50mM and diluted in sterile PBS to the desired mg/kg dose before intraperitoneal (IP) injection once daily unless otherwise indicated. MK-2206 (Selleck Chemicals), or its derivative compound ARI-5173 was resuspended in 15% Captisol and given orally by gavage at the indicated times. ARI compounds were generous gifts from the Bachovchin Laboratory (Tufts University School of Medicine) where they were synthesized in house. ARI-4175 and ARI-4268 were resuspended to stock concentrations of 20 mg/mL using sterile acidified (pH 2) water, further diluted to indicated µg/mouse doses, and administered orally by gavage once per day for five consecutive days, then given a two-day drug holiday. This 5 day on, 2-day off schedule was repeated as necessary.

2.2.10 Statistical Analysis

Statistics were performed using GraphPad Prism 5.02, utilizing Student's unpaired T-Test, One Way-ANOVA with Tukey post-test, Two-Way ANOVA, or

Kaplan Meyer Survival analysis as indicated. Significant p-values are listed, or noted as *P<0.05, **P<0.01, or ***P<0.001. Error bars represent standard error means, and P-values <0.05 were considered significant.

Chapter 3. AKT2 loss impairs BRAF mutant melanoma metastasis

3.1 Introduction

The PI3K/AKT pathway is the second most frequently altered pathway in melanoma (Hayward et al., 2017), but the underlying mechanisms that favor malignant transformation or metastasis remain obscure. PI3K pathway alterations like PTEN loss are associated with increased invasiveness and occur preferentially in BRAF mutant tumors (Shain et al., 2015). However, few studies have investigated how hyperactive AKT, and specifically the AKT isoforms, contribute to melanoma progression or metastasis. Given that AKT isoforms are known to functionally differ in their promotion of cancer-associated phenotypes like cell growth and metastasis (Gonzalez and McGraw, 2009), understanding differential roles the isoforms may play in melanoma is of clear utility when designing strategic therapeutic interventions.

Based on studies of both melanoma and non-melanoma tumor types, AKT2 is an attractive candidate. AKT2 is highly amplified in prostate cancer, and PTEN-null prostate tumors require AKT2 for maintenance and survival (Chin et al., 2014b). AKT2 is also required for invasive migration of PTEN-deficient glioblastoma (Zhang et al., 2009) in which AKT2 knockdown (KD) also attenuates chemoresistance (Cui et al., 2015; Cui et al., 2012). AKT2 synergizes with PTEN loss to promote metastasis in late-stage colorectal cancer (Rychahou et al., 2008), and AKT2 amplification was identified in a ductal carcinoma brain metastasis not present in the matched primary tumor sample (Brastianos et al., 2015), suggesting AKT2 aided metastatic disease. There is also specific rationale to target AKT2 in the BRAF mutant melanoma subtype, compared to other melanoma subtypes. It was found that AKT2 is preferentially activated in PTEN-null,

RAS-driven tumors, where it promotes an invasive phenotype (Nogueira et al., 2010), and PTEN loss is most common in the BRAF mutant melanoma subtype (Akbani et al., 2015). Additionally, a recent publication specifically implicated AKT2 in promoting melanoma metastasis through the suppression of PHLPP activity (Yu et al., 2018), a study which directly supports the data herein. AKT2 is widely implicated as a key regulator of tumor cell invasion and metastasis (Cheng et al., 2007; Liu et al., 2014; Rychahou et al., 2008; Sheng et al., 2015) and given the importance of end stage disease to clinical prognosis, an in-depth understanding of the mechanisms promoting melanoma metastasis and therefore a role for AKT2 in this process is of critical importance.

3.2 Results

3.2.1 AKT2 promotes melanoma cell migration, invasion, and EMT

Metastasis is responsible for the vast majority of melanoma mortality; therefore, we first endeavored to assess possible contributions of AKT isoforms to cell behaviors associated with cell migration and invasion, two critical early steps in the process of metastasis. To model AKT isoform depletion *in vitro*, we took advantage of a panel of human metastatic melanoma cell lines harboring the common driver mutation $BRAF^{V600E}$ and in which all three AKTs were phosphorylated due to PTEN loss (Figure 3.1, WM1799, UACC903, 1205LU, WM1158, and WM455). We infected the indicated cell lines with lentivirus expressing validated, doxycycline-inducible shRNA hairpins to AKT1, AKT2, or AKT3, or a non-targeting hairpin (shNT). Reproducible knockdown (KD) efficiency was ~50% for AKT1/3, and greater than 80% for AKT2 in each cell line tested, and the representative cell line WM1799 is shown as an example after 72 hours of incubation in DMSO- or Doxycycline (DOX)-containing media (Figure 3.2A). WM1799

was chosen as a representative cell line for downstream assays, but when possible, *in vitro* results were reproduced in additional melanoma cell lines to ensure generalizable conclusions but are omitted for brevity.

First, we assessed the contribution of AKTs to cell migration using a wound-healing assay. A scratch was made across a confluent cell monolayer using a pipette tip, and the resulting wound was visualized at 0h or 16h under low serum conditions. AKT2 depletion delayed wound closure in WM1799 human melanoma cells *in vitro* (Figure 3.2B) and in UACC903 and WM455 cells (data not shown) while AKT1 or AKT3 depletion had no effect.

We next assessed cell migration using a transwell assay, in which we added WM1799 cells to the upper chamber of a porous transwell in serum-free medium containing DMSO or DOX, and 16-24 hours later removed cells from the upper chamber and visualized the number of cells that migrated to the underside of the transwell membrane. AKT2 KD again reduced cell migration in response to a serum gradient in WM1799 cells (Figure 3.2C), and also in cell lines UACC903 and WM455 (data not shown).

Further, we hypothesized that AKT2 depletion would also reduce cellular invasion. To test this, we added cells to the upper chamber of porous membrane additionally coated with a Matrigel layer and incubated for 36h in serum free conditions as described above. Invasion through Matrigel was impaired by AKT2 depletion in WM1799 (Figure 3.2D), UACC903, and WM455 human melanoma cell lines (data not shown), consistent with its effects on cellular migration.

A.

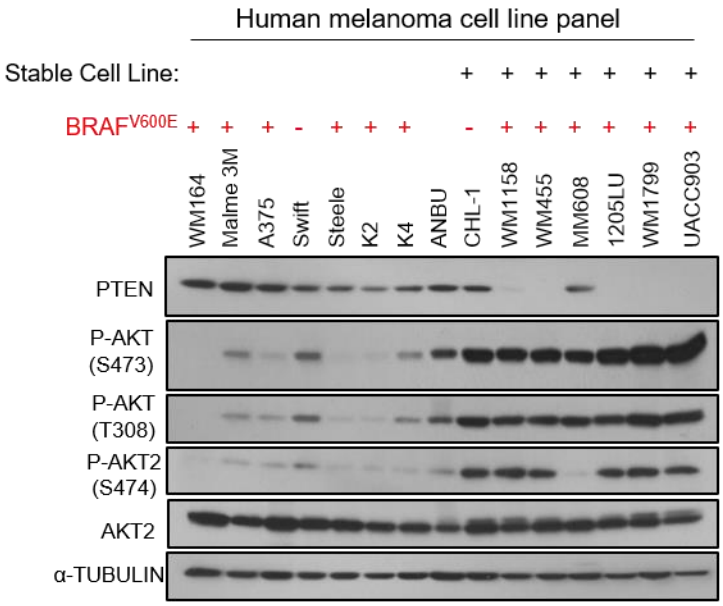

B.

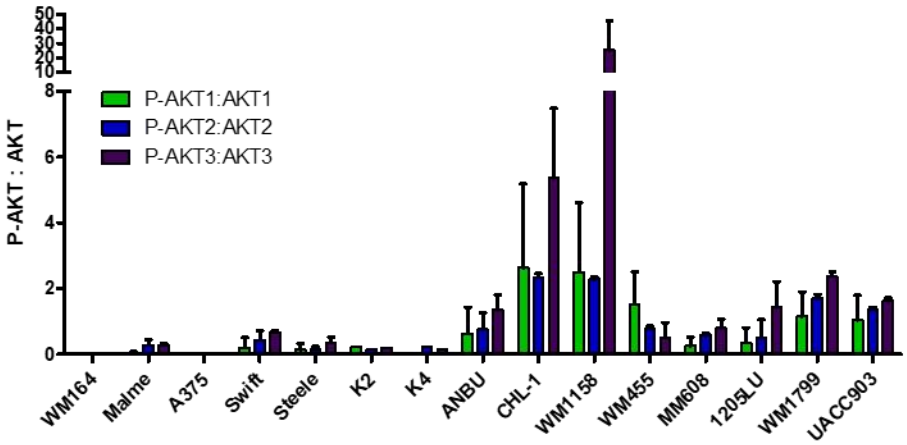

Low/ No P-AKT	pAKT1 only	pAKT2 only	pAKT3 only
WM164 A375	---	---	---

pAKT1 +pAKT2	pAKT2+pAKT3	pAKT1+pAKT2 +pAKT3	
---	Malme Swift Steele K4 MM608	K2 1205LU WM1799 UACC903	WM455 ANBU CHL-1 WM1158

Figure 3.1. AKT phosphorylation in a panel of metastatic human melanoma cell lines. A) Immunoblotting of total and AKT2 phosphorylation in a panel of human melanoma cell lines. B) Quantitation of immunoblotting by ImageJ for AKT isoform-specific phosphorylation across the panel of melanoma cell lines. Phospho-specific antibodies to were utilized to determine proportion of P-AKT1/2 protein to total AKT1/2 protein. For AKT3 specific phosphorylation, AKT3 was immunoprecipitated from total protein, and blotted for S472 phosphorylation. Similar results were obtained when P-AKT (S473) was immunoprecipitated and blotted for AKT3. (C) represents the aggregation of three independent experiments.

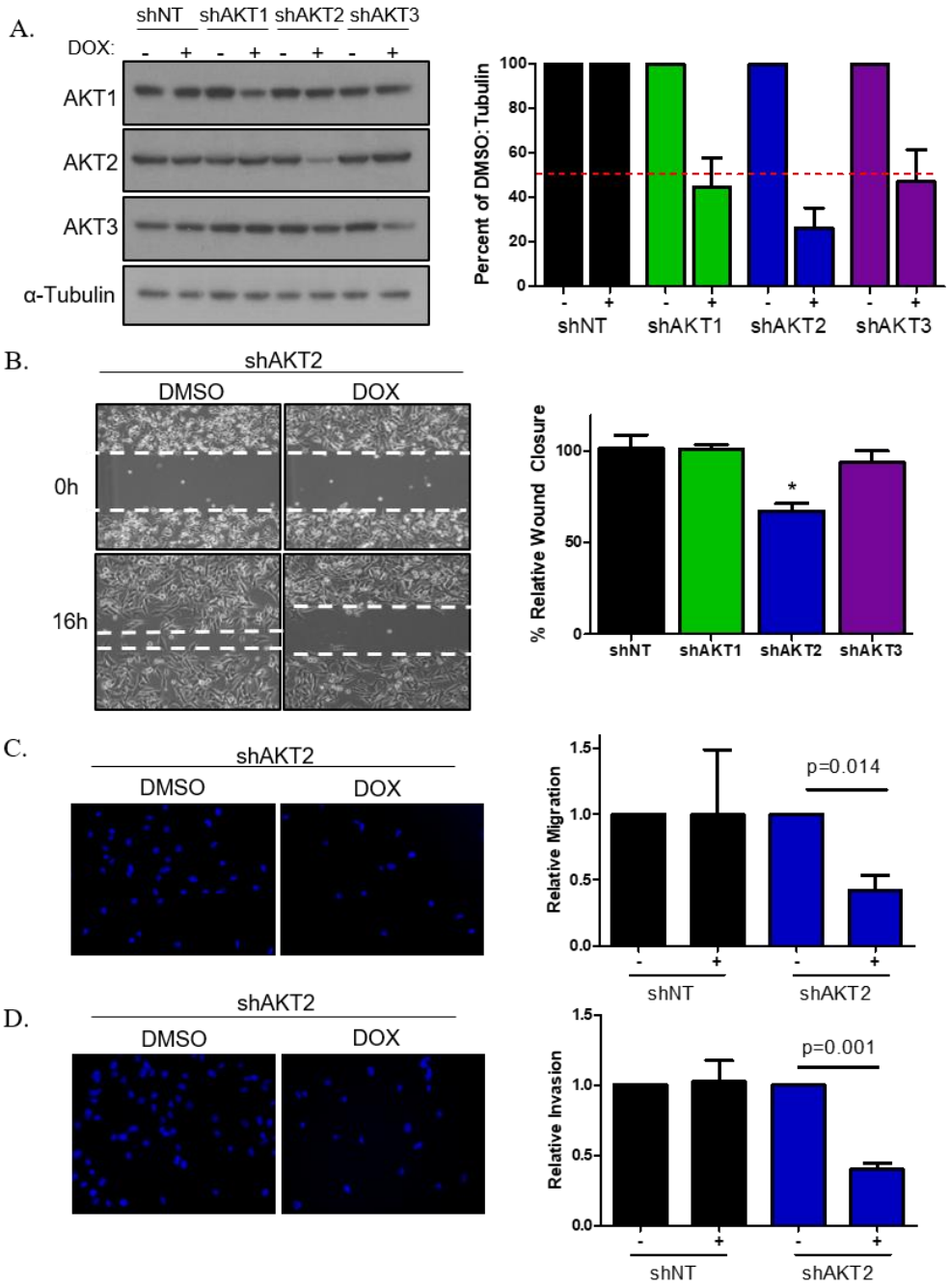

Figure 3.2. AKT2 promotes migration and invasion *in vitro*. A) Representative immunoblot showing AKT-isoform KD using doxycycline-inducible hairpins (left) with quantification of KD across three independent experiments using ImageJ (right). B) Representative image of a wound healing assay in AKT2 KD cells (left) with quantification of wound closure by ImageJ (n=3, right). C) Representative image of the underside of a transwell (left). Quantification of relative migration using ImageJ (n=3, right). D) Representative image of the underside of a Matrigel coated transwell (left) with quantification of relative invasion from (n=3, right). Relative migration/invasion refers to the number of cells/field normalized to the DMSO-treated control condition. Images at 20x magnification.

To extend our characterization and further investigate a potential role for AKT2 in cellular phenotypes pertinent to metastasis, we determined AKT2's role in anchorage-independent growth. WM1799 shAKT2 cells were seeded in soft agar, overlaid with either DMSO- or doxycycline-containing media to induce AKT2 KD. We observed that AKT2 KD reduced total colony number without significantly affecting colony size (Figure 3.3A). Such impairment in anchorage-independence might predict a requirement for AKT2 in modulating tumor growth *in vivo.* Therefore, we next assessed the ability of cells to grow subcutaneously in NOD/SCID mice, allowing palpable tumors to form before transitioning a subset of mice to doxycycline chow to induce AKT2 KD. We observed that AKT2 KD delayed tumor growth relative to control mice fed regular chow (Figure 3.3B), but tumors eventually reached similar endpoints in both groups, despite persistent AKT2 KD (Figure 3.3C). Analysis of tumor lysates at this endpoint by immunoblotting showed that AKT1 protein levels and phosphorylation were increased in mice fed doxycycline chow, compared to regular chow fed mice, suggesting possible AKT-isoform compensation is occurring as a means to support renewed or continued tumor growth (Figure 3.3D).

To rule out that the cellular phenotypes we observed were not due to a defect in cell growth, we also tested the effect of AKT2 KD on cell proliferation. First, cells were seeded in triplicate in 12-well plates and incubated with DMSO- or DOX-containing media. Cells were trypsinized and counted daily over a period of four days, and trypan blue exclusion was used to assess viability. We observed that AKT2 KD had no effect on overall cell growth or viability in 2D culture in a variety of cell lines including WM1799 (Figure 3.4A-D). As an additional assessment, we performed BrdU incorporation and

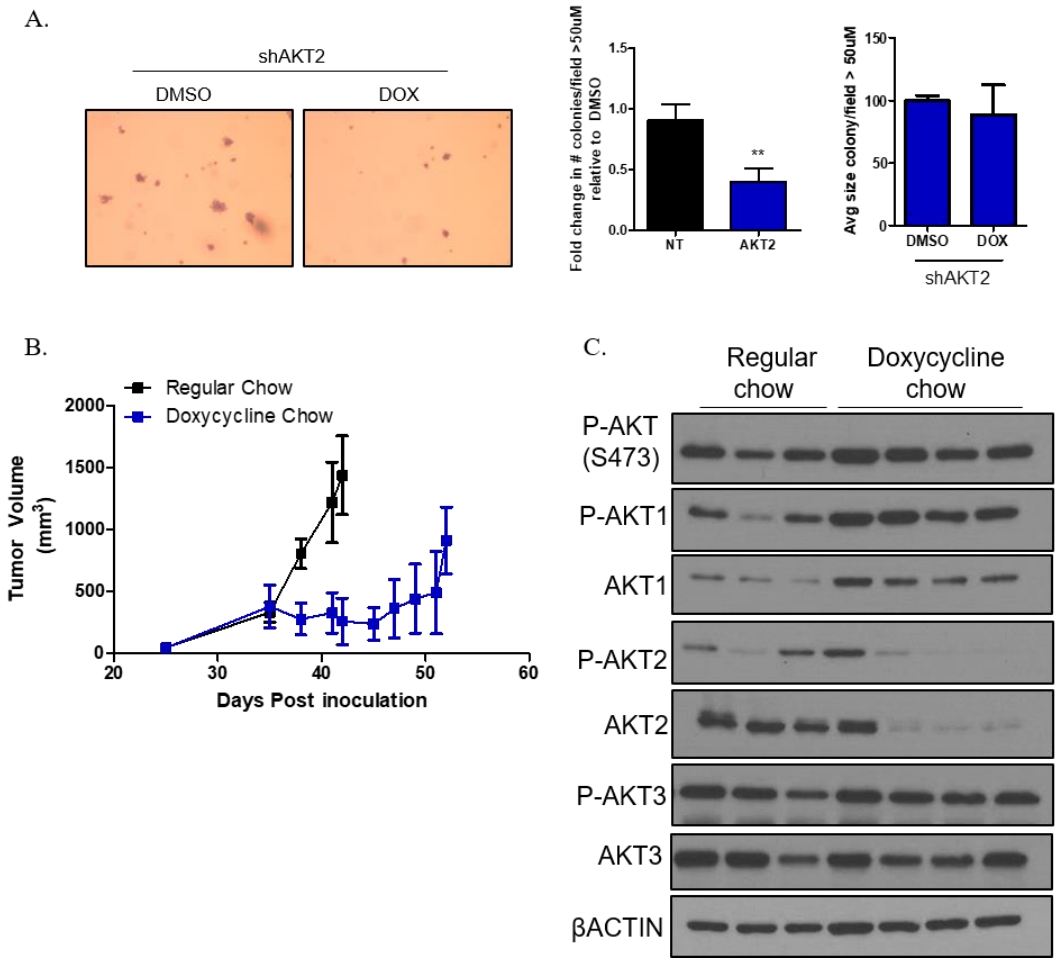

Figure 3.3 AKT2 depletion reduces anchorage independent growth *in vitro* and tumor growth *in vivo*. A) 10,000 WM1799 shAKT2 cells per well were seeded in 0.5% soft agar on a 1% agar layer in the presence of DMSO- or DOX-containing media for 3 weeks. Once macroscopic colonies were visible in DMSO-treated wells, cells were fixed using 10% neutral buffered formalin and stained with 0.005% crystal violet overnight (n=3, left) and colony number and size were quantified using ImageJ (right). Representative images from three independent experiments. B) NOD/SCID mice were injected subcutaneously with two million WM1799 shAKT2 cells and allowed to form palpable tumors before a subset of mice were switched to DOX-containing chow, and tumor size was measured using calipers (n=3-4 mice per group, *P=0.0483). Similar results were obtained in two independent experiments. C) Resulting tumors from (B) were collected at humane endpoints and analyzed by immunoblotting for AKT-isoform KD.

assessed cell cycle progression by propidium iodide staining after incubation for 96 hours in DMSO- or DOX-containing media, and again we did not observe a defect with AKT2 KD (Figure 3.4C-D).

Thus far, the phenotypes we observe as a result of AKT2 KD in human melanoma cells suggest that AKT2 contributes significantly to cellular migration, invasion, and anoikis avoidance, all properties of the epithelial-mesenchymal transition (EMT) (Lambert et al., 2017). We therefore interrogated the impact of AKT2 depletion on expression of EMT-associated genes. AKT2 KD reduced expression of pro-metastatic transcription factors ZEB1 and Snail, and the matrix-remodeling enzyme MMP2, concomitant with increased E-cadherin expression Figure 3.5A. These changes were specific to AKT2 depletion, as neither AKT1 nor AKT3 KD displayed consistent changes associated with EMT modulation (Figure 3.5A).

Additionally, we investigated whether AKT2 could modulate invasion-associated genes previously implicated in melanoma metastasis. AKT2 KD reduced expression of TEAD2 and TEAD3 (Figure 3.5A), as well as the melanocyte master regulator MITF- and epithelial-melanocyte stem cell regulator NFIB (Figure 3.5B). We previously established that WM1799 is $MITF^{lo}$ (data not shown) and therefore a reduction in MITF levels is predicted to inhibit invasion (reviewed in (Arozarena and Wellbrock, 2017). Consistent with reduced MITF-M protein levels (Figure 3.5C), AKT2 KD reduced expression of MITF target genes Tyrosinase (TYR) and Dopachrome Tautomerase (DCT, Figure 3.5B). Because MITF is maintained at very low levels in WM1799 cells, likely due to suppression by the MAPK pathway, it is known that MAPK inhibition, such as therapeutic treatment with the BRAF inhibitor Vemurafenib, reverses MITF suppression

and increases a differentiation program in melanoma (Haq et al., 2013; Joseph et al., 2010). To test the extent to which AKT2 depletion is able to inhibit melanocyte differentiation genes, we treated WM1799 cells with Vemurafenib to de-repress MITF and its target genes. We simultaneously inhibited AKT1, AKT2, or AKT3, and interrogated protein expression of the MITF-regulated pigment gene DCT, in addition to investigating AKT and MAPK signaling (Figure 3.5D). We observed that upon Vemurafenib treatment, DCT is dramatically upregulated, as expected, and consistent with MAPK inhibition, downstream ERK phosphorylation is suppressed. In addition, AKT2 depletion, but not AKT1 or AKT3, strongly inhibited the induction of DCT by Vemurafenib treatment (Figure 3.5D). The de-repression of MITF enhances melanocyte differentiation genes such that cellular morphology of melanoma cells undergoes a phenotypic switch, becoming reminiscent of primary, differentiated melanocytes with enhanced spindle-like cellular projections. AKT2 depletion was sufficient to blunt this morphological change, consistent with a potential role for AKT2 in suppressing a melanocyte differentiation program (Figure 3.5E).

Taken together, AKT2 depletion does not affect 2D growth, but may be promoting migratory and invasive behaviors in human melanoma cells by regulating an EMT-associated transcriptional program, which includes the suppression of a melanocyte-specific differentiation program.

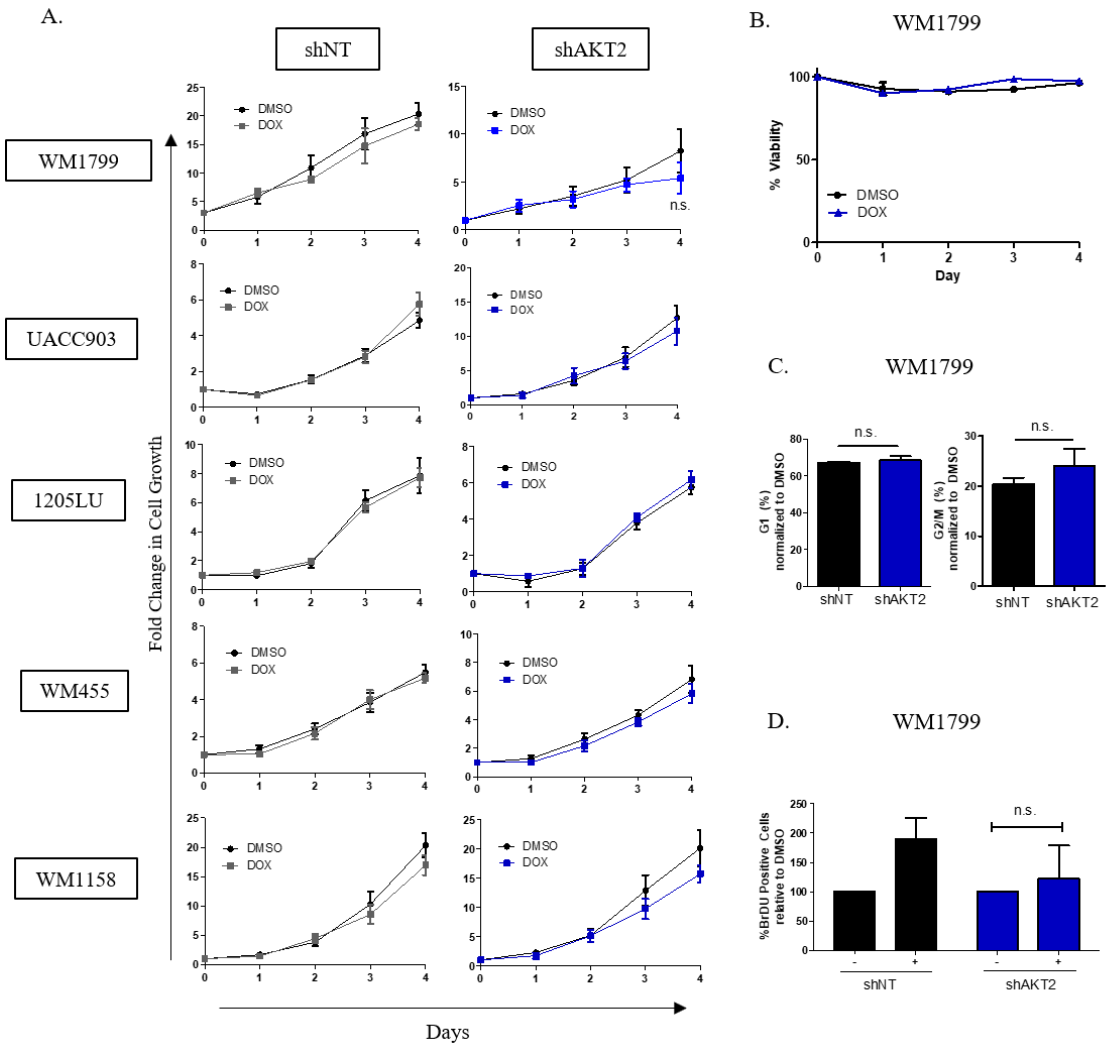

Figure 3.4. AKT2 is not required for cell proliferation *in vitro*. A) 30,000 human melanoma cells expressing DOX-inducible hairpins to shNT or shAKT2 were seeded in 12-well plates, then trypsinized and counted over a four-day period in the presence of DMSO- or DOX-containing media. Error bars represent SEM from two independent experiments, each performed in technical triplicate. B) Cell viability was assessed by trypan blue exclusion in WM1799 shAKT2 expressing cells from (A). C) Cell cycle analysis of WM1799 shAKT2 cells after 96h of DMSO or DOX treatment. Cells were fixed with ethanol, washed, and stained with propidium iodide 40 minutes prior to flow cytometry analysis. D) BrdU incorporation of WM1799 cells after 96h of DMSO or DOX treatment. BrdU was pulsed for one hour prior to fixation and preparation as in (C) for flow cytometry. Error bars are SEM of three independent experiments.

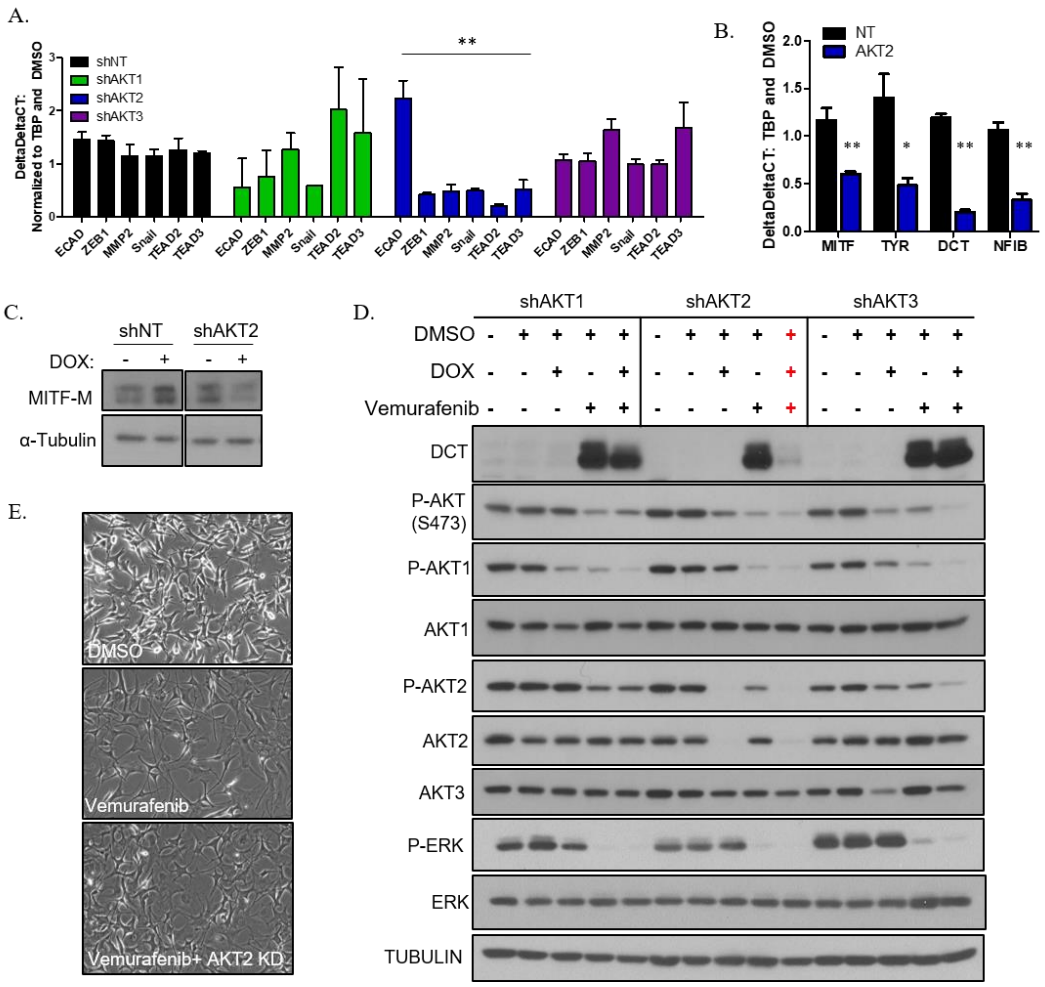

Figure 3.5. AKT2 depletion modulates EMT-associated transcription and suppresses a melanocyte differentiation program. A) RT-qPCR of EMT-TF's and invasion associated genes in WM1799 cells expressing shNT, shAKT1, shAKT2, or shAKT3 DOX-inducible hairpins. SEM from three independent experiments. B) RT-qPCR of melanocyte differentiation genes microthalmia transcription factor (MITF), Tyrosinase (TYR), Dopachrome Tautomerase (DCT), and Nuclear Factor 1B (NFIB). SEM from three independent experiments. C) MITF-M protein levels were assessed by immunoblotting in WM1799 cells expressing shNT or shAKT2 hairpins after 72h of DMSO or DOX treatment. D) WM1799 cells expressing doxycycline-inducible hairpins to AKT1, AKT2, or AKT3 were treated with DMSO, 1µg/mL Doxycycline (DOX), or 1 µM Vemurafenib for 72 hours, and DCT levels, AKT and MAPK signaling was assessed by immunoblotting. E) Representative images of cells from (D) at 20x magnification show cellular morphology differences after 72h of indicated drug treatment.

3.2.2 Prophylactic AKT2 depletion prevents metastatic cell seeding

In many tumors, EMT is essential for the early stages of metastatic dissemination, including intravasation and colonization of distant sites. To test whether AKT2 affects metastatic seeding, the WM1799 AKT2 KD cell line was engineered to express luciferase and cultured in DMSO- or doxycycline-containing media for 72h to prophylactically deplete AKT2. DMSO-treated cells were injected via the tail vein of NOD/SCID mice fed regular chow, while doxycycline-treated cells were similarly injected into mice fed doxycycline chow (Figure 3.6A). Mice maintained on regular chow displayed luminescent tumor nodules within 3 weeks, which progressed to advanced metastatic disease by 6 weeks (Figure 3.6B-C). Control mice developed numerous metastases at distant sites, consistent with lymphatic dissemination (under the forelimbs, head and neck, and lining the mesentery). In contrast to control mice, mice that received AKT2 KD cells and doxycycline chow remained healthy, with no detectable metastases by 6 weeks (Figure 3.6B-C). Additionally, none of the mice injected with AKT2 KD cells and fed doxycycline chow developed detectable metastasis, even at 12 weeks (Figure 3.6D-E). This finding suggests that AKT2 is required for metastatic seeding but does not distinguish whether AKT2 KD cells were eliminated from circulation or were simply latent in mice fed doxycycline chow. To address this question, we asked if tumors would emerge after doxycycline chow removal. A subset of mice injected with WM1799 AKT2 KD cells and fed doxycycline chow were switched to regular chow after the first 6 weeks, at which time they did not have detectable metastases. Mice were monitored weekly, and after an additional 6 weeks, none of the mice removed from doxycycline chow developed metastases (Figure 3.6F-G). These results suggest that initial lack of tumors in AKT2 KD

mice was unlikely due to dormant tumor cells. Rather, that AKT2 depletion may impair the ability of cell to survive in circulation, the seeding of invasive cells in the metastatic niche, or both processes together.

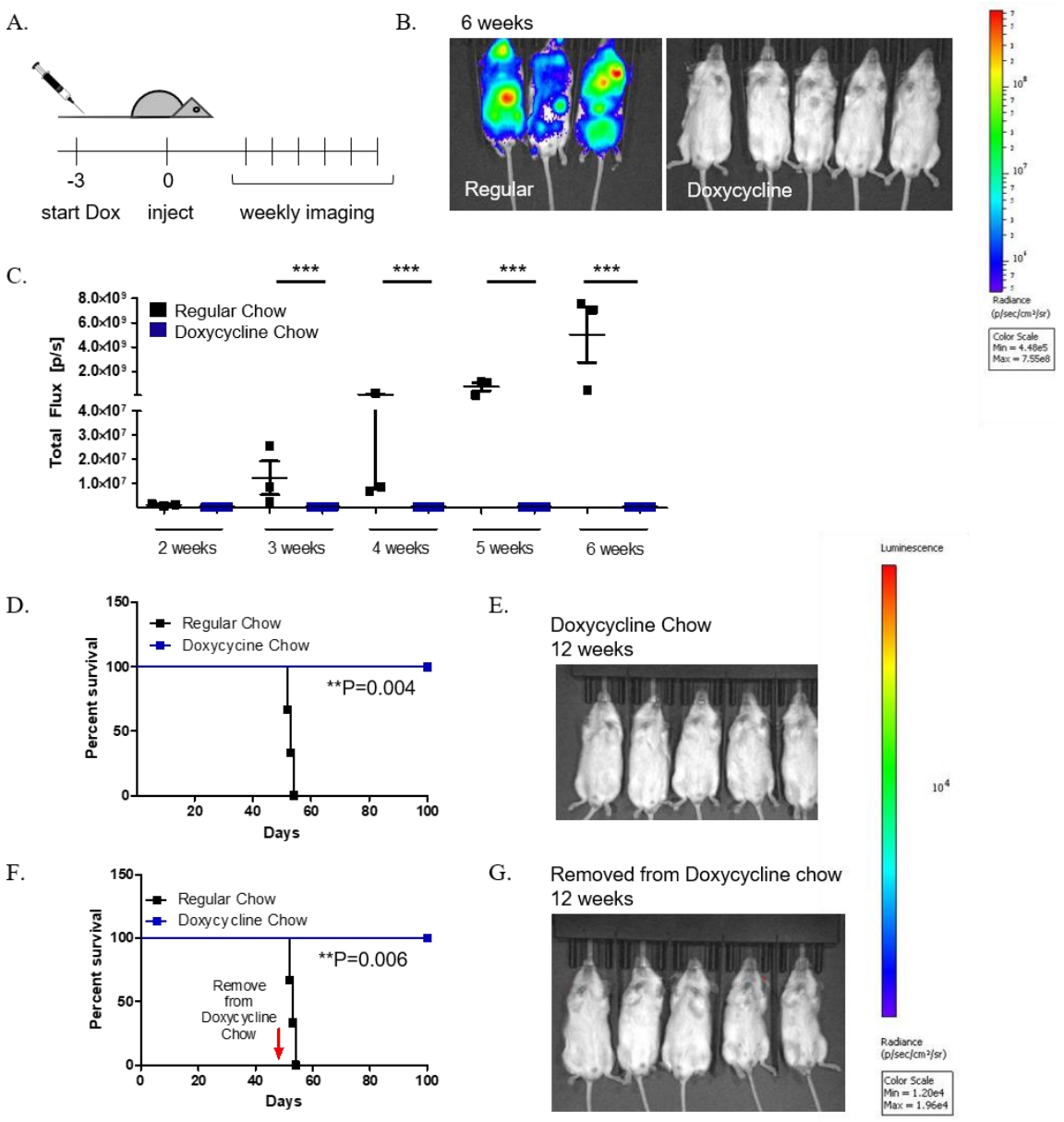

Figure 3.6. Prophylactic AKT2 depletion prevents metastatic disease. A) Experimental schematic of AKT2 depletion three days prior to tail vein injection of luciferized WM1799 cells expressing doxycycline inducible hairpins to AKT2. B) Intravital imaging at 6 weeks post-injection of NOD/SCID mice fed regular or doxycycline chow, that likewise received AKT2-expressing or AKT2-depleted cells, respectively. C) Quantification of luminescence over time in regular or doxycycline chow fed mice. D) Kaplan-Meyer survival curve of mice fed regular or doxycycline chow. E) Intravital imaging at 12 weeks post-injection of NOD/SCID mice fed doxycycline chow. F) Kaplan-Meyer survival curve of mice initially injected with AKT2-depleted cells and then removed from doxycycline chow after 6 weeks, compared to the same regular chow fed mice as in (D). G) 12-week intravital imaging of mice removed from doxycycline chow at 6-weeks post-injection. Statistics using Mantel-Cox or Gehan-Breslow-Wilcoxon Test.

3.2.3 AKT2 depletion delays metastatic onset and extends survival of melanoma-bearing mice

To determine whether AKT2 is important for growth or survival in the metastatic site in addition to metastatic cell seeding, we performed a tail vein assay in which untreated melanoma cells were allowed to seed the lungs, then followed by AKT2 depletion one day later through the introduction of doxycycline chow (Figure 3.7A). Control mice fed regular chow displayed advanced metastatic disease at 6 weeks (Figure 3.7B), with tumors observed at multiple sites. Mice fed doxycycline chow also displayed tumor nodules at 6 weeks, albeit the luminescence was significantly reduced compared to control mice (Figure 3.7B). Resulting metastases exhibited stable depletion of AKT2 protein and phosphorylation (Figure 3.7D), suggesting that AKT2 was not required for eventual growth of metastatic lesions. Nevertheless, AKT2 depletion after metastatic seeding conveyed a survival advantage, as AKT2 KD significantly improved overall survival in doxycycline chow fed mice versus regular chow mice (Figure 3.7C). These results are consistent with our previous findings that AKT2 KD initially affects growth of subcutaneous tumors (Figure 3.3B)**,** but tumors eventually grow, despite sustained AKT2 KD (Figure 3.3C). Taken together, AKT2 may promote growth in the metastatic niche, but is most important for invasive cell seeding, potentially through regulation of EMT and/or melanocyte-specific genes.

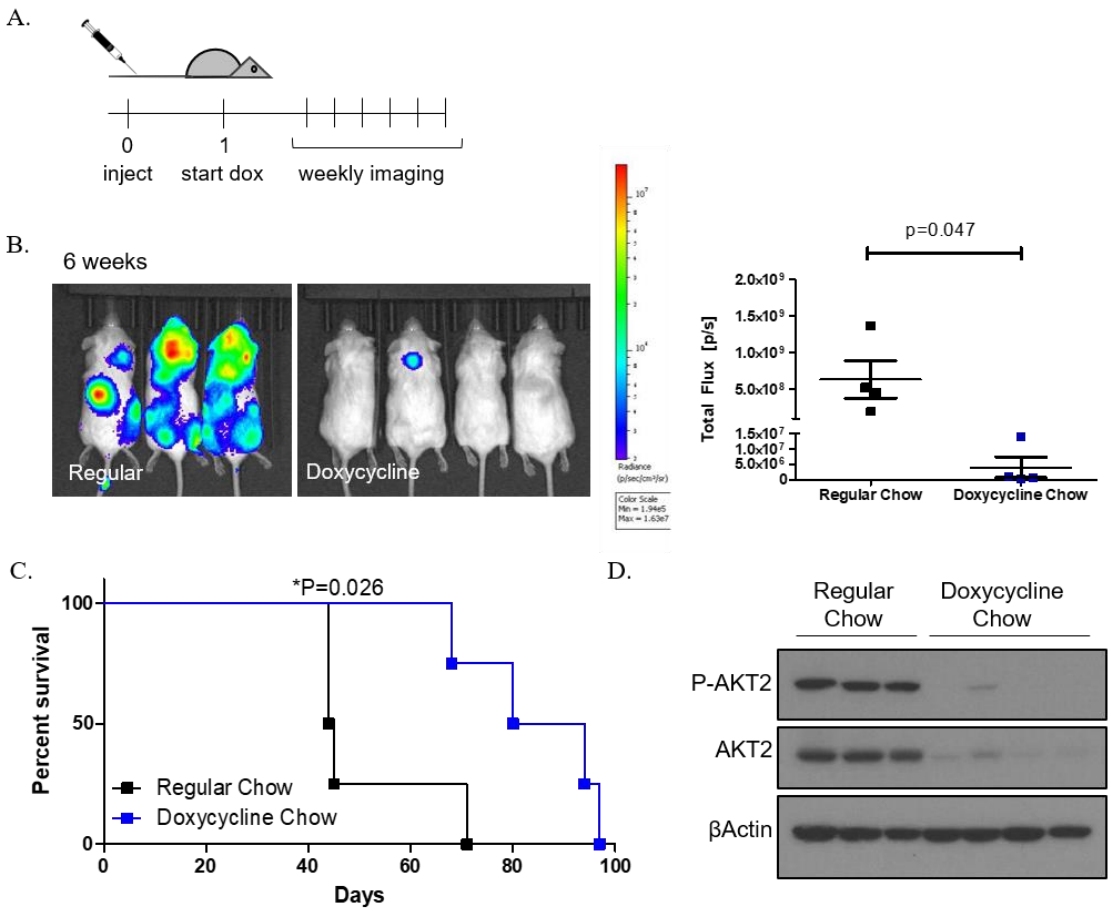

Figure 3.7. AKT2 depletion delays the onset of metastatic disease. A) Experimental schematic of tail vein injection of WM1799 shAKT2 cells followed one day later by the introduction of doxycycline chow and weekly intravital imaging. B) Intravital imaging at 6-weeks post injection of NOD/SCID mice fed regular or doxycycline chow (left) with quantification of relative luminescence at the same timepoint (right). C) Kaplan-Meyer survival curve of mice fed either regular or doxycycline chow. Statistics using Mantel-Cox Test. D) Immunoblotting for AKT2 levels and phosphorylation in metastases detected in regular or doxycycline chow fed mice.

3.2.4 AKT2 KO phenocopies the effect of AKT2 KD in reducing cell migration, invasion, and metastasis

To determine that AKT2 is important for cell behaviors associated with metastasis by an alternate mechanism, we took advantage of CRISPR/Cas9 gene editing to knockout (KO) AKT2 in human melanoma cell lines. Using guide RNAs specific to AKT1, AKT2, or AKT3, in addition to a non-targeting guide (NT), stable cell lines were generated and screened for AKT isoform KO. The AKT isoforms were efficiently depleted in seven individual human melanoma cell lines, as determined by immunoblotting, and the WM1799 cell line is shown as an example in Figure 3.8A.

Next, we tested whether AKT2 KO could reduce cell migration in either a wound healing assay or a transwell assay. AKT2 KO slightly but significantly reduced cell migration in both cases, compared with the NT cell line (Figure 3.8B). Similar results were obtained in AKT2 KO UACC903 and WM455 cell lines (data not shown). Additionally, we assessed the ability of AKT2 KO cells to invade through Matrigel coated transwells. We again observed that AKT2 KO cells had a slight defect in cellular invasion (Figure 3.8C) in comparison to WM1799 cells expressing a NT guide RNA. These results are consistent with our previous data using shRNA and suggest that AKT2 depletion impairs cell migration and invasion *in vitro*.

We further hypothesized that loss of AKT2 would impair metastatic seeding. To test this, we engineered NT and AKT2 KO WM1799 cells to express luciferase and injected them into the tail veins of NOD/SCID mice. We observed that mice injected with AKT2 KO cells had significantly reduced luminescence in comparison to mice injected with NT control cells (Figure 3.8D). Additionally, AKT2 KO mice had significantly

increased overall survival compared with control mice receiving NT cells (Figure 3.8E). As in previous assays, WM1799 cells readily metastasized and were identified in diverse locations consistent with both hematogenous and lymphogenous spread. Tumors were detected in the vicinity of the axillary, cervical, and inguinal lymph nodes, and one mouse exhibited luminescence within both right and left side inguinal lymph nodes at endpoint by intravital imaging. Tumors lining the GI tract, as well as snout or eye tumors were also common in both groups. By 50-70 days post-injection, moribund mice in the control group had extensive peripheral tumor masses on the snout and eye (3/9), but interestingly, AKT2 KO mice (2/9) had either localized tumors contained within the lung mass, or no detectable tumors. The latter was moribund due to hind limb paresis, possibly the result of a bone or spinal metastasis not visible by eye. Taken together, AKT2 KO had a slight but significant effect limiting metastatic potential of WM1799 cells, similar to previous results using shRNA-mediated KD, and reinforce the hypothesis that AKT2 may promote the process of melanoma metastasis.

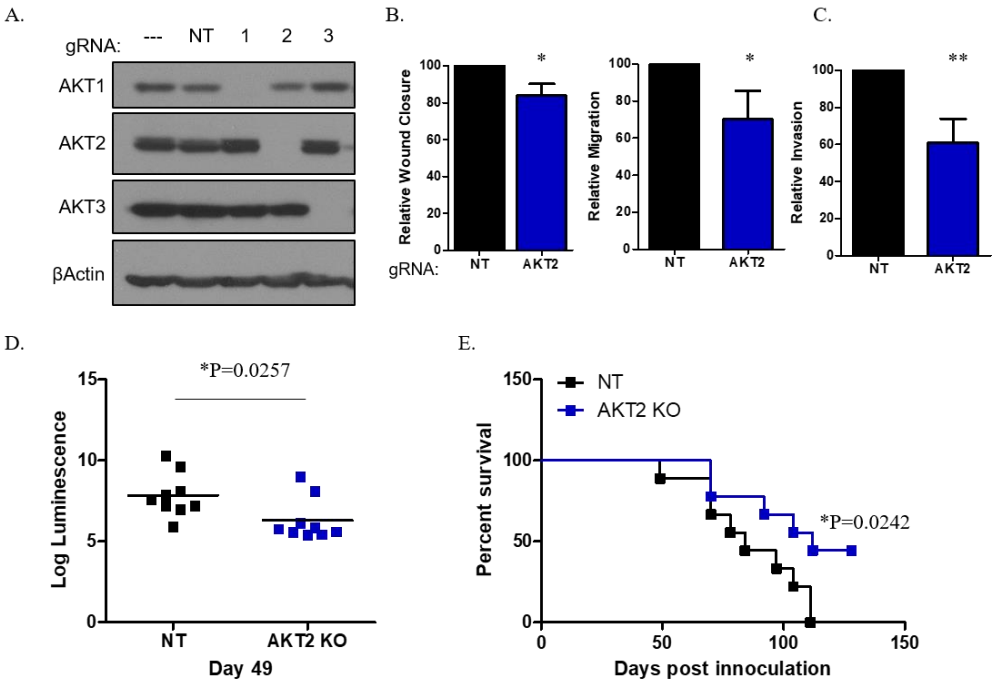

Figure 3.8. AKT2 KO impairs human melanoma cell migration, invasion, and metastasis. A) AKT isoform KO in WM1799 cells using CRISPR guide RNAs specific each AKT (1/2/3) or a non-targeting guide (NT). Lysates represent a pool of bulk selected cells, rather than subcloned populations. B) AKT2 KO impairs cellular migration compared to NT cells in a scratch assay (n=3, left) or in transwell assay (n=3, right). C) Quantification of relative invasion through Matrigel coated transwells (n=3) is reduced by AKT2 KO in comparison to NT cells. D) WM1799 AKT KO or NT cells were injected into the tail vein of NOD/SCID mice and luminescence was quantified at day 49 post-injection. E) Kaplan-Meyer survival curve of NOD/SCID mice injected with NT or AKT2 KO cells (n=9 per group).

3.2.5 AKT2 is important for melanoma cell metabolism and response to hypoxia

The next step was to identify a possible mechanism whereby AKT2 could support metastatic growth and survival. The PI3K/AKT pathway is known to support cancer cell metabolism by multiple means, and growth signals are tightly coupled to anti-apoptotic and pro-survival signals (Robey and Hay, 2009). Additionally, AKT2 has been specifically implicated in the recruitment of glucose transporters to the cell membrane, a necessary first step in supporting cellular metabolism (Jensen et al., 2010).

Given the importance of the AKT pathway to critical metabolic functions, we hypothesized that AKT2 disruption may cause broad changes in the metabolic profile of these cells. To investigate this, we took a metabolomic approach, using NMR to analyze the metabolites that were differentially expressed in WM1799 cells with inducible AKT2 KD. Preliminary analysis indicated no significant differences in metabolite expression profiles between DMSO and DOX treated shNT cells (data not shown), therefore, we opted to use DMSO treatment as a control for shAKT2 hairpin expression in further analyses. We treated WM1799 shAKT2 cells with DMSO or DOX for 96 hours before performing metabolite extraction and NMR analysis of three independent biological replicates. A principle component analysis indicates that the DMSO-treated biological replicates cluster tightly together, while the DOX-treated AKT2 depleted samples are more spread, but still cluster together compared with DMSO-treated controls (Figure 3.9A**)**. We went on to perform NMR and compare spectra between DMSO and DOX treated samples. To determine the percent representation of each metabolite, we standardized the amount of each metabolite to total cell number of each individual sample. Next, we calculated the fold change in metabolite percentage in AKT2 KD

DOX-treated samples relative to DMSO-treated controls. Surprisingly, among the nearly 45 identifiable metabolites, only a handful of these displayed enrichment greater than 1.5-fold compared to DMSO, and only one metabolite was suppressed by at least 50% (Figure 3.9B). Even fewer metabolites reached any level of statistical significance, according to the volcano plot shown in Figure 3.9C. Significantly enriched metabolites included Glycine, Creatine, and Creatine Phosphate, while uridine diphosphate (UDP)-Glucuronidate was suppressed.

Glycine is an essential component of a metabolic process known as one-carbon-metabolism, used to generate increased amounts of proteins, lipids, nucleotides, and redox substrates. One-carbon metabolism is prevalent in cancer cells and associated with malignant progression; melanoma cells have acquired gene amplification of one-carbon metabolic components to support sustained proliferation rates (Locasale, 2013). Importantly, carbon derived from glucose is often shunted toward one-carbon metabolism in a critical branch point in glycolysis; highly glycolytic tumor cells partially divert synthesized carbon products into one-carbon metabolism, and this metabolic plasticity is correlated with malignant progression (Locasale, 2013). We hypothesized that if AKT2 depletion disrupted the process of glycolysis by hampering glucose utilization, the cancer cell may be forced to compensate by increasing utilization of one-carbon metabolism.

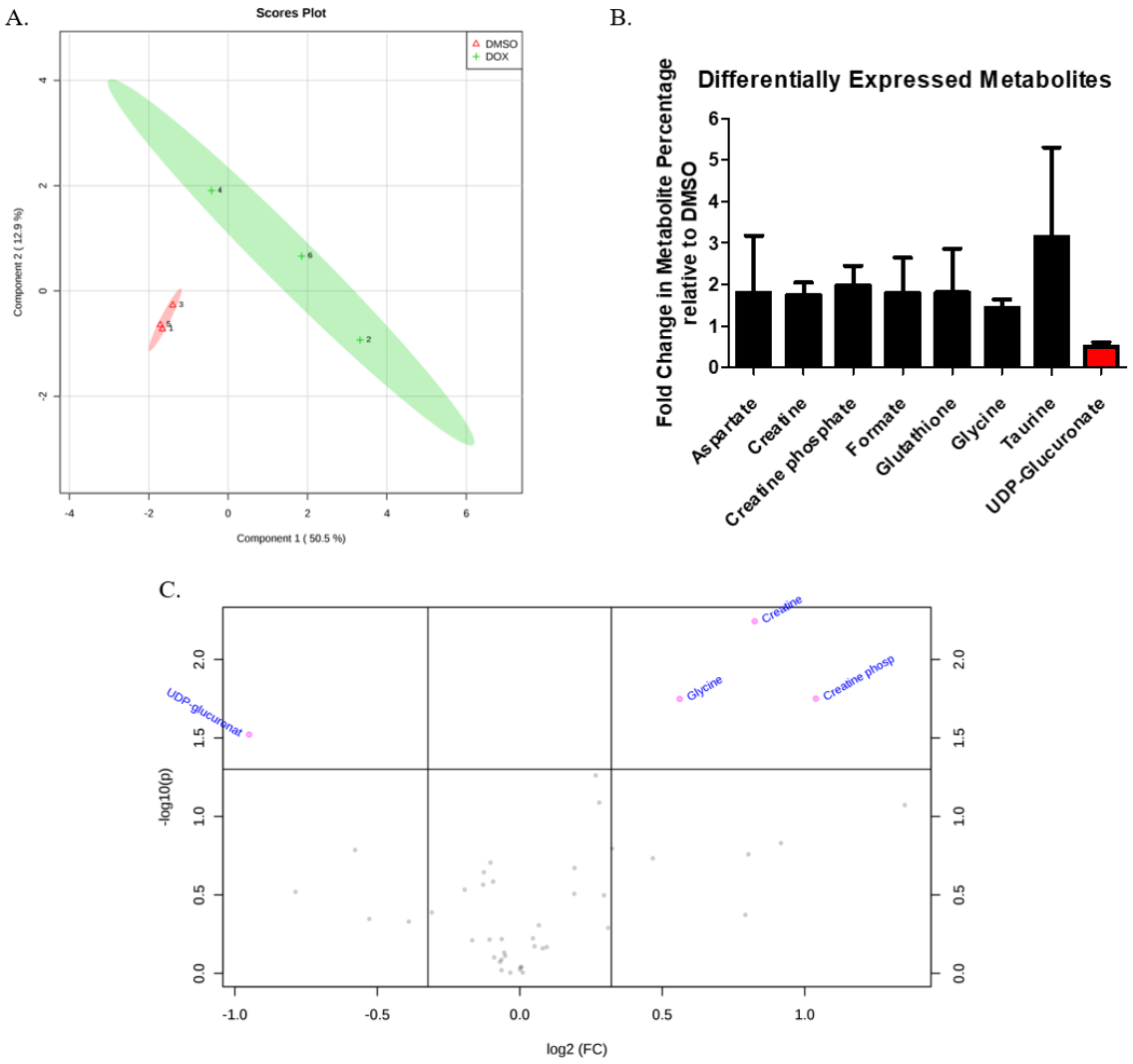

Figure 3.9. AKT2 depletion alters the metabolite profile of WM1799 human melanoma cells. A) WM1799 shAKT2 cells incubated with DMSO-or DOX-containing media for 96 hours were scraped into ice-cold methanol to isolate cellular metabolites, and then analyzed by NMR spectroscopy. A principle component analysis of three independent biological replicates shows clustering according to treatment group. B) Analysis of NMR data comparing fold change in AKT2 depleted DOX treated cells in comparison to DMSO-treated control group. Metabolites with >1.5-fold enrichment (black) or >0.5-fold suppression (red) are indicated. C) A volcano plot showing significantly enriched or suppressed metabolites across 3 independent biological replicates.

To determine whether AKT2 KD directly disrupts glycolysis, we employed a Seahorse glycolytic rate assay (GRA). This assay is similar in concept to conventional lactate assays, which measure acidification of cellular medium as a result of metabolic activity. However, this assay calculates and subtracts the contribution of mitochondrial acidification to more accurately quantify cellular glycolysis. In brief, proton efflux rate (PER), a measure of media acidification, is quantified in real time as chemicals inhibit mitochondrial respiration or glycolysis. First, basal PER is sampled in a series of three basal measurements. Next, the instrument injects a Rotenone/Antimycin A mixture (Rot/AA) that blocks mitochondrial metabolism by inhibiting the electron transport chain. In response, cellular metabolism must compensate by undergoing a metabolic switch to glycolysis, and an increase in the proton efflux rate (PER) will be detected. Finally, injection of 2-deoxy-D-glucose (2DG) inhibits glycolysis, and PER levels drop in parallel with cellular metabolism.

Using WM1799 cells expressing shNT or shAKT2 hairpins, we performed a glycolytic rate assay after 48 or 72 hours of incubation with DMSO- or DOX-containing media. The representative GRA plot of WM1799 cells expressing AKT2 hairpins is shown in Figure 3.10A. Fold changes in basal glycolytic metabolism between shNT DOX-treated and shAKT2 DOX-treated WM1799 cells revealed that AKT2 KD suppressed basal glycolytic metabolism (Figure 3.10B). Further, it was apparent that AKT2 depletion was suppressing glycolytic function in comparison to mitochondrial respiration, since the PER levels remained unchanged after Rot/AA injection (Figure 3.10A). This is further reflected in the quantification of compensatory glycolysis, which was significantly reduced in AKT2 depleted cells compared to DOX-treated WM1799

shNT cells (Figure 3.10C). These results show that AKT2 KD is inhibiting glycolysis in WM1799 human melanoma cells, consistent with our hypothesis.

While AKT2 can mediate glycolytic activity through the control of glucose transporters, hyperactive AKT can also stimulate HIF1α, which upregulates glycolytic enzymes (Robey and Hay, 2009). This metabolic response is important for the ability of tumor cells to adapt to hypoxic environments, a common feature of the metastatic niche. To determine whether AKT2 influenced the ability of cells to upregulate or stabilize HIF1α in response to hypoxic conditions, we performed an experiment in which we simulated hypoxia by treating cells in culture with cobalt chloride, a known hypoxia mimic (Wu and Yotnda, 2011). We pre-treated WM1799 shNT or shAKT2 cells with DMSO- or DOX-containing media for 24 hours before adding cobalt chloride to the culture medium, and protein was collected 8 or 24 hours after hypoxia induction and analyzed by immunoblotting (Figure 3.11A). AKT2 protein was efficiently depleted in shAKT2 cells as expected, concomitant with loss of AKT2 phosphorylation. We observed robust HIF1α induction by 8 hours in WM1799 shAKT2 cells and 24 hours in WM1799 shNT cells (Figure 3.11B-C). Consistent with our hypothesis, HIF1α expression was markedly reduced in cells with AKT2 depletion, in comparison to matched DMSO-treated samples (Figure 3.11B-C). Additionally, cleaved PARP, an indicator of apoptosis, was observed in 24-hour cobalt chloride treated AKT2 depleted cells, but not in other samples, suggesting that AKT2 depletion sensitizes cells to hypoxia-induced cell death (Figure 3.11B).

As an additional approach to investigate the effect of AKT2 on the cellular response to hypoxia, we also treated AKT2 KO WM1799 cells with cobalt chloride. The

results were similar to those seen in KD cells, in which HIF1α was stabilized by cobalt chloride treatment, but to a lesser degree than NT control cells (Figure 3.11C-D). Taken together, these results suggest that AKT2 partially mediates cellular response to hypoxia via the induction or stabilization of HIF1α.

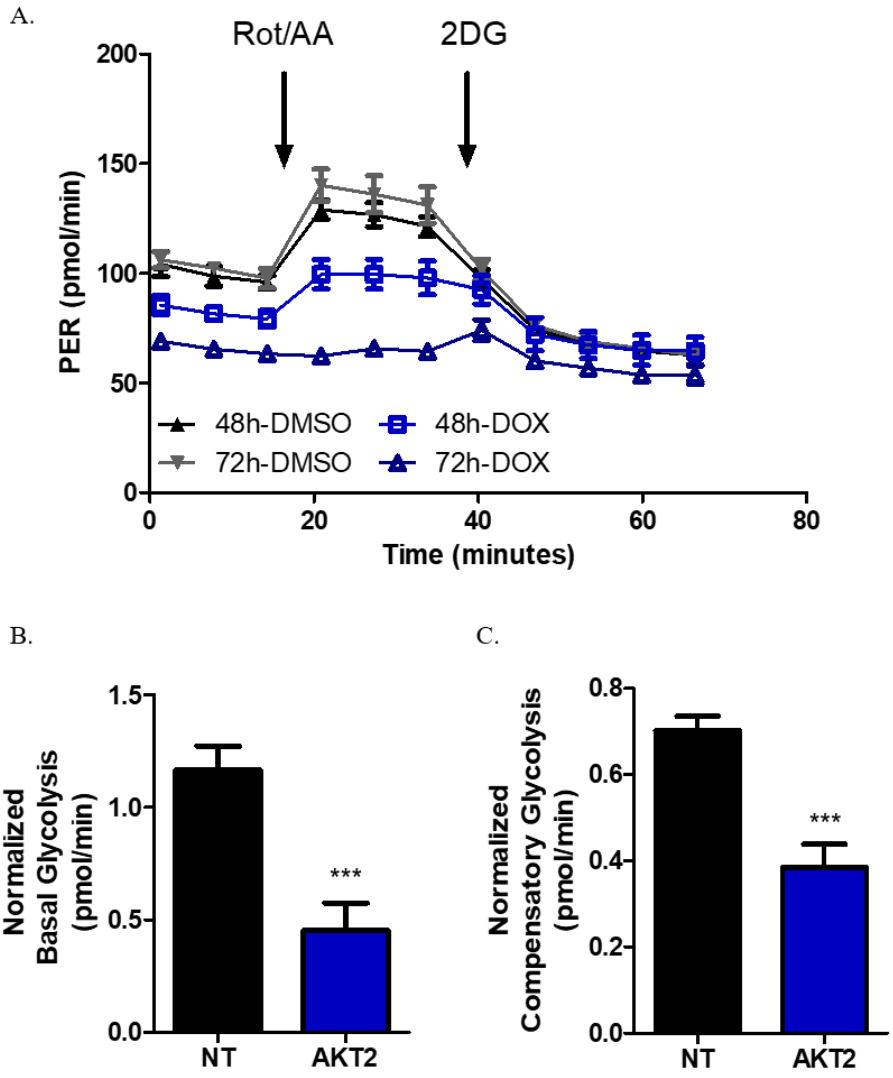

Figure 3.10. AKT2 depletion impairs glycolysis in human melanoma cells. A) WM1799 shAKT2 cells were incubated in DMSO-or DOX-containing media for 24 or 48h, then 21,000 cells were passaged into Agilent plates and incubated as indicated for a further 24h. A representative plot shows the results of a glycolytic rate assay (GRA) in which proton efflux rate (PER) was measured over time following injection of first Rotenone/Antimycin A (Rot/AA) followed by 2-deoxy-D-glucose (2-DG). Three independent experiments, each in triplicate, were performed with similar findings. B) Basal glycolysis (indicative of PER before Rot/AA injection) was quantified over three independent experiments and compared to DOX-treated WM1799 shNT cells. C) Compensatory glycolysis (indicative of PER after Rot/AA injection) was quantified as in (B) from three independent experiments.

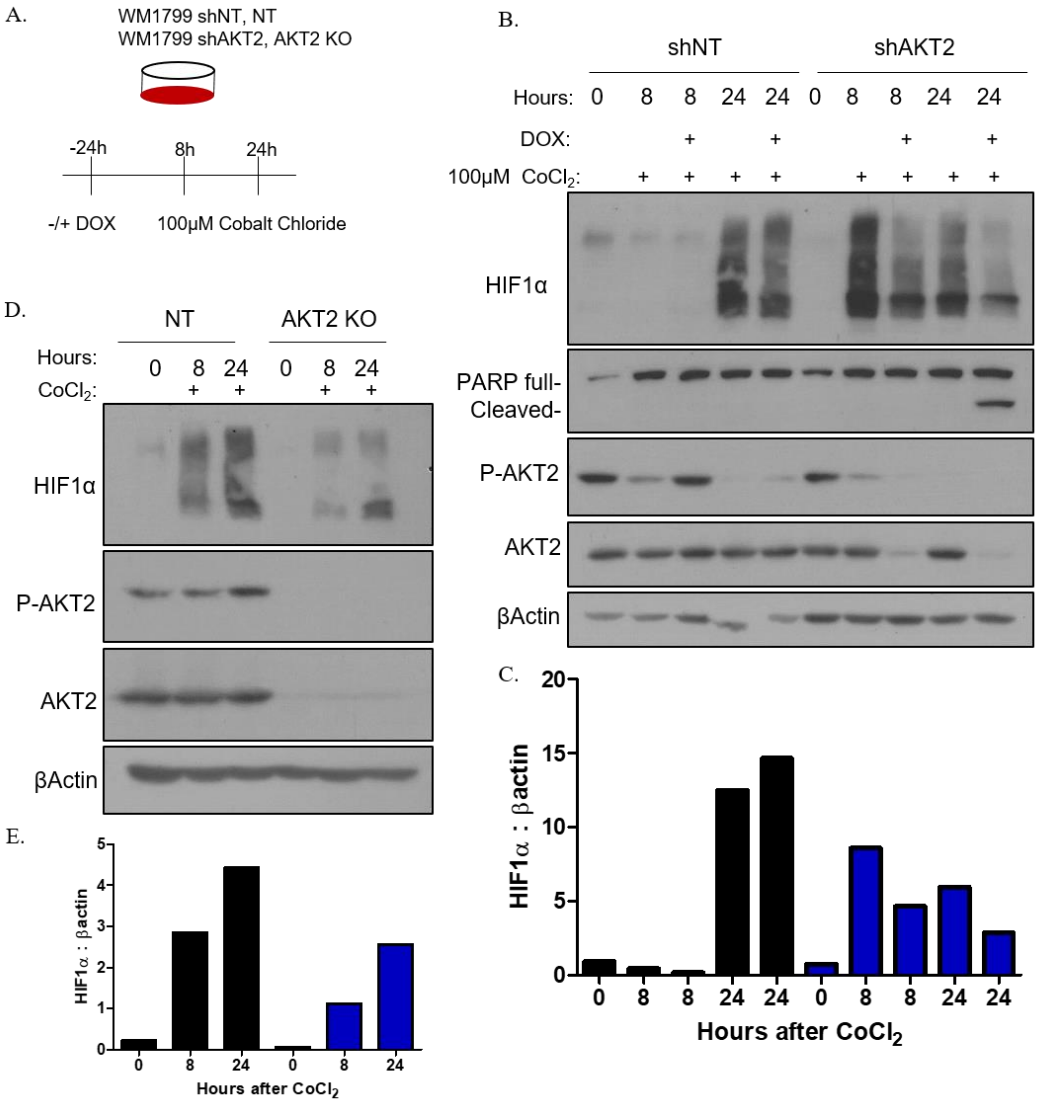

Figure 3.11. AKT2 loss blunts HIF1α response during simulated hypoxia. A) Experimental design for experimentally induced hypoxia using cobalt chloride treatment. WM1799 human melanoma cells incubated for 24h with DMSO- or DOX-containing media, then treated with 100μM cobalt chloride (final concentration) before both adherent and floating cells were harvested at the indicated timepoints. B) Immunoblotting for HIF1α, PARP, AKT2, and AKT2 phosphorylation (S474) after cobalt chloride treatment in shNT or shAKT2 WM1799 cells treated as in (A). C) Quantification of immunoblots from (B) using ImageJ. D) NT or AKT2 KO WM1799 cells where treated with cobalt chloride as indicated and subjected to immunoblotting for AKT2 and HIF1α. E) Quantification of immunoblots from (D) using ImageJ.

3.2.6 Investigating the phospho-AKT substrate landscape in WM1799 human melanoma cells

Our results thus far have implicated the AKT2 isoform in a variety of functions pertaining to metastasis but given that AKT2 is an intracellular kinase far upstream of these diverse processes, we thought it likely that downstream substrates are mediating the phenotypes we observe. To get a snapshot of the landscape of potential cellular mediators, we performed a mass spectrometry analysis of AKT phospho-substrates in WM1799 cells.

First, we used an antibody specific to the AKT-phospho-substrate binding motif (R/K)X(R/K)XX(T*/S*) to immuno-precipitate proteins with this recognition sequence from WM1799 shAKT2 cells incubated in DMSO- or DOX-containing media for 48 hours, as well as treatment with the BRAF inhibitor Vemurafenib, either alone or in combination with AKT2 depletion (Figure 3.12A). We then used magnetic beads to capture the bound protein complexes and submitted them for analysis by mass spectrometry.

Our results show that with this approach we were able to identify 14 phospho-substrates when immunoprecipitating with the AKT-consensus motif in WM1799 shAKT2 DMSO treated cells that were not present in the IgG negative control sample (Table 3.1). Similarly, we identified 11 phospho-substrates in WM1799 shAKT2 DOX-treated samples (Table 3.2). Additionally, there were 10 phospho-substrates in the Vemurafenib treated group (Table 3.3), and 11 in the combined Vemurafenib and DOX-treated group (Table 3.4). No substrate was common to all four groups, but there were at least 3-4 substrates in each group that were also found in other groups. Some of these

substrates are known AKT phospho-targets, such as TBC1D4, and NDRG1. In the case of these proteins, the modified site was also annotated AKT consensus site. However, the majority of peptides that we identified were not annotated targets, and the modified peptide residue did not match an AKT consensus site. One substrate, SSFA2, was modified at serine 739, an R-X-X-S consensus site, which is an alternate AKT-substrate binding motif, but not the consensus site recognized by the antibody we used. In most cases, the identified position was a serine or threonine phosphorylation site but did not match the AKT-binding consensus motif. This does not preclude the existence of AKT-consensus sites elsewhere in the protein sequence, but this was not additionally investigated. Furthermore, some potential substrates identified in this screen, such as NCKAP5L and CCDC138, are also not well annotated with regard to protein function, or their function was unknown.

Only two substrates identified in WM1799 shAKT2 DOX-treated cells were significantly associated with gene ontology (GO) terms. TDRD5 and ACRBP together were associated with three separate GO terms, spermatid development, spermatid differentiation, and cell maturation (Figure 3.12B). There were no significantly associated GO terms among proteins from the other groups, and these two proteins did not contain the AKT consensus site at the modified residue annotated in our screen. However, many phospho-proteins we identified, while not significantly enriched GO terms, may bear investigation for their potential involvement in cell motility, cytoskeletal rearrangement, or other aspects of cell movement, which could be participating in AKT2-mediated metastatic promotion.

Taken together, with this phospho-proteomic screen we have generated an actionable list with myriad potential substrates that could be facilitating AKT-induced cell invasion phenotypes but require substrate validation and testing in future studies.

A.

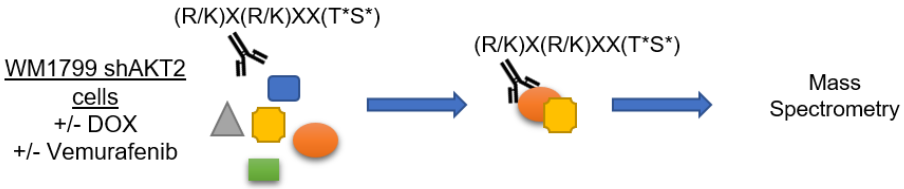

B.

Gene Ontology terms associated with proteins in WM1799 AKT2 KD cells	Corrected P-value	Genes annotated to the term
spermatid development	0.00672	TDRD5, ACRBP
spermatid differentiation	0.0072	TDRD5, ACRBP
cell maturation	0.00759	TDRD5, ACRBP

Figure 3.12. Identification of AKT-phospho-substrates by Mass Spectrometry. A) Schematic experimental design. WM1799 shAKT2 cells were cultured in DMSO- or DOX-containing media for 96 hours, and then immunoprecipitated with an antibody specific to the AKT-phosphorylation consensus site binding motif. Immunoprecipitated proteins were subjected to Mass Spectrometry after a Trypsin digestion using a TripleTOF 5600. Protein fragments were identified using UniProt database. B) Gene ontology terms associated with phospho-substrates identified in WM1799 shAKT2 DOX-treated cells.

Table 3.1. Phospho-proteins identified by Mass Spectrometry in WM1799 shAKT2 DMSO-treated cells

Gene Name	Description	Biological Process
CAMK2D	Calcium/Calmodulin Dependent Protein Kinase II Delta	calcium modulation
TBC1D4	TBC1 Domain Family Member 4	Rab GTPase, AKT mediated insulin modulation
SSFA2	sperm specific antigen 2	cytoskeletal
TCOF1	treacher collins syndrome 1	RNA binding, transcription
PLEC	plectin-1	cytoskeletal, motility
NDRG1	N-Myc Downstream Regulated 1	hypoxia inducible anti-apoptotic protein
GLYR1	Glyoxylate Reductase 1 Homolog	Oxidoreductase, chromatin remodeling
PCM1	Pericentriolar Material 1	cell cycle, centrosome localization
ATP5O	ATP Synthase, H+ Transporting, Mitochondrial F1 Complex, O Subunit	Component of F-type ATPase found in the mitochondrial matrix
PRSS1	Protease Serine 1	protease
SVIL	supervillin	Actin cytoskeleton binding protein
ABCA1	ATP Binding Cassette Subfamily A Member 1	ATP-binding cassette (ABC) transporter
MARS2	Methionyl-TRNA Synthetase 2, Mitochondrial	translation, oxidative phosphorylation
CARD14	Caspase Recruitment Domain Family Member 14	adaptor/scaffold

Table 3.2. Phospho-proteins identified by mass spectrometry in WM1799 shAKT2 doxycycline-treated cells

Gene Name	Description	Biological Process
MYH10	Myosin Heavy Chain 10	motility/chemotaxis
TBC1D4	TBC1 Domain Family Member 4	Rab GTPase, AKT mediated insulin modulation
TCOF1	treacher collins syndrome 1	RNA binding, transcription
PLEC	plectin-1	cytoskeletal, motility
NDRG1	N-Myc Downstream Regulated 1	hypoxia inducible anti-apoptotic protein
ITPR2	Inositol 1,4,5-Trisphosphate Receptor Type 2	ER membrane receptor calcium channel protein
NCKAP5L	NCK Associated Protein 5 Like	microtubule bundle formation
KIAA1217	Sickle tail protein homolog	cell development/differentiation
ACRBP	acrosin binding protein	cell development/differentiation
TDRD5	Tudor domain containing protein	represses transposable elements in spermiogenesis by DNA methylation
CCDC138	coiled coil domain containing protein 130	cilia basal body/centriolar satellite protein

Table 3.3. Phospho-proteins identified by mass spectrometry in WM1799 shAKT2 Vemurafenib-treated cells

Gene Name	Description	Biological Process
ADGRG7	Adhesion G-protein coupled receptor G7	orphan receptor
CAMK2D	Calcium/calmodulin-dependent protein kinase type II	calcium modulation
GPNMB	glycoprotein non-metastatic melanoma protein B	Type I transmembrane glycoprotein
MYH10	Myosin Heavy Chain 10	motility/chemotaxis
MYH9	Myosin Heavy Chain 9	motility/chemotaxis
NPM1	Nucleophosmin 1	centrosome duplication, protein chaperoning, cell proliferation
SLAIN2	SLAIN motif-containing protein 2	Promotes cytoplasmic microtubule nucleation and elongation
SSFA2	Sperm-specific antigen 2	cytoskeletal
THRAP3	Thyroid hormone receptor-associated protein 3	pre-mRNA splicing, circadian rhythm
TTC28	Tetratricopeptide repeat protein 28	may be involved in the condensation of spindle midzone microtubules

Table 3.4. Phospho-proteins identified by mass spectrometry in WM1799 shAKT2 cells co-treated with Vemurafenib and doxycycline

Gene Name	Description	Biological Process
MYH10	Myosin-10	motility/chemotaxis
SSFA2	Sperm-specific antigen 2	cytoskeletal
ACTB	Actin	cytoskeletal
TOP1	DNA topoisomerase 1	DNA replication
SVIL	Supervillin	actin binding protein
H1FX	Histone H1x	replication-independent histone, histone H1 family
EIF5B	Eukaryotic translation initiation factor 5B	initiation of translation
NDRG1	hypoxia inducible anti-apoptotic protein	cell development/differentiation
RP1L1	Retinitis pigmentosa 1-like 1 protein	microtubule polymerization
TTN	Titin	cardiac structural protein
ZC3HAV1	Zinc finger CCCH-type antiviral protein 1	Viral replication inhibitor

3.3 Summary and Significance

In this chapter, we took advantage of a panel of human melanoma cell lines to investigate the contribution of AKT isoforms to cell behaviors associated with metastasis. Our results show that the AKT2 isoform mediates cell migration and invasion, without affecting 2D growth in culture. Further, we observed that AKT2, but not AKT1 or AKT3, modulates an EMT-associated transcriptional program. Further, AKT2 depletion suppresses the expression of melanocyte specific regulators. In addition, prophylactic AKT2 depletion can prevent metastatic seeding of the invasive niche *in vivo*. We also observed that AKT2 depletion was sufficient to transiently reduce tumor growth after metastatic cell seeding, suggesting that AKT2 may affect the ability of cells to grow or survive in the metastatic niche, despite a lack of requirement for cell growth *in vitro.* We discovered that AKT2 depletion suppressed glycolysis and also hampered HIF1α induction during simulated hypoxia, suggesting possible mechanisms whereby AKT2 supports cells growth or survival during the metastatic process. Lastly, we screened for possible phospho-substrates that may play a role in effecting diverse downstream phenotypes. We found both known and unknown AKT phospho-substrates involved in cellular processes mediating metabolism and cell motility. These interesting candidates will require further validation but provide promising targets in an ongoing effort to understand the process of melanoma metastasis.

Taken together, these results provide evidence that AKT2 supports the metastatic process in melanoma, in line with recently published work (Yu et al., 2018). Understanding the mechanism of metastatic dissemination is crucial for future therapeutic design, and we have specifically implicated AKT2 in the initial steps of metastatic

seeding. In addition, we have correlated AKT2 with expression of critical melanocyte-specific differentiation regulators, which has not been previously described. Because frontline targeted therapies directly modulate the melanocyte differentiation process (Haq et al., 2013; Joseph et al., 2010), this novel finding could have implications for co-treatment regimens involving BRAF and AKT inhibitors.

Chapter 4. AKT1 promotes BRAF mutant melanoma initiation and tumor progression

4.1 Introduction

The PI3K/AKT pathway is well known to regulate cell growth and survival (Manning and Cantley, 2007). Of the three AKT isoforms, loss of AKT1 causes perinatal lethality, and mice that survive into adulthood demonstrate a 20% reduction in body weight (Cho et al., 2001b). In contrast to AKT2 deficiency, AKT1 loss has no effect on insulin regulation or glucose metabolism *in vivo* (Cho et al., 2001a; Cho et al., 2001b).

Tumors frequently display hyperactivation of PI3K/AKT signaling, and an activating mutation in AKT1 at residue E17K in the PH domain was identified in a variety of breast, ovarian, and colorectal cancers, mutually exclusive to PTEN loss or other activating mutations (Carpten et al., 2007). AKT1 supports oncogenic transformation of mammary tumors (Maroulakou et al., 2007) but suppresses EMT and cellular migration in breast cancer cells (Irie et al., 2005). In melanoma, an AKT1 mutation, Q79K, was identified that increased association at the plasma membrane and amplified adaptive resistance to BRAF inhibition (Shi et al., 2014). AKT1 has also been implicated in melanoma metastasis (Cho et al., 2015) but the role of AKT1 in melanoma cell proliferation or in supporting melanoma initiation has not been investigated.

4.2 Results

4.2.1 AKT1 promotes melanoma cell proliferation *in vitro*

Given the well-known function of AKT1 in regulating cell proliferation, we hypothesized that AKT1 would be important for this process in melanoma cells. Using inducible shRNA KD, we investigated whether AKT1 depletion would reduce cell

proliferation *in vitro*. First, we seeded human melanoma cell lines expressing shAKT1 hairpins in triplicate in 12-well plates and incubated them in DMSO- or DOX-containing media for a total of 96 hours. Every 24 hours, cells were trypsinized and counted using trypan blue exclusion as a marker for live cells. We observed that after the 48-hour time point in the majority of cell lines, we counted fewer human melanoma cells, with the greatest difference at 96 hours, in which there were significantly fewer cells than in DMSO-treated groups (Figure 4.1A). This result was consistent across at least four BRAF mutant human melanoma cell lines. To assess cell proliferation by an alternate approach, we performed propidium iodide staining for DNA content after 96h of incubation in DMSO- or DOX-containing media in WM1799 and UACC903 cells. Our results show that a slight increase in the percentage of cells in the G1fraction, with a concomitant decrease in observed G2/M cells, was seen in both cell lines with AKT1 KD (WM1799, Figure 4.1C-D). In addition, we assessed BrdU incorporation at this timepoint in WM1799 cells and observed an expected decrease in the observed percentage of BrdU positive cells with AKT1 KD, relative to DMSO-treated controls (Figure 4.1E).

The observed dependence on AKT1, in contrast to AKT2, for cell proliferation in vitro would suggest that AKT1 KD would impair anchorage independent growth. To assess this, we seeded single cells in soft agar and grew colonies in the presence of DMSO- or DOX-containing media. We observed fewer colonies in WM1799 cells when AKT1 was depleted Figure 4.2A-B). While there was a trend toward a reduction in colony size with AKT1 KD, this decrease was not statistically significant (likely due to variation in the shNT control) (Figure 4.2C). These results are consistent with the

hypothesis that AKT1 plays an important role in supporting cell proliferation in human melanoma cells *in vitro*.

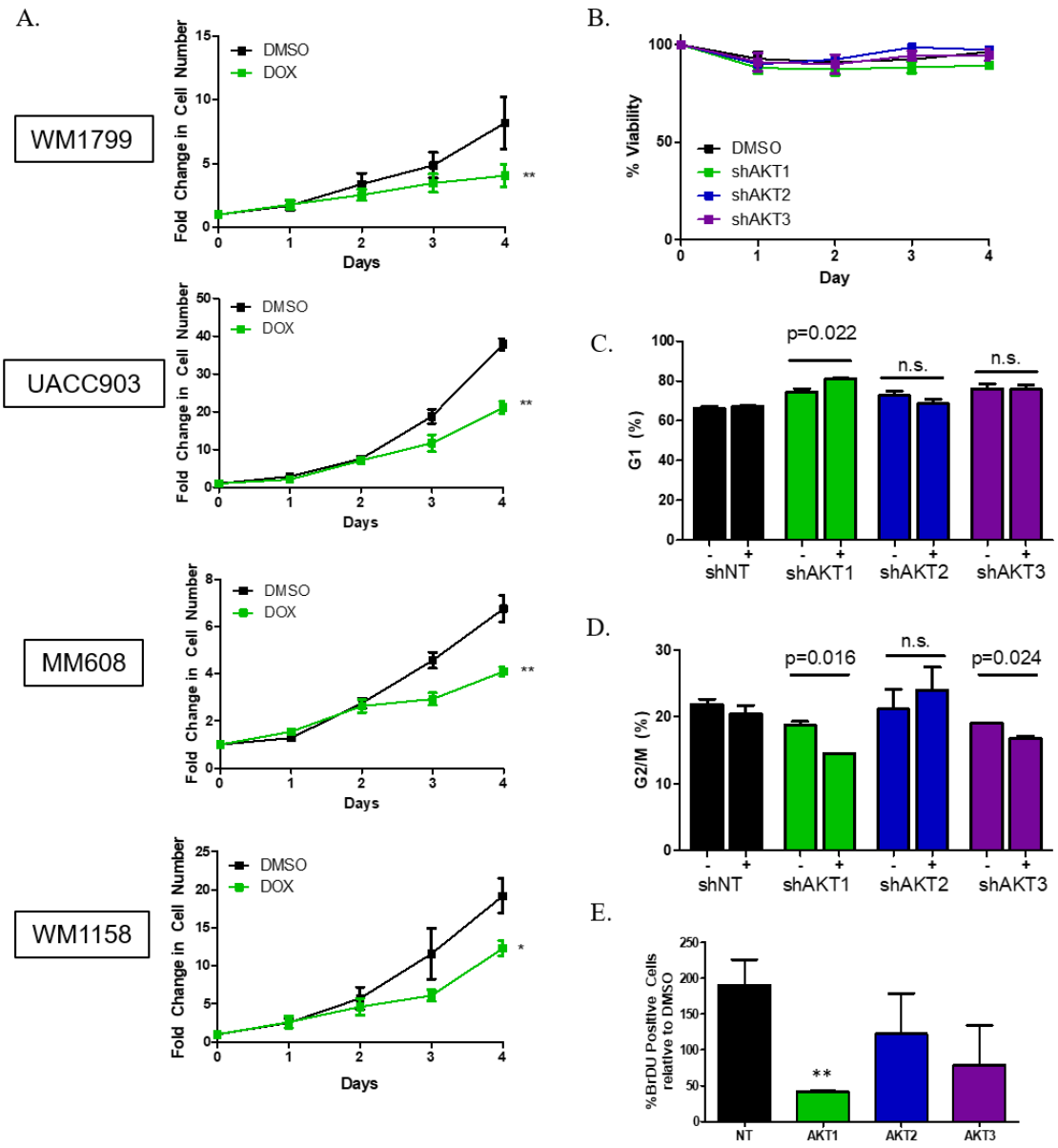

Figure 4.1. AKT1 KD reduces cell proliferation in human melanoma cell lines. A) 30,000 human melanoma cells were seeded in 12-well plates and live-cell number was counted over a period of 4 days. Fold change in cell number was lower in DOX-treated cells compared to DMSO-treated cells. Fold changes represent the average of two independent experiments for each cell line. B) Cell viability according to trypan blue exclusion in WM1799 cells from (A) shows no significant differences in cell viability with AKT-isoform KD. C) Cell cycle analysis of WM1799 cells by propidium iodide staining shows a slight increase in G1 cells with AKT1 depletion. D) Cell cycle analysis of WM1799 cells by propidium iodide staining shows a slight decrease in the observed percentage of G2/M cells with AKT1 depletion, SEM from three independent experiments. E) BrdU incorporation in WM1799 cells after 96h of DOX treatment shows that relative to DMSO-treated cells, AKT1 KD cells have a reduction in observed BrdU positivity. SEM from three independent experiments.

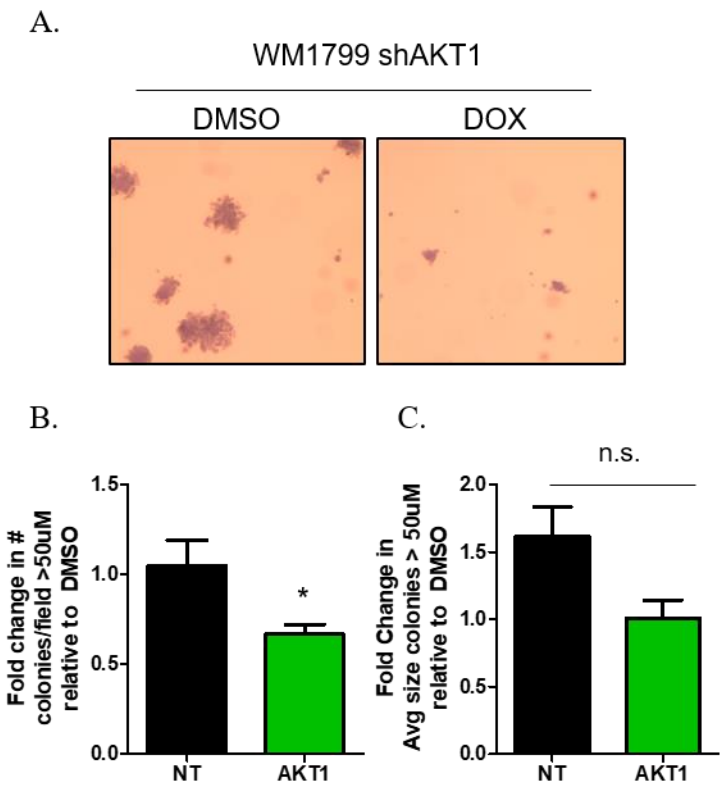

Figure 4.2. AKT1 depletion reduces anchorage independent growth. A) WM1799 cells were seeded in soft agar in the presence of DMSO- or DOX-containing media, and after 3 weeks were fixed with formalin and stained with 0.005% crystal violet overnight. Representative images are 4x magnification. Experiment was repeated three times. B) Quantification of total number of colonies greater that 50µm in DOX-treated shNT or shAKT1 WM1799 cells compared to DMSO-treated cells, using ImageJ. C) Quantification of the change in average size colonies greater than 50µm in shNT compared to shAKT1 WM1799 cells, using ImageJ.

4.2.2 AKT1 is important for cell proliferation *in vivo*

Our results thus far suggest that AKT1 is important for cell proliferation, and this would predict a role for supporting melanoma tumor growth *in vivo*. To further test this hypothesis, we took advantage of the human the melanoma cell line WM1799 expressing inducible AKT1 shRNA hairpins, and injected cells subcutaneously in NOD/SCID mice. We waited for tumors to become palpable before starting a subset of mice on Doxycycline chow, to induce AKT1 KD *in vivo*. We additionally injected a separate group of NOD/SCID mice with WM1799 cells expressing shNT hairpins, to ensure that tumor growth was not affected by the presence of Doxycycline chow in our mice. We observed that while no difference in tumor growth was seen with a non-targeting hairpin (Figure 4.3A), AKT1 depletion reduced tumor growth in NOD/SCID mice (Figure 4.3). However, this delay in tumor formation was transient, and tumors that reached humane endpoints were analyzed by immunoblotting for AKT isoform levels and phosphorylation. We observed similar levels of AKT isoform phosphorylation and total protein levels across groups, making it difficult to confirm that AKT1 knockdown was responsible for the delay in tumor growth. We reasoned that knockdown avoidance, while unlikely, was possible, and could be playing a role in the transient tumor reduction we observed.

To circumvent the ability of cells to avoid doxycycline-induced KD, we utilized AKT isoform KO cells generated by CRISPR/Cas9. We hypothesized that AKT1 KO cells would also display a proliferation defect in culture in support of our KD results. However, we were not able to observe that cells lacking AKT1 had a proliferation defect. Contrary to our previous results using shRNA and showing that AKT1 KD inhibits cell

proliferation, stable AKT1 KO cells showed no defect in cell proliferation by cell counting (Figure 4.4A). Additionally, there was an increase in the number of colonies observed in soft agar (Figure 4.4B), an opposite result. However, when we performed additional tumor forming experiments by injecting WM1799 AKT isoform KO cells subcutaneously in NOD/SCID mice, we observed that AKT1 KO cells appeared to have delayed tumor initiation (Figure 4.4C). In contrast, WM1799 NT cells or cells with AKT2 or AKT3 KO had no difference in their tumor-forming ability or relative tumor growth. However, once AKT1 KO tumors formed, there appeared to be no difference in relative growth or eventual tumor size at humane endpoints (data not shown). Because AKT1 KO cells were injected in parallel with AKT3 KO cells, this ostensible delay was not likely due to variation in cell injection or host tumor take.

Taken together, these results suggest that AKT1 supports the growth of melanoma tumors *in vivo* and is important in promoting melanoma cell proliferation but highlight the potential for cellular plasticity in overcoming AKT1-mediated growth suppression.

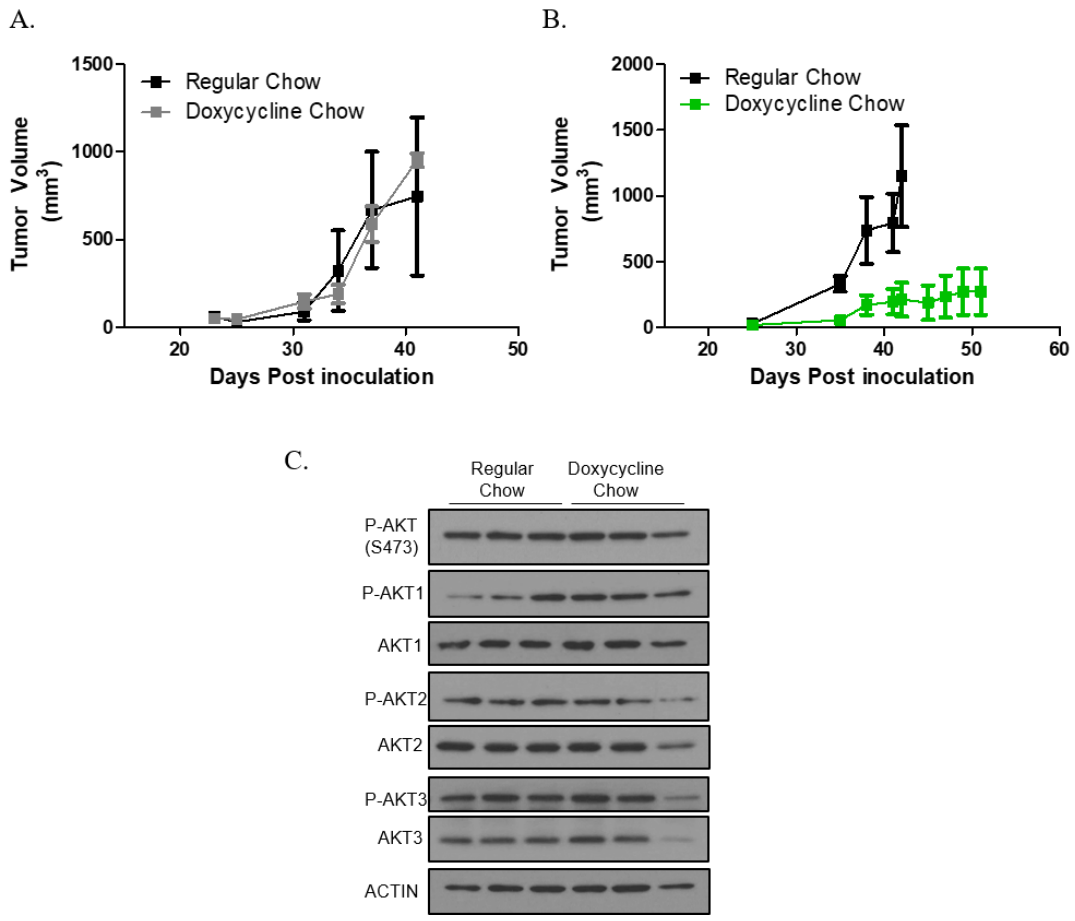

Figure 4.3. AKT1 depletion inhibits tumor growth *in vivo*. A) Two million WM1799 shNT cells were injected subcutaneously into NOD/SCID mice (n=3-4 per group) and tumors were allowed to form before a subset of mice were switched to doxycycline containing chow and tumors were measured every other day using calipers. P=n.s. B) Two million WM1799 shAKT1 cells were injected subcutaneously in NOD/SCID mice (n=3 per group), and a subset of mice were switched to doxycycline chow once tumors were palpable. Tumors were then measured with calipers and followed as in (A), *P=0.0124. C) Immunoblot analysis of tumors from (B) at humane endpoints.

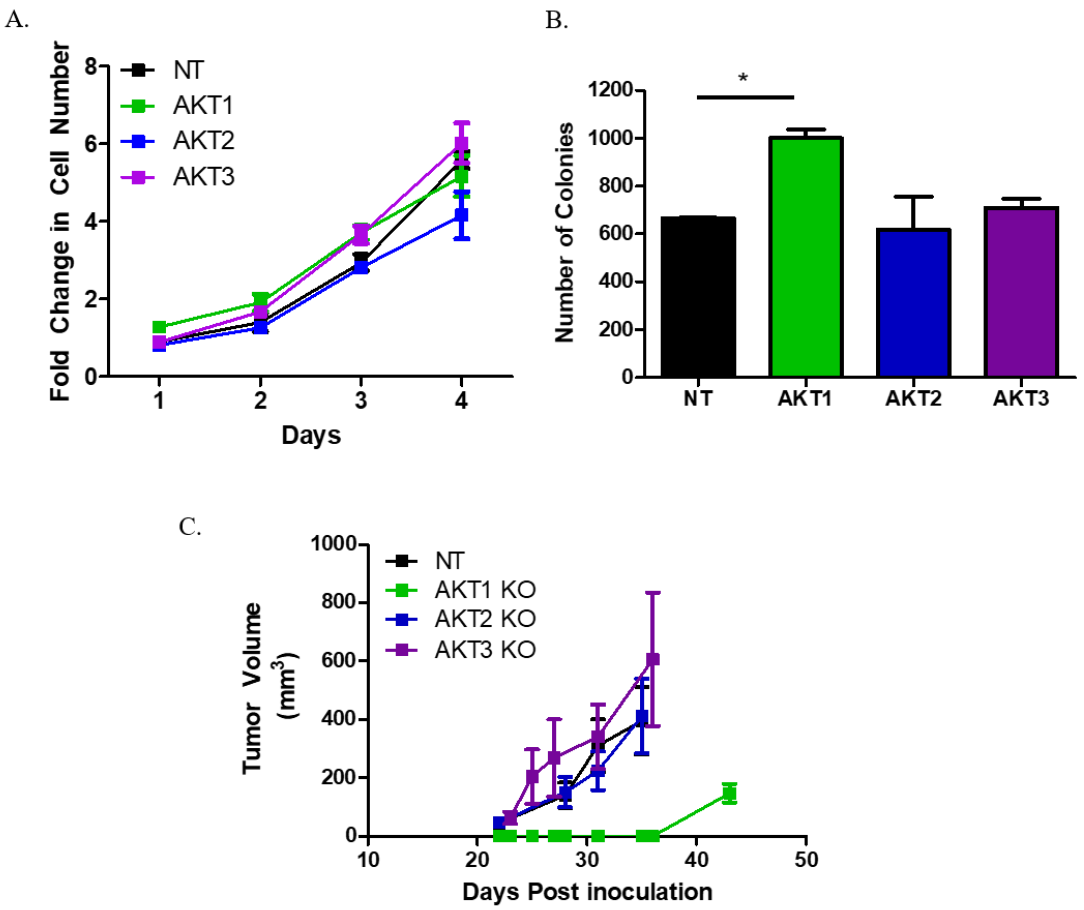

Figure 4.4. AKT1 KO does not limit cell proliferation or anchorage independent growth *in vitro* but delays tumor growth *in vivo*. A) 30,000 stably AKT isoform KO WM1799 cells were seeded in triplicate into 12-well plates and live cell number was assessed at indicated timepoints using an automated cell counter with trypan blue exclusion. B) WM1799 AKT isoform KO cells (10,000 per well) were seeded in soft agar and after three weeks, colonies were fixed, stained with crystal violet, and totally number of colonies was quantified using ImageJ. C) Two million WM1799 cells with AKT isoform KO were injected subcutaneously in NOD/SCID mice. Once palpable, tumors were measured with calipers approximately every other day (n=5-10 mice per group).

A.

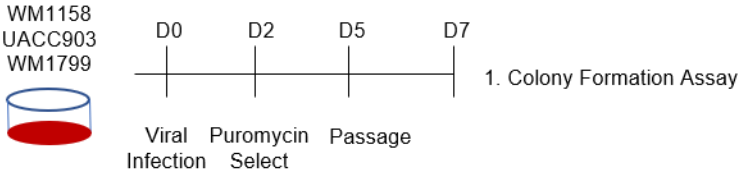

B.

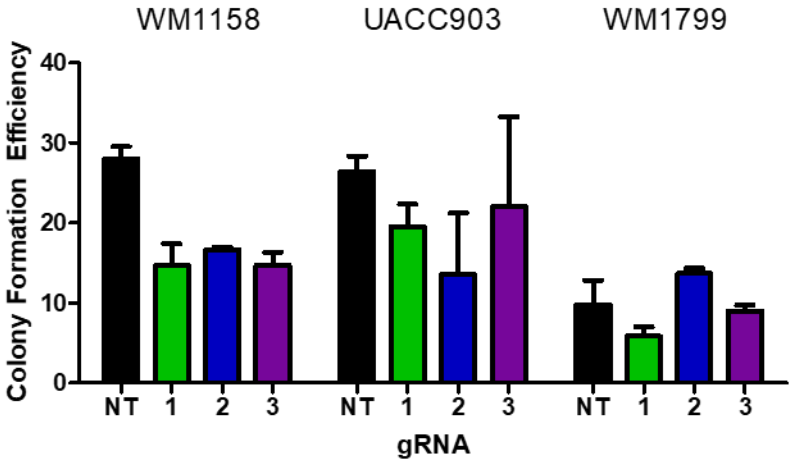

Figure 4.5. AKT1 KO reduces colony forming efficiency in human melanoma cells. A) Experimental schematic of viral infection, puromycin selection, and utilization of cells for downstream assays. Three independent cell lines WM1158, WM1799, and UACC903 were infected with viruses encapsulating NT, AKT1, AKT2, or AKT3 KO LentiCRISPRV2 plasmid DNA, and selected for expression using puromycin for three days. Cells were passaged once as an initial expansion before being used for the downstream assay indicated. B) Human melanoma cells were plated at low density (100-150 cells) in 6-well plates, and quantification of colony forming efficiency is represented as the total number of colonies as a percent of possible colonies, counted in triplicate for each indicated guide RNA in the three human melanoma cell lines.

4.2.3 AKT1 KO is not well-tolerated in human melanoma cells

Given the result and that AKT1 KO only delayed but did not prevent tumor initiation, we hypothesized that cells could possibly undergo selective "re-wiring" to acclimatize to the lack of AKT1, and eventually overcome a requirement for AKT1 in cell proliferation. To test this hypothesis, we designed an experiment in which we would newly infect cells with guide RNAs to NT, AKT1, AKT2, or AKT3, across three independent cell lines and analyze cellular phenotypes immediately after selection, in an attempt to visualize any transient growth defects or compensation that may occur. The first phenotype we investigated was colony forming efficiency. We infected human melanoma cells with NT or AKT isoform guide RNAs, selected them for three days with puromycin to achieve AKT isoform KO, and then passaged them once for an initial expansion. Two days later, we plated the cells at extreme low-density of 100-200 cells per well in 6-well plates, in triplicate (Figure 4.5A).

Our results show that across three independent cell lines (WM1158, UACC903, WM1799), there was a trend toward a reduction in colony forming efficiency with AKT1 depletion (Figure 4.5B). Compared with NT, no cell line except WM1158 showed a significant difference in colony formation efficiency, and this was not specific to AKT1 KO in this cell line. A similar result was obtained in UACC903 cells, which showed a decrease in colony formation with each AKT isoform guide RNA. In WM1799 cell lines however, only the AKT1 guide RNA showed a trend toward reduced colony forming efficiency, but again, this decrease was not significant (Figure 4.5B).

To extend our characterization, we analyzed AKT isoform protein levels by immunoblotting, in cells after one passage post-selection (Figure 4.6A). It is worth noting

that each of the guide RNAs selected for use in each cell line were also previously validated as able to achieve specific AKT isoform KO, but data showing this validation is omitted for brevity. Analysis of P1 protein showed that KO of both AKT2 and AKT3 was consistently achieved across all cell lines, but AKT1 protein remained detectable (Figure 4.6B**)**. None of three individual guide RNAs were able to achieve AKT1 KO, although the third of three guide RNAs is perhaps the most efficient, as protein levels are reduced but not absent in UACC903 and WM1799 cell lines (Figure 4.6B). This could explain the non-significant trend toward a reduction in colony forming efficiency that we previously observed.

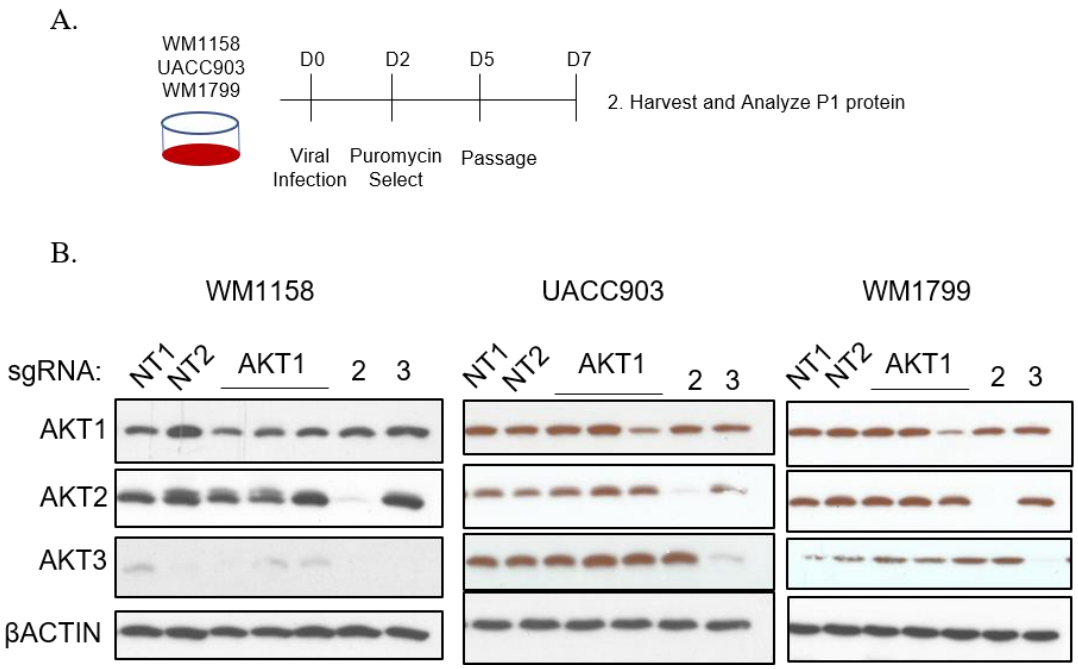

Figure 4.6. AKT1 protein persists in human melanoma cells after CRISPR/Cas9 gene editing. A) Experimental schematic of viral infection, puromycin selection, and utilization of cells for downstream assays. Three independent cell lines WM1158, WM1799, and UACC903 were infected with viruses encapsulating NT, AKT1, AKT2, or AKT3 KO LentiCRISPRV2 plasmid DNA, and selected for expression using puromycin for three days. Cells were passaged once as an initial expansion before being used for the downstream assay indicated. B) Immunoblot analysis of P1 protein in three separate human melanoma cell lines infected with the indicated guide RNAs.

Lastly, we used a subset of cells from the same bulk infected cell population from the above assays and single cell sorted them into 96-well plates containing conditioned medium from the parental line. We hypothesized that if AKT isoform loss affected the ability of individual cells to grow, we would predict that a lower percentage of colonies might result from single cells in AKT1 KO wells as compared to cells infected with alternate guide RNAs. Two 96-well plates containing single-cells were sorted for each guide RNA, and then the percentage of wells containing colonies was quantified and compared (Figure 4.7A). Additionally, up to twelve clones from each plate were randomly chosen for expansion and analyzed by immunoblotting to confirm AKT isoform KO. The results show that the percent growth of single cell colonies varied tremendously between individual human melanoma cell lines. Further, AKT1 KO did not appear to change the observed incidence of colonies per plate (Figure 4.7B). However, when a variety of clones were picked and expanded from the WM1799 cell line, none of the resulting clonal cell lines had AKT1 KO (Figure 4.7C). This phenomenon was not specific to AKT1 however, as clones that were analyzed from bulk populations infected with AKT2 or AKT3 guide RNAs also did not have AKT isoform KO (data not shown). No further clones from additional cell lines were analyzed however, so it remains unknown if this was the case in the WM1158 cell line, and no viable clone were obtained from UACC903 cells.

Taken together, these data suggest that AKT1 loss in human melanoma cell lines is not easily achieved, however the mechanisms promoting AKT1 protein retention are not clear. Specifically, an outstanding question is how puromycin selected cells, which should represent cells expressing both Cas9 and the respective guide RNA, are able to

retain AKT1 protein levels initially, but over time lose detectable AKT1 protein expression. To more fully dissect the role of AKT1 in promoting melanoma cell proliferation and tumor initiation, we decided to take a genetic approach.

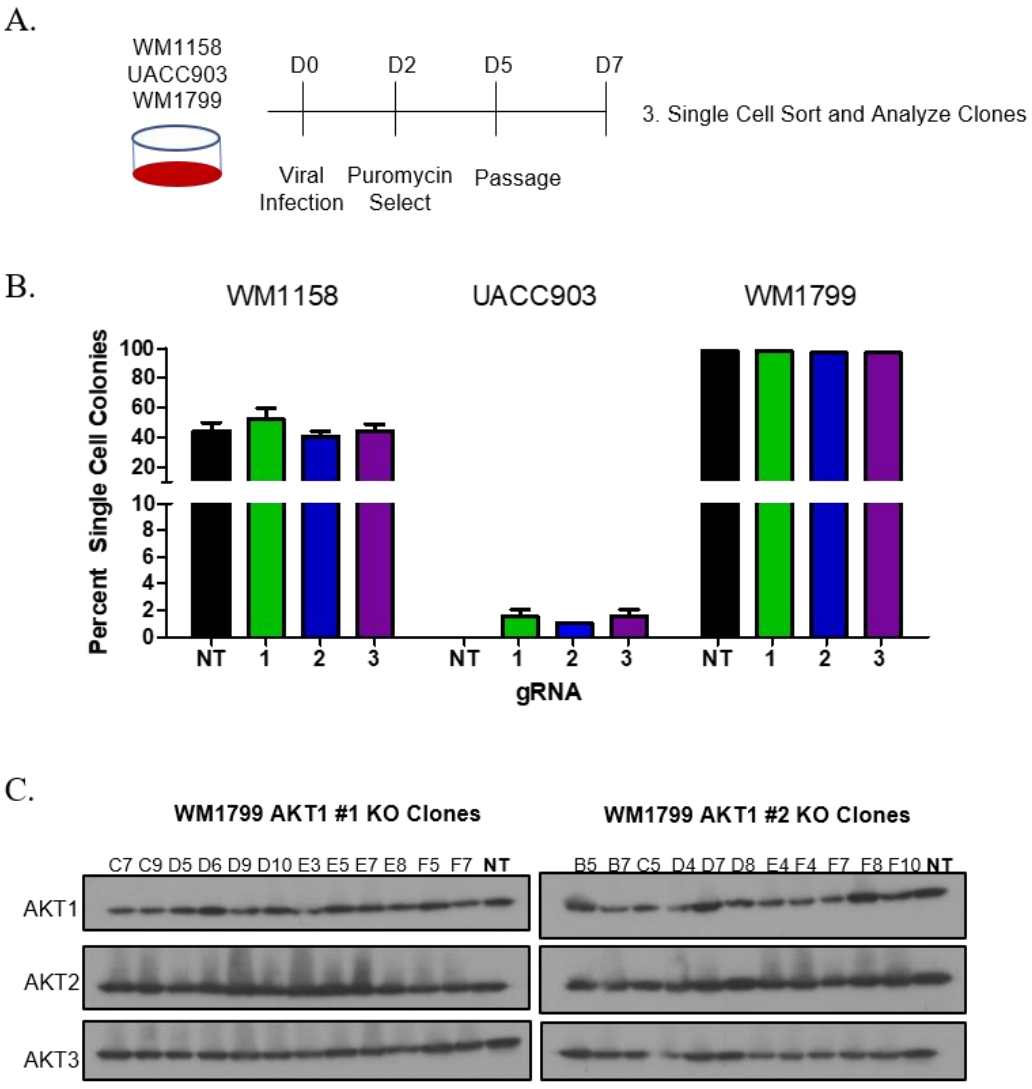

Figure 4.7. Single cell colony formation and clone validation after AKT isoform KO in human melanoma cells. A) Experimental schematic of viral infection, puromycin selection, and utilization of cells for downstream assays. Three independent cell lines WM1158, WM1799, and UACC903 were infected with viruses encapsulating NT, AKT1, AKT2, or AKT3 KO LentiCRISPRV2 plasmid DNA, and selected for expression using puromycin for three days. Cells were passaged once as an initial expansion before single cell sorting and clone isolation for analysis. B) Percent single cell colonies obtained from individual human melanoma cell lines infected with the indicated guide RNAs. Percentage of colonies represents the total number of colonies that grew in two independent single-sorted 96-well plates. C) Immunoblot analysis of 11-12 individual clones picked from two separate 96-well plates (#1 and #2, respectively) containing WM1799 cells infected with an AKT1 KO guide RNA, with cells expressing a NT guide RNA (last well) as a control for AKT1 protein expression.

4.2.4 Akt1 promotes $BRAF^{V600E}$ murine melanoma initiation

In an effort to more fully understand the role of Akt1 in melanoma initiation, we chose to investigate whether Akt1 germline ablation could alter melanoma penetrance in a murine model. The lab previously developed a mouse model of $BRAF^{V600E}$-driven spontaneous melanoma in which Akt phosphorylation is observed in tumors but not normal skin (Goel et al., 2009), suggesting Akt is important for tumor initiation in this model, and ideal for dissecting the role of individual Akts to the tumor initiation process. First, we isolated cell lines (Tufts University Mouse Melanoma, TUMM) from spontaneously arising primary tumors from mice which have melanocyte-targeted human $BRAF^{V600E}$ and cooperating Arf loss (see Materials and Methods for genotypes). The Arf tumor suppressor is commonly lost in human melanomas and increases melanoma penetrance in our model (Luo et al., 2013). Analysis of Akt isoform phosphorylation in TUMM lines indicated ubiquitous total Akt phosphorylation on the activating residue serine 473, and readily detectable phosphorylation of the Akt1 isoform (Figure 4.8A). Additionally, consistently detectable Akt3 phosphorylation was observed in most cell lines, however, Akt2 phosphorylation was not as readily detectable in the cell lines tested (Figure 4.8A). These results suggest that active Akt2 may be less important than activating phosphorylation of Akt1 or Akt3 for primary melanoma formation, at least in this BRAF-driven model.

Taken together with our previous data suggesting a role for AKT1 in human melanoma cells, this data is consistent with the hypothesis that Akt1 may support cell proliferation, while Akt2 may not be required for melanoma growth. However, since we had also observed previously that Akt2 is important for metastasis but not for cell

proliferation in human melanoma cell lines, we wondered if Akt2 could play a similar role in murine melanoma cells. To investigate if there is a requirement for Akt2 phosphorylation during the process of metastasis, distinct from melanoma initiation, we injected SM1-750 cells (to be described in depth in Chapter 5) into the tail veins of C57BL6/J mice. We saw that these cells readily colonized the lungs (Figure 4.8B) and metastasized to distant organs such as the brain and liver (Figure 4.8D). Isolation of discrete lung metastases from individual mice and analysis of Akt2 phosphorylation revealed that in contrast to cell lines injected into the tail vein, which initially lacked detectable Akt2 phosphorylation, the majority of lung metastases displayed increased levels of detectable Akt2 phosphorylation (Figure 4.8C). Additional follow-up studies attempted to determine if Akt2 phosphorylation was enhanced by extraneous factors such as subcutaneous tumor growth, low oxygen conditions, or 3D non-adherent culture conditions, but none of these other scenarios resulted in detectable changes in Akt2 phosphorylation (data not shown). These collective results suggest that while Akt1 may be vital for murine melanoma initiation, Akt2 may be important for the process of murine metastasis.

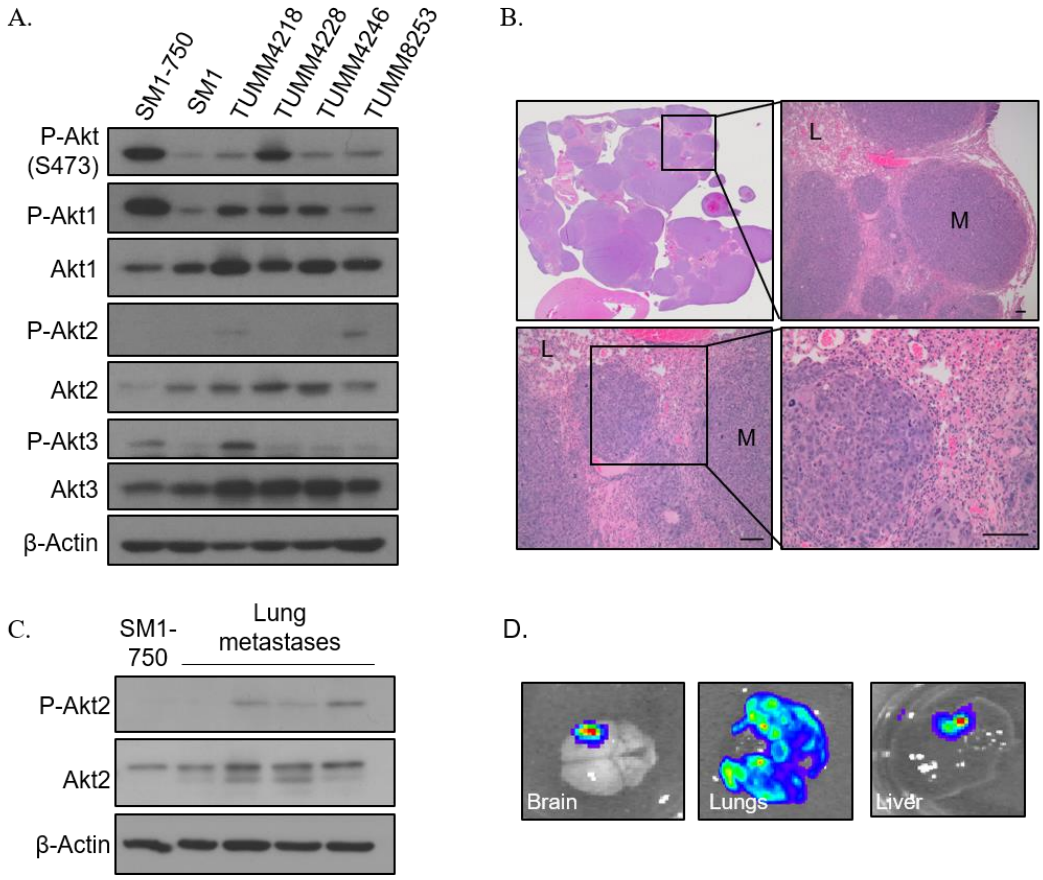

Figure 4.8. Characterization of Akt levels and phosphorylation in $BRAF^{V600E}$ murine melanoma cell lines and metastases. A) Cell lines were isolated from individual tumors containing $BRAF^{V600E}$ and/or cooperating Arf loss, and were screened for Akt isoform phosphorylation and protein levels by immunoblotting. B) The metastatic potential of SM1-750 cell lines was evaluated by injecting $1x10^6$ cells into the tail veins of C57BL6/J mice (n=4), and then lungs were fixed, paraffin embedded, and stained with H&E at 4 weeks post-injection. Scale bar 100μm. L=lung, M=metastasis. C) Metastases were isolated from lungs of individual mice and were analyzed for Akt2 protein and phosphorylation by immunoblotting. D) Intravital imaging of organs isolated from C57BL6/J mice at 4 weeks post injection shows the presence of tumor cells in the brain, lungs, and liver.

Table 4.1. Akt1 germline ablation extends survival of melanoma prone mice

Genotype	Median Survival (Days)	P-Value	Cohort Size (#)	Tumor Incidence
$BRAF^{V600E}$; $Arf^{-/-}$	102	--	96	54/96 (56.3%)
$BRAF^{V600E}$; $Arf^{-/-}$; $Akt1^{-/-}$	125	**0.0025	50	27/50 (54%)
$BRAF^{V600E}$; $Arf^{-/-}$; $Akt2^{-/-}$	101	n.s.	87	45/87 (51.7%)
$BRAF^{V600E}$; $Arf^{-/-}$; $Akt3^{-/-}$	109.5	n.s.	86	45/86 (52.3%)

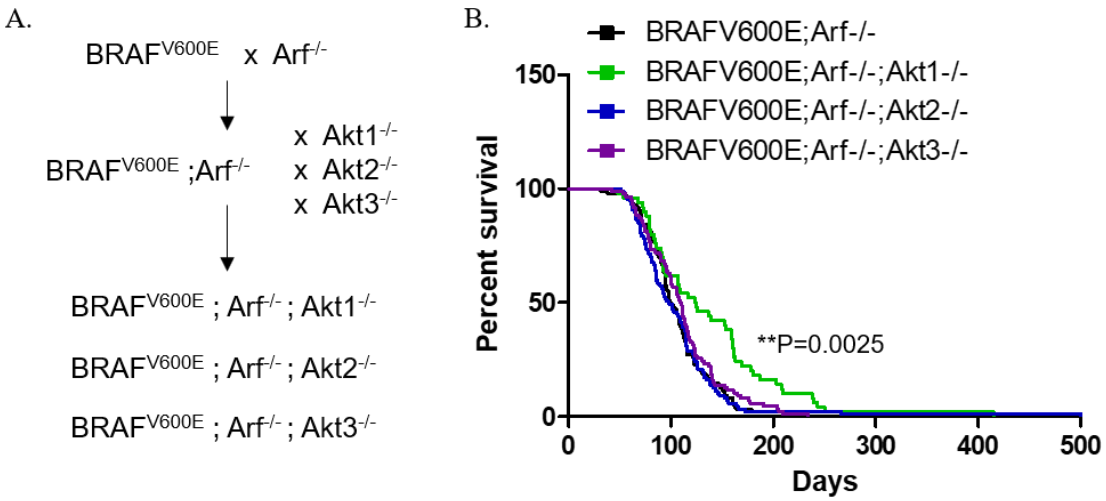

Figure 4.9. Akt1 genetic ablation extends overall survival of melanoma prone mice. A) Breeding scheme to generate Akt null melanoma prone mice. Whole body Akt isoform KO mice were crossed with mice expressing melanocyte specific $BRAF^{V600E}$ in addition to mice with whole body Arf loss. Resulting mice have combined loss of Arf and Akt, with melanocyte-specific $BRAF^{V600E}$ expression. B) Overall survival was evaluated using Kaplan-Meyer Survival analysis, to test the effect of Akt isoform loss on overall survival of melanoma prone mice. **P<0.01 by Log-Rank (Mantel-Cox) Test.

To further determine a requirement for Akt1 in melanoma initiation, we crossed $BRAF^{V600E}$; $Arf^{-/-}$ mice to Akt isoform KO mice, generating melanoma prone mice with germline ablation of each individual Akt isoform (Figure 4.9A). This work was done in collaboration with the post-doctoral researcher Jodie Pietruska, PhD.

Our results, summarized in Table 4.1, indicate that germline ablation of the Akt1 isoform, but not the Akt2 or Akt3 isoforms, extends overall survival of melanoma prone mice (Figure 4.9B). Akt1 loss enhanced survival median from 102 to 125 days, despite no significant difference in overall tumor incidence (Table 4.1). Median survival of Akt2 KO mice was nearly identical to control BRAFV600E; $Arf^{-/-}$ mice and while Akt3 KO mildly extends overall survival, this was not a statistically significant benefit (Table 4.1). We also identified the cause of death for each mouse and noted when a tumor was present. Neither the overall tumor incidence (Table 4.1) or tumor-free survival differed with Akt2 or Akt3 loss, but Akt1 loss appeared to enhance survival of tumor-bearing mice (**P=0.0016 by log-rank test, data not shown). It should be mentioned that these results do not represent melanoma-free survival, and tumor incidence may also refer to tumors other than melanoma, such as lymphomas or sarcomas which are commonly associated with Arf loss. Given that the overall penetrance of murine melanoma in $BRAF^{V600E}$;$Arf^{-/-}$ mice is roughly 40% percent (Luo et al., 2013), it is likely that Akt1 loss extends overall survival at least in part by limiting melanoma incidence. However, at this time, attempts to dissect the direct contribution of Akt isoform loss to melanoma penetrance with respect to parsing tumor origin and identity are still ongoing.

As an additional approach to characterize how Akt may impact melanoma initiation or progression, we combined genetic loss of Akt with UV-irradiation exposure.

As previously mentioned, UV irradiation is the largest environmental contributor to melanoma development, and as a result, melanomas are enriched for UV-signature mutations (Lawrence et al., 2013; Siegel et al., 2017). It was previously determined that $BRAF^{V600E}$;$Arf^{-/-}$ mice are sensitized to UV irradiation, such that the spectrum of tumors is shifted toward melanoma formation (Luo et al., 2013). We took advantage of this to understand how Akt isoform loss may affect mice exposed to UV-irradiation. Specifically, mice were exposed to 750 mJ/cm^2 of UV-B irradiation at post-natal day (PND) 3.5 and monitored for tumor formation (Figure 4.10A). Only mice with $BRAF^{V600E}$ expression developed tumors, in comparison to Arf null mice lacking $BRAF^{V600E}$ expression (data not shown), recapitulating previously published results (Luo et al., 2013). The tumors were unpigmented but subcutaneous, supporting a likely origin from epidermal melanocytes. $BRAF^{V600E}$; $Arf^{-/-}$ mice that were UV-irradiated had a median survival of 69 days (Table 4.2), reduced in comparison to a 102-day median survival in non-irradiated mice (Table 4.1). While results from Akt1 ablated mice are still in process, our results from Akt2 ablated mice show that Akt2 KO had no effect on overall survival of UV-irradiated mice (Figure 4.10), despite a slight increase in median survival (Table 4.2). In contrast, Akt3 ablation enhanced median survival from 69 to 82 days, a significant survival benefit in comparison to UV-irradiated control mice (Table 4.2).

Taken together, these results support an important role for Akt1 in promoting melanoma, as melanoma prone mice had enhanced overall survival when Akt1 was ablated. Akt2 does not appear to be required for melanoma initiation or progression, but

in murine cell lines, may promote metastasis. Additionally, Akt3 may play an important role in the process of UV-initiated melanoma progression.

Table 4.2. Akt3 germline ablation extends median survival of UV-irradiated melanoma prone mice.

Genotype	Median Survival (Days)	P-Value	Cohort Size (#)	Tumor Incidence
$BRAF^{V600E}$; $Arf^{-/-}$	69	--	29	27/29 (93.1%)
$BRAF^{V600E}$; $Arf^{-/-}$; $Akt1^{-/-}$	--	--	--	--
$BRAF^{V600E}$; $Arf^{-/-}$; $Akt2^{-/-}$	78	n.s.	28	26/28 (92.8%)
$BRAF^{V600E}$; $Arf^{-/-}$; $Akt3^{-/-}$	82	**0.009	14	10/14 (71.4%)

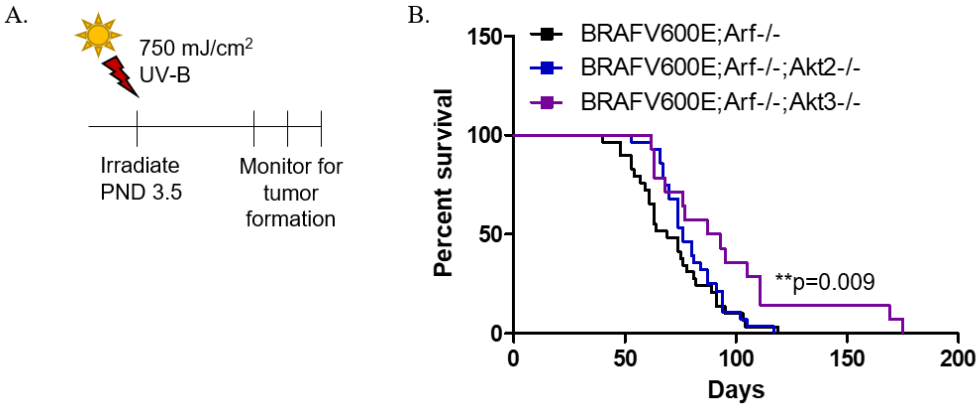

Figure 4.10. Akt3 germline ablation extends overall survival of UV-irradiated melanoma prone mice. A) Experimental schematic. $BRAF^{V600E}$;$Arf^{-/-}$;$Akt^{-/-}$ mice were irradiated with 750mJ/cm^2 of UV-B at post-natal day (PND) 3.5 to induce melanoma formation. B) Kaplan-Meyer survival curves of UV-irradiated melanoma prone mice by genotype. **P<0.01 by Log-Rank (Manel-Cox) Test.

4.3 Summary and Significance

In this chapter, we evaluated the role of AKT1 in melanoma cell proliferation and tumor initiation. We observed that AKT1 KD impairs cell proliferation and cell cycle progression in a variety of human melanoma cells using shRNA. We found that AKT1 supports subcutaneous tumor growth *in vivo*, consistent with the finding that AKT1 KD impairs anchorage independent growth. Additionally, we probed the dynamics of AKT1 KO, finding that AKT1 persisted in gene edited cells and may be required for the growth of single cells.

Lastly, we interrogated a requirement for Akt1 in murine melanoma initiation, by genetically ablating Akt isoforms in a murine model of melanoma. We observed that among the isoforms, murine tumors show Akt1 and Akt2 phosphorylation but Akt2 is not phosphorylated. Similarly, Akt1 ablation in murine melanomas extends the survival of melanoma prone mice, but ablation of Akt2 has no effect. Lastly, UV irradiation of melanoma prone mice increases melanoma penetrance, and surprisingly, Akt3 ablation in this context extends overall survival while Akt2 does not.

Taken together, these results provide evidence that Akt1 may be important in promoting melanoma initiation and tumor progression. While Akt1 is well known to support cell proliferation in other cancers, this role has not been exclusively described in melanoma. Furthermore, our novel mouse model combines environmental and genetic risk factors to model Akt isoform loss in melanoma, which has not been done previously. With Akt inhibitors in clinical development, clarifying the role of Akt pathway effectors could help inform and define improved therapeutic strategies moving forward.

Chapter 5. Tumor targeted and combination therapies for improved delivery and efficacy of AKT and other kinase inhibitors *in vivo*

5.1 Introduction

A major drawback associated with targeted therapy has been the development of resistance mechanisms that make single-agent inhibition ineffective over the long term. Combination therapy, often using single agents that synergize together, is a more effective anti-tumor strategy, but few promising compounds with anti-melanoma efficacy have been identified. As discussed previously, combination therapies largely consist of dual kinase inhibition within the MAPK pathway, or dual immune checkpoint blockade, but few studies have sought to combine targeted therapies with immunomodulatory approaches in melanoma thus far.

It is well known that the tumor microenvironment plays an essential role in supporting tumor growth, immune-evasion, and metastatic potential (Quail and Joyce, 2013). Fibroblast activation protein (FAP) is a serine protease, and as the name implies, it is a marker of activated fibroblasts that are present during embryogenesis, tissue damage, and wound healing, but generally absent in adult tissues (Keane et al., 2013). It was noted that FAP is aberrantly expressed in tumor-associated fibroblasts (Kraman et al., 2010; Lee et al., 2005), and FAP expression on tumors correlated with poor prognosis (Liu et al., 2015). FAP is also found in reactive stromal fibroblasts surrounding melanoma lesions (Huber et al., 2003), which makes it a useful antigen for tumor-targeting to the microenvironment.

Many studies have used FAP as a tumor marker to produce vaccines, and mice immunized against FAP are protected from tumor formation or experience tumor

regression in a variety of carcinoma models (Chen et al., 2015; Kraman et al., 2010; Lee et al., 2005). Further, use of inhibitors of FAP or similar serine proteases has shown efficacy against growth of established tumors, in part by mediating anti-tumor immune responses (Walsh et al., 2013). While the mechanisms of this immune-mediated anti-tumor activity is incompletely understood, serine protease inhibitors have been shown to trigger a form of proinflammatory cell death in monocytes and macrophages known as pyroptosis (Okondo et al., 2017) through activation of an inflammasome sensor protein mediated by caspase-1 (Okondo et al., 2018).

The exploitation of FAP as a tumor microenvironmental marker and its activity as a serine protease have been harnessed for tumor-targeted therapeutics. First, a peptide carrier containing a preferential FAP cleavage site is conjugated to a cytotoxic compound of interest. In this conjugated form, the peptide renders the cytotoxic compound inactive by limiting its ability to cross cell membranes, and this conjugated molecule is known as a prodrug. Once the prodrug reaches the vicinity of the tumor microenvironment where FAP is expressed, the peptide moiety is cleaved, and the cytotoxic compound becomes active, delivering its intended cytotoxic effects within the tumor microenvironment (Brennen et al., 2012). In murine breast and prostate cancer models, FAP-activated prodrugs had slower clearance from tumor tissue than circulation, persisted within the tumor, and had marked anti-tumor activity (Brennen et al., 2014). Other types of targeted prodrugs have been used with some success in melanoma recently (Liu et al., 2017a) but to date, no FAP-activatable prodrugs have been utilized as anti-melanoma therapies.

We sought to determine first whether tumor-targeted approaches using FAP could be harnessed for enhanced delivery of AKT-inhibitors to the tumor microenvironment,

and further, whether inhibiting serine protease activity like FAP would synergize with approved targeted therapies such as the $BRAF^{V600E}$ inhibitor Vemurafenib for enhanced anti-melanoma activity.

5.2 Results

5.2.1 Adaptation of a murine melanoma cell line for syngeneic tumor studies

While tumor studies performed in immunocompromised mouse models are useful for their tolerance of human material, the presence of an immune system is a critical element when designing and testing immune-modulating therapies. Recently, a $BRAF^{V600E}$-driven murine model of melanoma, termed SM1, was developed which is syngeneic to fully immunocompetent mice (Koya et al., 2012). Briefly, the SM1 melanoma cell line was derived by Ribas and colleagues from a spontaneous $BRAF^{V600E}$ melanoma, passaged in a C57BL6/J mouse, and was subsequently isolated for growth in culture (Steps 1-4, Figure 5.1A). After obtaining SM1 cells as a generous gift, we found it did not readily grow with more than 50% frequency in our C57BL6/H mice (H; Hinds), and the majority were able to resolve tumor lesions within 1-2 weeks of implantation (data not shown). Therefore, we further passaged SM1 cells in C57BL6/H mice within our colony and re-derived the cell line for use in subsequent tumor studies (Steps 5-7, Figure 5.1A). The resulting cell line, known as SM1-750, reproducibly formed tumors with 100% penetrance in immunocompetent C57BL6/H and J mice within 14 days, with robust growth efficiency such that tumors reached maximum allowable size limits within 30-40 days.

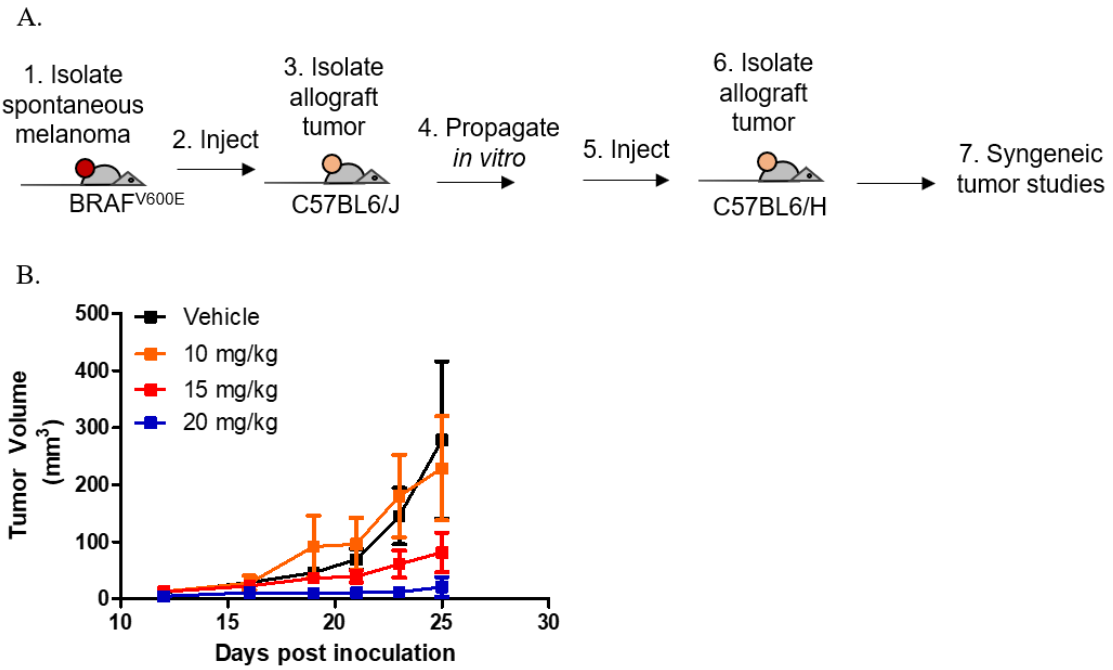

Figure 5.1. SM1-750 is a Vemurafenib responsive syngeneic tumor model. A) Experimental schematic of the derivation and propagation of the SM1 murine melanoma model (Steps 1-4), to make the SM1-750 model (Steps 5-7) used in future studies. B) Two million SM1-750 cells were injected subcutaneously in C57BL6/H mice and treated with indicated doses of the BRAF inhibitor Vemurafenib by daily intraperitoneal injection. Tumors were measured using calipers. N=5 mice per group.

To further characterize this cell line model, we validated that in accordance with its $BRAF^{V600E}$ mutational status, resulting allograft tumors were responsive to inhibition by the BRAF inhibitor Vemurafenib. To test this, we subcutaneously injected SM1-750 cells in C57BL6/J mice and waited for palpable tumors to form. Once tumors reached 3-5mm in diameter, mice were randomized into treatment groups receiving vehicle treatment, or experimental doses of 10, 15, and 20 mg/kg of Vemurafenib. Consistent with published results in SM1 cells (Koya et al., 2012), SM1-750 tumors displayed a dose-response dependent inhibition of tumor growth (Figure 5.1B). However, while growth was severely inhibited during treatment, we did not observe tumor regression, and discontinuation of daily Vemurafenib dosing resulted in tumor re-growth. This transient, but dose-dependent inhibition makes this tumor model ideal for testing novel combination therapies.

5.2.2 Characterization of small molecule AKT inhibition in SM1-750 murine melanomas

An inhibitor currently in clinical development for the inhibition of AKT signaling is MK-2206, an allosteric inhibitor of hyperactive AKT. This drug inhibits all isoforms of AKT, and as a result, has broad toxicity and myriad off-target effects. We hypothesized that conjugating MK-2206 to a FAP-cleavable peptide moiety, thereby creating an inactive prodrug, would reduce off-target effects, target MK-2206 to the tumor, and enhance its efficacy. The Bachovchin lab at Tufts University was able to synthesize an inactive FAP-cleavable prodrug of MK-2206, which they denoted ARI-5173. However, before we could directly compare the anti-tumor activity to that of ARI-5173, we first

had to determine if MK-2206 alone had the ability to inhibit AKT in murine SM1-750 cells, and the necessary dose to use for *in vivo* tumor studies.

To begin studying the efficacy of MK-2206 alone, we first treated SM1-750 cells in culture. SM1-750 cells were treated with increasing doses of MK-2206, from 1-12μM, or an equivalent concentration of DMSO for a period of 72 hours. We observed that compared to DMSO-treated cells, AKT phosphorylation on the S473 residue became undetectable with increasing MK-2206 dose (Figure 5.2). AKT1-specific phosphorylation was comparable to control at the 1μM dose, with a dose dependent reduction starting at 5μM. AKT2 phosphorylation was not detectable, as expected for the majority of murine melanoma cell lines (Figure 5.2). Downstream AKT signaling was inhibited by MK-2206 with as little as 1μM showing a decrease in phosphorylation of downstream AKT target PRAS40. Additionally, we observed that cleaved PARP, an indicator of apoptotic cell death, was increasingly detectable at doses of 5μM and higher (Figure 5.2). This suggests that MK-2206 has the ability to inhibit AKT signaling and induce cell death in this murine cell model, and therefore may be suitable to test *in vivo.*

Based on published literature, MK-2206 displays anti-tumor activity in a variety of tumor models *in vivo*, with oral doses ranging from 120-360 mg/kg 3x weekly (Hirai et al., 2010). However, in murine melanoma, a dose of 480 mg/kg/wk was reported (Marsh Durban et al., 2013), therefore we chose to dose our mice with either 360mg/kg three times weekly, or a single weekly dose of 480mg/kg as an initial pilot experiment. We injected C57BL6/H mice subcutaneously with SM1-750 melanoma cells, and after palpable tumors reached 3-5mm in diameter, we initiated a dosing schedule of vehicle (15% Captisol, n=3), 240 mg/kg three times per week (n=3) or a single weekly dose of

480 mg/kg. All doses were given orally by gavage, as recommended and previously described in the aforementioned reports (Hirai et al., 2010; Marsh Durban et al., 2013). Our results, shown in Figure 5.3, show that mice receiving MK-2206 experienced significant toxicity. MK-2206 was initially effective, as tumors shrank within 24 hours of the initial dose, but the majority of mice could not tolerate additional dosing (Figure 5.3A). Mice given MK-2206 lost significant weight very quickly; mice experiencing loss of >15% of their initial body weight are considered moribund and require humane euthanasia. Two of three mice in both MK-2206 experimental groups met this criteria within 24 hours of the initial dose (Figure 5.3B). The third and final mouse in both groups received a second dose of either 240mg/kg or 480mg/kg on schedule, and this continued dosing schedule was not tolerated. While a molecular characterization of vital organs by histology was not carried out, necropsies of the deceased mice showed inflammation of the intestinal tract and colon with visibly enlarged blood vessels, as well as a pale enlarged liver (data not shown). This toxicity is consistent with the given oral route of administration, as drug exposure would first occur within the gut and then be absorbed and metabolized by the liver. These results confirm our hypothesis that MK-2206 has anti-tumor activity but is not a viable therapy due to its wide toxicity. We therefore decided to move forward with testing the tumor-targeted prodrug version of MK-2206, ARI-5173, in murine melanomas.

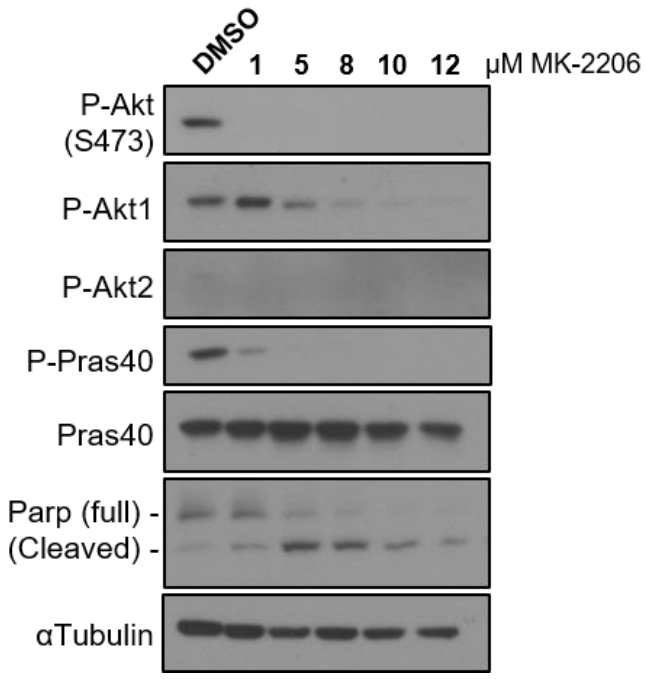

Figure 5.2. MK-2206 inhibits Akt phosphorylation and downstream signaling in the SM-750 murine melanoma cell line. MK-2206 was dissolved in sterile DMSO, and further diluted in culture media to the indicated concentrations. Cells were treated for a period of 72h before analysis by immunoblotting with the indicated antibodies.

A.

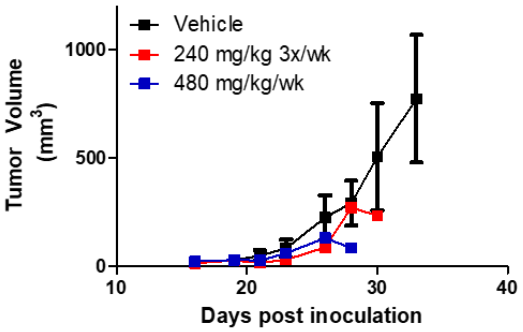

B.

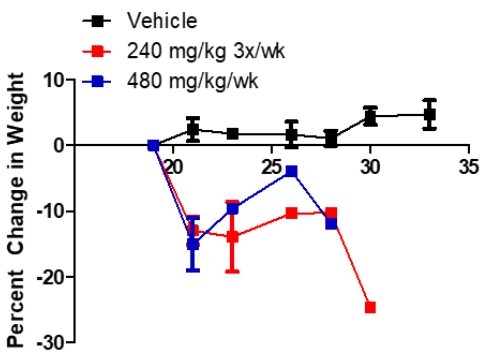

Figure 5.3. MK-2206 inhibits tumor growth of SM1-750 murine melanomas. A) C57BL6/H mice (n=3 per group) were injected subcutaneously with two million SM1-750 cells and when tumors reached 3-5mm in diameter, mice were gavaged with vehicle (15% Captisol), MK-2206 (240mg/kg 3x/wk), or MK-2206 (480mg/kg/wk). Tumors were measured using calipers. B) Percent change in weight (y-axis, grams) over the treatment period (x-axis, days post inoculation) for each group.

5.2.3 ARI-5173, a tumor-targeted prodrug of the AKT inhibitor MK-2206

Before evaluating tumor inhibition by ARI-5173 in established tumors, we first wanted to confirm that our SM1-750 tumor bearing mice had detectable FAP activity, sufficient to cleave the prodrug to its active form. To do this, we isolated subcutaneous SM1-750 tumors from C57BL6/H mice and submitted them to the Bachovchin lab for routine analysis of FAP activity using enzymatic methods previously described (Keane et al., 2013). The results show that FAP activity, while variable in 3 individual SM1-750 tumors samples, is elevated (Figure 5.4A) compared to mouse plasma FAP activity, which is typically measured at levels <0.5 pmol AMC/min/mg tissue (Keane et al., 2013). This result suggests that SM1-750 tumors have FAP activity and may be capable of cleaving an FAP-activatable prodrug.

Next, we wanted to ensure that oral administration of ARI-5173 would concentrate to the tumor microenvironment. To test this, we designed an experiment in which we administered a single dose of either ARI-5173 or Vehicle to mice bearing subcutaneous SM1-750 tumors, and then measured the amount of MK-2206 that was present in the tumor compared to the plasma. We hypothesized that mice treated with ARI-5173 would have enhanced MK-2206 in the tumor compared with the plasma. We treated mice orally with a single dose of either 120mg/kg or 240 mg/kg of ARI-5173, and after just four hours collected samples for comparison. Our results show that consistent with enhanced FAP activity in the tumor microenvironment of SM1-750 tumor bearing mice, there was up to three times more MK-2206 detected in tumors compared to plasma (Figure 5.4B). While we cannot rule out that proteases other than FAP may have cleaved

the ARI-5173 prodrug, it is highly likely that ARI-5173 was cleaved to MK-2206 at the site of the tumor microenvironment by FAP activity.

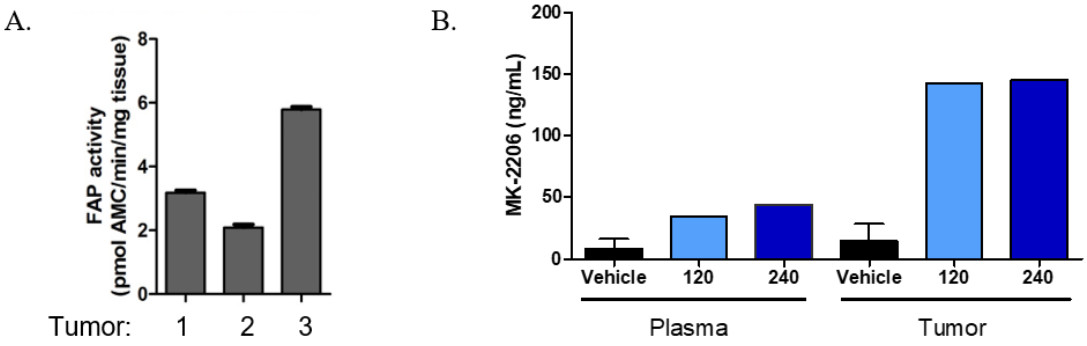

Figure 5.4. FAP activity is present in SM1-750 tumors and cleaves the inactive prodrug ARI-5173 to active MK-2206 at the site of the tumor. A) FAP activity was measured in 3 independent SM1-750 tumors from C57BL6/H mice. B) C57BL6/H mice bearing SM1-750 tumors were dosed with vehicle, 120mg/kg, or 240mg/kg of ARI-5173, and four hours later, tumor and plasma samples were collected and assayed for MK-2206 cleaved by FAP using mass spectrometry.

Next, we endeavored to investigate whether treating tumor bearing mice with ARI-5173 would be an improved therapeutic strategy in comparison to MK-2206 alone. Because MK-2206 showed toxicity at 240mg/kg, we opted to use half the concentration, a dose of 120mg/kg. Our previous experiment also showed that using 240mg/kg of ARI-5173 did not result in increased MK-2206 concentrated to the tumor compared to a dose of 120mg/kg (Figure 5.4B), therefore we chose this dose as the optimal concentration for both drugs in this initial study. Unfortunately, because ARI-5173 must be synthesized and is not commercially available, our limited supply only allowed for administration of two doses at 120mg/kg. Therefore, we opted to adjust our dosing strategy in order to maximize tumor inhibition by giving two sequential doses of ARI-5173 or MK-2206 without allowing one day recovery in between doses.

The results of this experiment show that giving just two early drug doses was not sufficient to inhibit tumor growth in either the MK-2206 or ARI-5173 groups (Figure 5.5A). However, when percent change in tumor growth is plotted pot-treatment for each individual tumor (n=3), it is apparent that ARI-5173, but not MK-2206, does achieve a transient tumor inhibition (Figure 5.5B). This subtle effect is lost when mice are grouped together and could represent inter-individual differences in FAP expression. Mice receiving MK-2206 did not lose substantial weight compared to previous experiments, consistent with a lower, less toxic dose Figure 5.5C). Interestingly, one mouse receiving ARI-5173 experienced 10% weight loss, and this mouse also had the largest initial inhibitory tumor response. Further studies with sustained dosing regiments and dissection of FAP activity, in addition to an analysis of intra-tumoral cellular signaling will be required to determine if tumor-targeted ARI-5173 has enhanced efficacy compared to

MK-2206. However, these initial pilot studies give credence this approach, and demonstrate the FAP-activatable MK-2206 prodrug ARI-5173 has potential for enhanced selectivity and efficacy against melanoma tumors.

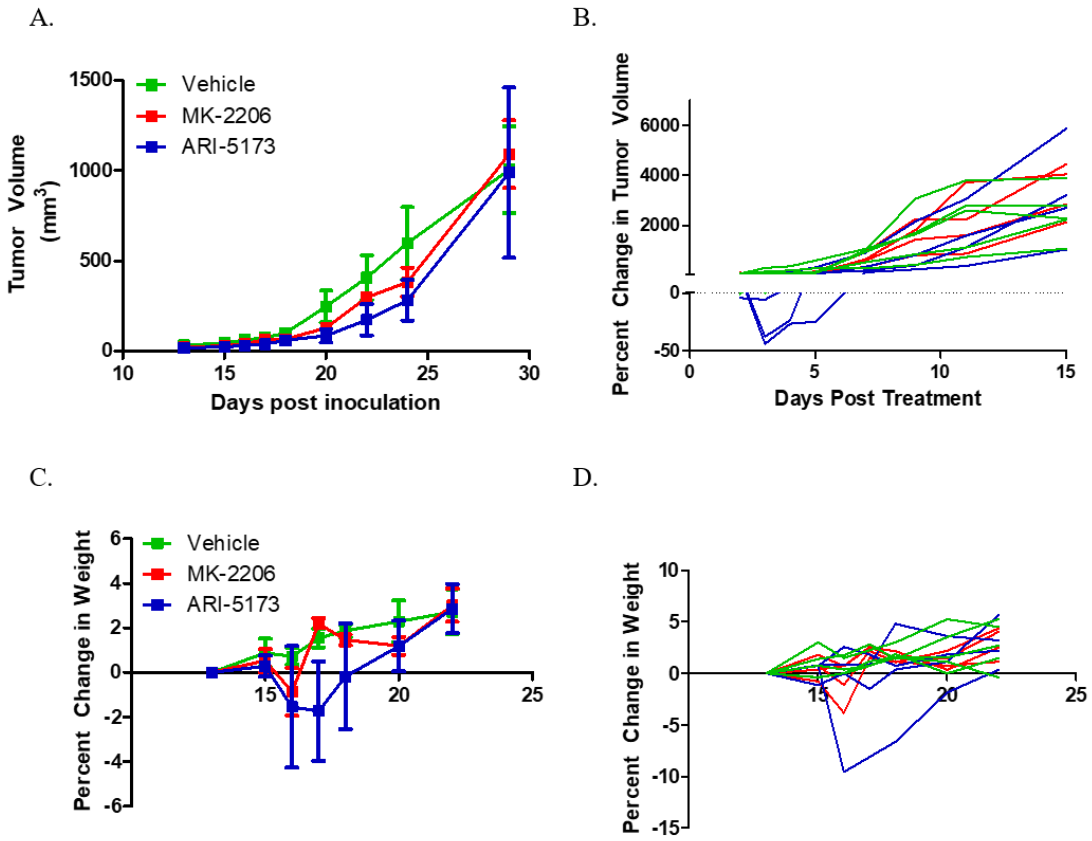

Figure 5.5. The FAP-activatable prodrug ARI-5173 has transient anti-tumor activity in SM1-750 murine melanomas. A) C57BL6/J mice bearing SM1-750 tumors (N=3-4 per group) were dosed by gavage with 120mg/kg of MK-2206, 120mg/kg ARI-5173, or Vehicle at days 15 and 16 post-inoculation, and tumors were measured using calipers. B) Percent change in tumor volume was calculated and individual tumors are represented. C) Percent change in weight for each group. D) Percent change in weight (y-axis) for each individual mouse is plotted as a function of days post-inoculation (x-axis). Green=Vehicle, Red=MK-2206, Blue=ARI-5173.

5.2.4 ARI-4175 is a serine protease inhibitor with immune-mediated anti-tumor activity that synergizes with BRAF inhibition in murine melanomas

In addition to its utility as a tumor antigen or marker of the tumor microenvironment, the serine protease FAP has also been implicated in supporting tumor progression and metastasis in a variety of tumor types. Because we established that FAP serine protease activity occurs in our SM1-750 tumors, we hypothesized that inhibiting FAP may have anti-tumor effects. As an initial approach, we took advantage of the pan-inhibitor denoted as ARI-4175 (Figure 5.6A), which has been shown to efficiently inhibit the dipeptidyl peptidase-4 activity and/or structure homolog (DASH) family of enzymes, including FAP, and initiate immune-mediated tumor regression in murine rhabdomyosarcoma, colon cancer, and breast cancer models (Donahue et al., 2014; Duncan et al., 2013). We sought to determine if ARI-4175 would have efficacy against melanoma, and further, if it may be a viable co-treatment with targeted therapies such as Vemurafenib.

As an initial experiment, we injected SM1-750 tumor cells in C57BL6/J mice and waited for palpable tumors to form. Next, we tested a previously published dosing and treatment schedule involving 200µg of ARI-4175 per mouse given daily by gavage for five consecutive days, followed by a two day rest period (Donahue et al., 2014). With this dosing scheme, we were able to achieve moderate anti-tumor activity, but the difference in tumor growth was not significantly different between the two groups (Figure 5.6B).

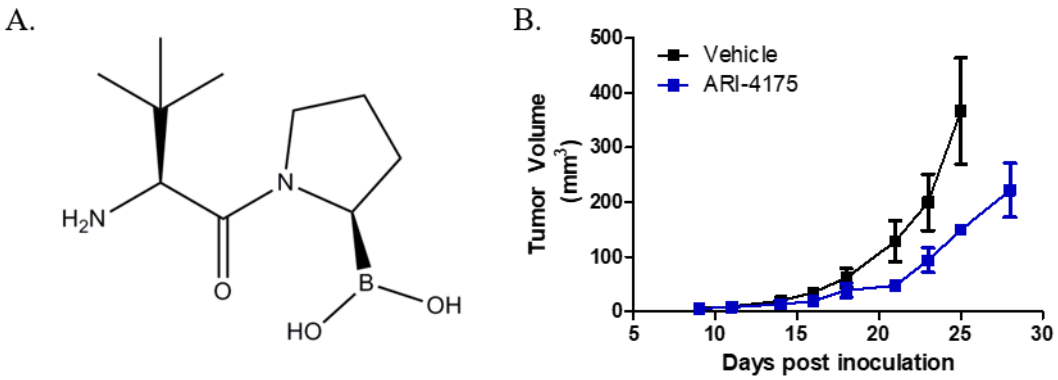

Figure 5.6. The pan-DASH serine protease inhibitor ARI-4175 inhibits tumor growth of SM1-750 murine melanomas. A) The chemical structure of ARI-4175, a boronic acid and pan-DASH serine protease inhibitor. B) C57BL6/J mice were injected subcutaneously with two million SM1-750 cells, and vehicle or ARI-4175 dosing was administered at 200µg/mouse by gavage on a five day on two day off schedule. P=n.s.

Next, we performed a combination treatment with the BRAF inhibitor Vemurafenib. We injected C57BL6/J mice with SM1-750 cells and waited for palpable tumors to form. Once tumors reached 3-5mm in diameter, we randomized the mice into one of four treatment groups (n=8-10 mice per group). The mice either received vehicle combination treatment (control), 30mg/kg Vemurafenib given daily by i.p. injection, ARI-4175 given orally by gavage on a five day on, two-day rest schedule, or the combination. The drugs were not given simultaneously; Vemurafenib was dosed in the morning, and ARI-4175 was dosed six to eight hours later. The results were highly encouraging, with mice tolerating a full 2 weeks of sustained dosing. Mice receiving the combination treatment had substantially reduced tumor growth, and this was significantly less than control mice, and less than either ARI-4175 or Vemurafenib treatment alone (Figure 5.7A). Two-Way ANOVA statistical analysis confirmed that the combination treatment was synergistic in comparison to the other treatment groups. This is best illustrated by examining the percent change in tumor growth, which shows that ARI-4175 and Vemurafenib were nearly identical in their ability to inhibit tumor growth relative to vehicle treatment, but the combination treatment was superior in its ability to inhibit SM1-750 tumor growth (Figure 5.7B). However, one contraindication of the ARI-4175 treatment seemed was enhanced weight loss observed in both the ARI-4175 and combination groups. Mice lost nearly 15% of their total body weight, the maximum allowable under protocol guidelines (Figure 5.7C**)**. However, the two-day drug holiday was sufficient for mice to recover their full weight, and once treatment was discontinued, mice appeared to suffer no residual weight loss and gained additional weight relative to vehicle or Vemurafenib treated mice (Figure 5.7C).

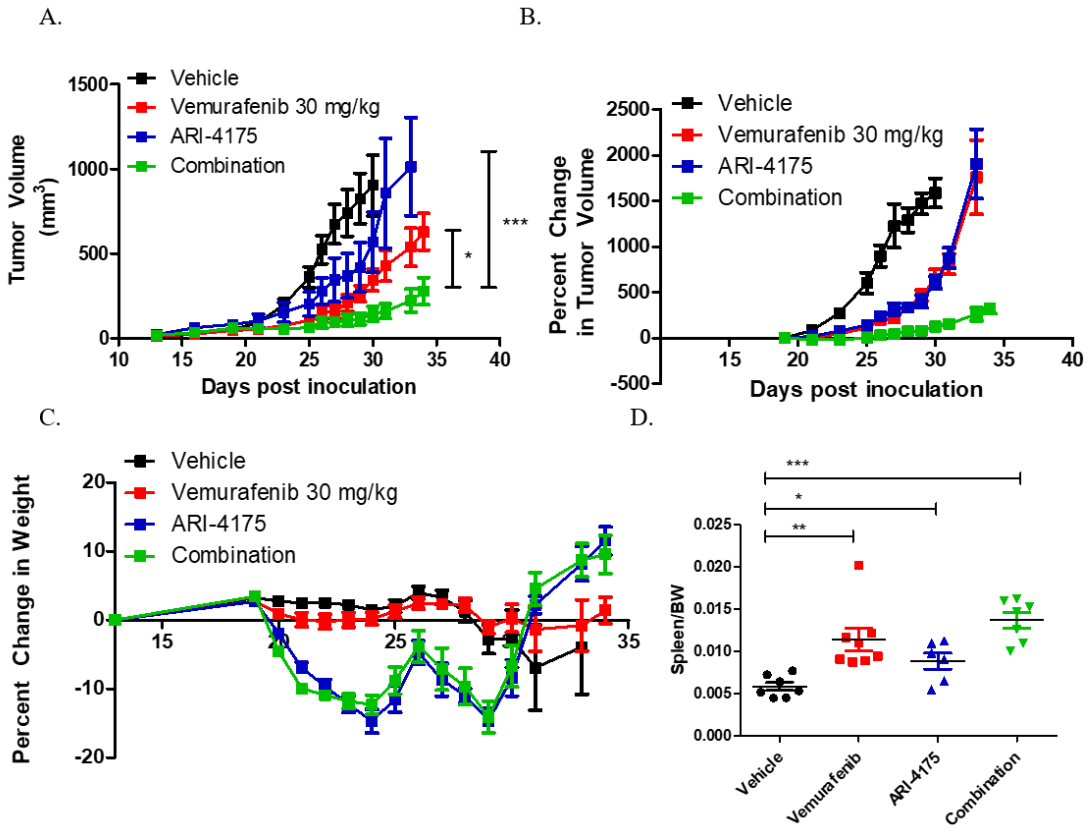

Figure 5.7. ARI-4175 synergizes with Vemurafenib to inhibit SM1-750 melanoma growth. A) C57BL6/J mice bearing SM1-750 subcutaneous tumors were randomized into groups (n=10 per group) receiving vehicle, 30mg/kg Vemurafenib i.p., 200µg/mouse ARI-4175 by gavage, or the combination, for five days on, two days rest for two weeks. Tumor growth was measured using calipers. B) Percent change in tumor volume was calculated for each group. C) Percent change in body weight (g) was recorded for each group plotted against days post inoculation. D) Spleen/Body Weight Ratio (g) is plotted for each treatment group.

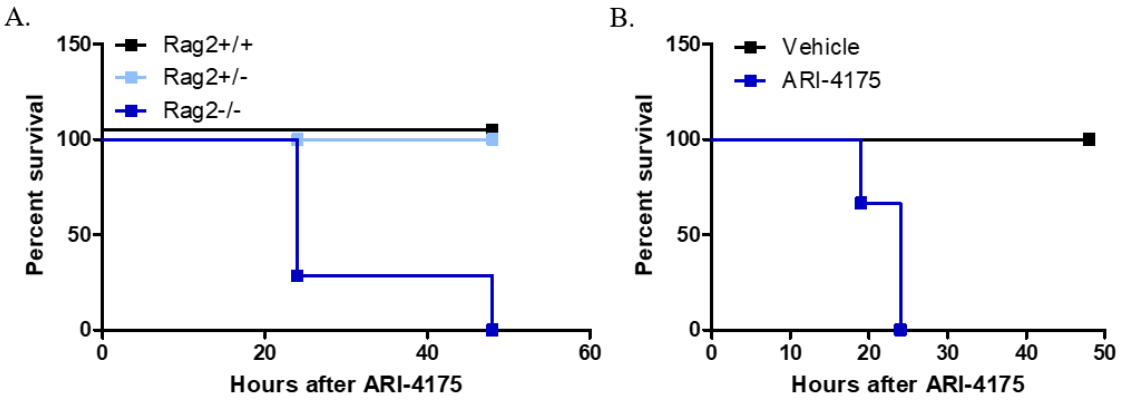

Figure 5.8. ARI-4175 is not well-tolerated in immune-deficient mice. A) Rag2 mice of varying genotypes were given a single dose of 200µg/mouse of ARI-4175 by gavage, and Kaplan-Meyer survival is plotted as a function of hours after administration. B) TCRα KO mice (n=2-3 per group) were treated with Vehicle or a single dose of 200µg/mouse of ARI-4175 by gavage, and Kaplan-Meyer survival is plotted as a function of hours after administration.

Because previous reports indicate that ARI-4175 causes tumor regression or inhibition via an immune-mediated mechanism of action, we endeavored to test the hypothesis that ARI-4175 was also mediating its anti-melanoma effects via the immune system. During the necropsies from the experiments described above we observed that spleens appeared to be enlarged. When we plotted the spleen weight to body weight ratio in the different groups, we could indeed observe a statistically significant increase in spleen size in all treatment groups compared to vehicle, with the largest difference in the mice receiving combination treatment (Figure 5.7D). Subsequent histological examination showed areas of extramedullary hematopoiesis, that is, increased production of hematopoietic cells within the spleen, such as lymphocytes (data not shown) that may account for the enhanced spleen weight.

To confirm that ARI-4175 was acting via an immune-mediated mechanism, we attempted to repeat the previous tumor dosing experiment in immune-deficient Rag2 mice, lacking B-cells and T-cells. We hypothesized that tumor bearing Rag2 mice would be insensitive to ARI-4175 treatment, if the mechanism of tumor inhibition involved immune cells. However, when we treated Rag2 mice with equivalent doses of ARI-4175 that had been well-tolerated in C57BL6/J mice previously, Rag2 mice experience acute toxicity, and this was genotype dependent, such that $Rag^{+/+}$ and $Rag^{+/-}$ mice were insensitive compared to $Rag^{-/-}$ mice (Figure 5.8A). This result was recapitulated in immune-deficient NOD/SCID mice (data not shown), as well as in T-Cell receptor alpha knockout (TCRα KO) mice (Figure 5.8B) highlighting that ARI-4175 may require T-cells to mitigate toxicity possibly mediated by other hematopoietic changes. These results

suggest that in order to test whether ARI-4175 mediates tumor inhibition via the immune system, and alternative experimental approach is required.

5.2.5 ARI-4268, a next-generation serine protease inhibitor

Given the serious toxicity observed following administration of ARI-4175 to immune-deficient mice, the Bachovchin lab modified the chemical structure and created a new variant of ARI-4175, a next generation compound denoted as ARI-4268 (Figure 5.9A). This compound was purported to be less toxic to immune-deficient mice and represented a practical alternative to ARI-4175. An initial dose-escalation pilot experiment in TCRα KO mice confirmed that ARI-4268 had improved tolerability, as no acute adverse effects were observed within a period of one week during daily oral administration (data not shown).

To test whether ARI-4268 had anti-tumor efficacy in our model, we initiated a pilot experiment in which C57BL6/J mice bearing subcutaneous SM1-750 tumors (n=3 per group) were randomized into three groups receiving vehicle, a low dose of 160µg/mouse of ARI-4268, or a very high dose of 1280µg/mouse ARI-4268. The dosing schedule was similar to methods used for ARI-4175, in which daily doses by gavage were given for five consecutive days, with a two-day drug holiday in between. We observed, somewhat surprisingly, that ARI-4268 was much less effective at producing an anti-tumor response in this model, and neither a low or high dose showed any appreciable differences in tumor growth (Figure 5.9B). Our sample size was likely not large enough to observe statistical differences, since tumor weight after two weeks of dosing at the study endpoint showed a trend toward a reduction in weight (Figure 5.9C). Spleen weight also showed a trend toward an increase, similar to previously observed results using ARI-

4175, but again this was not significant (Figure 5.9D). Notably, however, ARI-4268 did cause a dose-dependent increase in progressive weight loss (Figure 5.9D), similar to previous results using ARI-4175. Taken together, these results indicated that ARI-4268 is less effective as a single agent than ARI-4175, although better tolerated in immune-deficient mice. Further studies investigating combination therapy with Vemurafenib will be necessary to determine if ARI-4268 is a viable candidate for therapeutic intervention in melanoma.

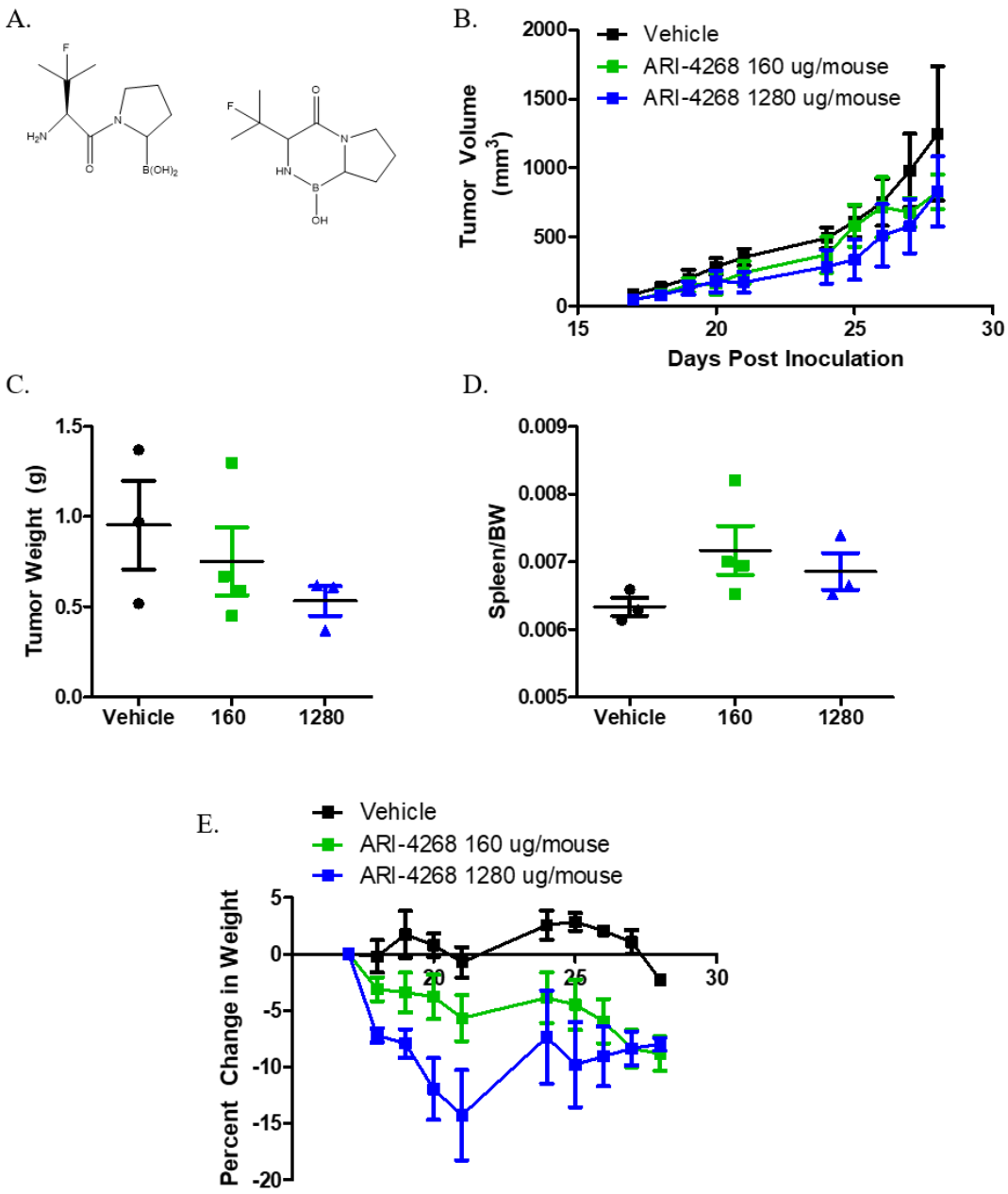

Figure 5.9. ARI-4268 does not inhibit SM1-750 murine melanoma growth. A) Chemical structure of ARI-4268, modified from the structure of ARI-4175. B) C57BL6/J mice bearing subcutaneous tumors (n=3 per group) were treated with indicated doses of ARI-4268 and tumor size was measured using calipers. C) Tumors were collected and weighed 24 hours after the last dose, at day 28 post-inoculation. D) Spleen to body weight ratio (g) was calculated for each group at day 28. E) Percent change in weight (g) was calculated for each group and plotted as a function of days post inoculation (x-axis).

5.3 Summary and Significance

In this chapter, we investigated tumor-targeted therapy as a method to increase the specificity of targeting the AKT inhibitor MK-2206 to the tumor microenvironment, and limit toxicity from systemic off-target effects. Our results using a syngeneic murine melanoma tumor model, SM1-750, demonstrate increased activity of the serine protease FAP in SM1 tumors, which we then used to activate prodrugs that are inactive in circulation until cleaved at the site of the tumor microenvironment by FAP activity. This approach was marginally effective, and we observed slight but promising change in percent tumor inhibition with our FAP prodrug ARI-5173, but not with equivalent dose of the AKT-inhibitor MK-2206. To date, there are no tumor-target therapies utilizing MK-2206 in melanoma, and therefore, optimizing dose schedule and frequency could represent a novel approach and major step forward in the utilization of AKT inhibition as melanoma therapy.

In addition, we took advantage of the FAP activity in an alternate manner to directly inhibit its activity using the pan-DASH serine protease inhibitor, ARI-4175, and this treatment synergized with BRAF targeted therapy to drastically inhibit tumor growth. However, this treatment was toxic to non-immune mice, and we additionally tested a next-generation inhibitor, ARI-4268, to determine if it was a viable alternative. ARI-4268 was less efficient at reducing tumor growth than ARI-4175, but was tolerated at high doses, and could be effective in combination with Vemurafenib.

Overall, the work presented here outlines several exciting novel therapeutic approaches with promising efficacy against melanoma. Further work can expand on

optimizing treatment strategies and combination approaches to enhance the arsenal of available treatment options for melanoma patients.

Chapter 6. Discussion

6.1 AKT2 Loss impairs BRAF mutant melanoma metastasis

6.1.1 AKT2 promotes cell migration, invasion, and an EMT-like process in melanoma

Although often considered to be functionally monolithic, it is now clear that individual AKT isoforms play markedly disparate roles in various tumor types. Hyperactivation of AKT signaling pathways occurs as a consequence of PTEN loss or following other oncogenic events such as gene mutation, amplification, or ectopic activation of PTEN-independent signaling pathways, and in our characterization of common genetic alterations in multiple human melanoma cell lines, we found a significant correlation between PTEN loss and elevated P-AKT, as well as phosphorylation of each AKT isoform contributing to total P-AKT (S473). However, by no means was this relationship exclusive, which should be considered for future analyses. For example, some cell lines (see CHL-1, Figure 3.1A) have robust total P-AKT, phosphorylation of all three isoforms, while also displaying PTEN protein expression. Because we did not test for PTEN functionality, mutations or other alterations could result in loss of function without loss of protein expression per se. Additional events, such as PI3K or AKT copy number variations could also be affecting AKT phosphorylation, independent of PTEN function. While the AKT isoforms may also be playing specific roles in these cell lines as well, our analysis focused on cell lines lacking detectable PTEN protein, in which we also show have phosphorylation of multiple AKT isoforms. The subsequent studies therein are consistent with data from other tumor types, in which expression of each AKT isoform has different functional consequences with respect to tumor-associated phenotypes.

Many studies indicate that AKT2, in contrast to AKT1 or AKT3, plays a unique role in driving cell migration, invasion, and EMT (Zhou et al., 2006), especially in breast cancer (Cheng et al., 2007; Iliopoulos et al., 2009; Irie et al., 2005), but in our human melanoma cell lines, we provide evidence that AKT2 may influence the melanocyte-specific TF MITF (Figure 3.5), which has not been previously described. MITF is regulated in part by the TF's BRN2 and PAX3, which other studies have shown may control melanoma invasiveness in response to PI3K signaling (Bonvin et al., 2012), but the exact mechanism was not determined. BRN2 expression is associated with enhanced migration in melanoma cells, mediated in part through the TF NFIB (Fane et al., 2017), which plays a pivotal role in melanocyte stem cell behavior within the hair follicle (Chang et al., 2013). Interestingly, we showed that AKT2 KD strongly inhibited NFIB transcriptional expression (Figure 3.5B), consistent with its role as pro-invasive mediator in melanoma (Fane et al., 2017). However, preliminary studies showed that AKT2 does not directly phosphorylate NFIB or MITF (data not shown), suggesting that if AKT2 is mediating melanoma cell invasion through NFIB, there are additional as yet unidentified intermediaries.

Possible regulation of melanocyte differentiation factors by AKT2 also may have consequences for targeted therapy. Not only is PI3K/AKT upregulation a major resistance mechanism in response to BRAF inhibition (Perna et al., 2015; Shi et al., 2013), but alterations in the PI3K/AKT pathway, such as PTEN loss, can alter how melanoma cells respond to BRAF inhibition (Fedorenko et al., 2015; Paraiso et al., 2011). Further, BRAF inhibition can induce changes in extracellular matrix (ECM) remodeling that were shown to be PTEN dependent (Fedorenko et al., 2015). PTEN loss may be

promoting AKT2 induction leading to ECM changes. Our results show that MMP2, involved in ECM degradation, was downregulated following AKT2 KD (Figure 3.5A). Further exploration of ECM remodeling by AKT2, especially in the context of BRAF inhibition, could provide additional insight into the mechanism of AKT2 in promoting cellular remodeling, a key step toward metastasis.

MicroRNAs regulate EMT-related processes in some cancers, and AKT2 regulates a diverse set of microRNAs across many cancer types (Honardoost and Rad, 2017). MicroRNAs are increasingly appreciated as metastasis drivers in melanoma (Mobley et al., 2012), and are reasonable candidates to investigate as driving AKT2-mediated invasive properties downstream. The mir200 microRNA family is regulated by AKTs in breast cancer (Iliopoulos et al., 2009), and AKT2 has been specifically implicated in the mir200-driven migratory phenotype of osteosarcoma cell lines (Liu et al., 2017b). However, a preliminary analysis of transcriptional changes in three candidate microRNAs, including mir200c, did not show any transcriptional changes with AKT2 KD in the human melanoma cell line WM1799 (data not shown). If AKT2 is indeed mediating changes in cell migration and EMT through one or more microRNAs, a larger broad-based analysis or microRNA screen will likely be necessary.

6.1.2 AKT2 depletion prevents metastatic seeding and delays metastasis of seeded cells

We observed that prophylactic AKT2 KD results in elimination of metastatic cells from NOD/SCID mice (Figure 3.6), but when cells are allowed to seed the lungs prior to AKT2 depletion, metastasis is only delayed (Figure 3.7). These results suggest that AKT2 is critically important in the early metastatic process, as cells intravasate. However, while AKT2 depletion impairs features of EMT, the exact mechanism whereby

WM1799 utilize AKT2 for intravasation should be further explored. In mice receiving WM1799 cells intravenously, the majority of mice did not display lung nodules, and instead showed metastases to the bowel and in the vicinity of lymph nodes. This pattern of dissemination suggests lymphogenous spread, and perhaps, extravascular migratory metastasis (EVMM) is impaired by AKT2 depletion. In contrast, one outstanding question is whether cells simply die while in the circulation, and if cell death is responsible for the lack of cells observed in mice injected with AKT2 depleted cells. One way to address this concern is to do a time course experiment, in which luciferase expression is quantified in whole blood within hours of tail vein injection and then over time to measure relative amounts of circulating cancer cells. In addition, a histological examination of the lungs at various timepoints after injection will help determine if WM1799 cells lodge in the lungs and subsequently migrate out of this niche via EVMM or some other mechanism, or if they undergo cell death, either in circulation or within the lungs. Studies examining the extravasation of breast tumor cells in real time have noted that expression of TWIST and beta-1-integrin are critical for intravascular cell migration (Stoletov et al., 2010). We noted that TWIST levels were unchanged transcriptionally following AKT2 KD (data not shown), although some studies suggest AKT2 is downstream of TWIST (Cheng et al., 2007). An analysis of critical integrins such as integrin β1 following AKT2 depletion should be a priority for future work.

Our observation that prophylactic AKT2 depletion drastically impairs metastatic seeding is in partial contrast with the results from a similar experiment using AKT2 KO cells, in which the phenotype is similar but much less dramatic (Figure 3.8). This may be partially explained by several factors. First, there may be AKT isoform compensation,

such that WM1799 cells increase AKT1 levels or phosphorylation when AKT2 is deleted. This is plausible, given that in AKT2-depleted subcutaneous tumors, AKT1 levels and phosphorylation increased. AKT1 has been previously implicated in the enhancement of melanoma metastasis (Cho et al., 2015), suggesting that AKT1 could also support cell growth or survival in the metastatic niche. Further examination of AKT1 levels in WM1799 AKT2 KO cells, or direct study of the role of AKT1 in metastatic ability of melanoma cells is required to clarify whether AKT1 plays and additional role in the metastatic ability of human melanoma cells. Additionally, these studies should utilize CRISPR/Cas9 gene edited cells, since the shRNA-mediated KD efficiency of AKT1 in our cells was just 50%. It is likely that this level of inhibition, while sufficient to observe proliferation changes, may not be adequate to observe migratory or invasive changes, as we saw no difference in the migratory ability of our cells with AKT1 KD.

It is also worth noting that tumor cells which enter the circulation via the tail vein easily lodge in terminal capillary beds within the lungs; intravasation or extravasation may not be necessary, but cellular survival and cell proliferation in the niche are required. Our results have shown that cell proliferation in 2D does not require AKT2 (Figure 3.4), but AKT2 depletion may impair cell growth or survival in 3D conditions (Figure 3.3). Interestingly, mice receiving AKT2 KO cells intravenously that also became moribund at similar timepoints as control mice had localized growth of tumors within the lungs, uncharacteristic for the WM1799 cell line which appeared to preferentially form distant metastases in the bowel, snout, and elsewhere. This could suggest that AKT2 loss limits the ability of WM1799 cells to extravasate into broader circulation, limiting their growth to the site of cellular seeding. However, WM1799 AKT2 KO cells represent a mixed

population and not a clonal KO cell line, and we cannot exclude the possibility that AKT2 protein remains in a subset of cells. Because distant metastases did form in a subset of NOD/SCID mice injected with AKT2 KO cells, we should confirm that AKT2 protein is absent, and therefore determine preliminarily if distant metastases require AKT2 protein expression.

While depletion of AKT2 may limit seeding of the metastatic niche and therefore tumor spread, the elimination of extant metastatic lesions in cancer patients remains the primary clinical hurdle, since patients frequently present with disseminated disease. Our results suggest that AKT2 depletion in established murine tumors is partially beneficial toward enhancing survival. Additionally, that AKT2 KO cells have no apparent subcutaneous growth defect (Figure 4.4) but show delayed metastasis (Figure 3.8) should be considered. These findings highlight a potential role for AKT2 in supporting growth of metastases, and the precise underlying mechanisms, while presently undetermined, are a high priority for future work. Inhibitors that purport isoform-specificity may be useful in testing for efficacy against established metastases. The AKT2-selective ATP-competitive inhibitor (Cat#124029, EMD Millipore) has shown efficacy in previous studies *in vivo* (Barazia et al., 2015), and could be worthwhile approach to consider.

As an extension to any of the follow up experiments so far described, a fundamental experiment that should be performed, ideally in parallel with any proposed experiment, is an AKT2-specific rescue. It should be confirmed that the effects observed as a consequence of AKT2 depletion by KD or KO are indeed a result of AKT2-specific loss-of-function. Rescuing with a WT AKT2 construct that is also non-targetable by shRNA is a necessary first step. A secondary question is also whether kinase activity is a

required component of the observed phenotypes, and to address this, a kinase-dead rescue construct could be used. These experiments should also be performed before moving downstream to interrogate mechanistic details.

6.1.3 AKT2 is important for melanoma cell metabolism and response to hypoxia

An AKT2-specific role in maintaining glucose homeostasis is well-documented (Cho et al., 2001a), and metabolic re-wiring in melanoma can both facilitate metastatic dissemination and support melanoma growth and survival within the metastatic niche (Fischer et al., 2017; Ratnikov et al., 2017). As such, we investigated the role of AKT2 in glycolytic function of melanoma cells to better understand how AKT2 may support growth of extant lesions.

Using a combination of metabolomics and a glycolytic rate assay, we observed that AKT2 depletion impaired basal and compensatory glycolysis (Figure 3.10). Because metabolism is important for supporting cellular survival during seeding of the niche as well as growth within the niche, it is plausible that AKT2 depletion could impair either or both processes, via several possible mechanisms. First, active AKT2 is required for GLUT1 mobilization, an early metabolic step (Beg et al., 2017), and GLUT1 utilization specifically enhances the metastatic properties of melanoma cells (Koch et al., 2015). If GLUT1 is important for cell survival in the metastatic niche by AKT2-mediated induction, then expression of GLUT1 concurrent with AKT2 depletion should rescue metastatic cell seeding. Additionally, future experiments could explore the specific enzymatic processes governing stepwise glycolytic function, to interrogate in more detail which metabolic steps are altered by AKT2 depletion.

Another possible route in which AKT2 may regulate melanoma cell metabolism is via its substrate PGC1α. AKT2 directly phosphorylates and inhibits PGC1α (Li et al., 2007), and PGC1α was recently shown to suppress melanoma metastasis (Luo et al., 2016). Preliminary analysis of transcriptional PGC1α levels with and without AKT2 KD did not show differences (data not shown), but because PGC1α is also regulated by MITF in melanoma cells (Haq et al., 2013), it is possible that AKT2 is involved in the regulation of PGC1α through MITF. Further studies should examine the precise relationship between MITF, AKT2, and PGC1α.

PI3K/AKT signaling controls the regulation of HIF1α, a key transcriptional regulator involved in the hypoxia response to low oxygen conditions, environmental conditions ubiquitous within the metastatic niche. We observed that during simulated hypoxia, AKT2 KD or KO impaired the induction or stabilization of HIF1α 8-24 hours after cobalt chloride treatment (Figure 3.11). At present, it is not clear if impaired HIF1α induction plays a role in limiting the metastatic capacity of melanoma cells during the metastatic process. Future studies should investigate whether there is a requirement for HIF1α during metastatic seeding, and if expression of factors downstream of AKT2 can rescue the HIF1α response. The mir-21 microRNA has been implicated in malignant progression of melanoma (Melnik, 2015) and AKT2 has been shown to induce mir-21 in response to hypoxia in both breast and ovarian cancer models (Polytarchou et al., 2011). Future studies should first investigate whether mir-21 levels differ in melanoma cells after AKT2 depletion, and subsequently, whether mir-21 expression can rescue hypoxia-related defects resulting from AKT2 depletion.

6.1.4 Identification of AKT phospho-substrates by IP-mass spectrometry in human melanoma cells

Although AKT signaling pathways are key drivers of tumor progression, selective targeting of AKT isoforms with clinically relevant small molecules has remained unfeasible to date. An alternative approach to targeting the AKT pathways is through the development of inhibitors to AKT isoform-specific substrates. AKT isoforms achieve their non-overlapping functions in part through differential substrate phosphorylation (Gonzalez and McGraw, 2009) and in an effort to understand potential substrates of that may be of specific relevance in WM1799 cells, we performed IP-mass spectrometry for proteins phosphorylated at the AKT-consensus site (Figure 3.12). Our results revealed a number of both known and unknown AKT phospho-substrates. The only significantly enriched gene-ontology terms were related to the biological process of spermatid differentiation. Interestingly, the implicated proteins TDRD5 and ACRBP have been previously shown to support cancer growth; sperm cells undergo rapid cell division requiring mitotic spindle stabilization, a mechanism aberrantly co-opted by cancer cells (Whitehurst et al., 2007; Whitehurst et al., 2010).

Several other candidates, while not associated with significant gene ontology processes, may also be promising candidates for follow up and validation. However, it is worth noting that the AKT consensus site was not identified as the modified region in our mass spectrometry results, and therefore, these candidates may not be bona fine AKT substrates. This does not preclude an AKT consensus site (or sites) elsewhere in the protein, and validation by immunoprecipitation and site-specific mutation are necessary before candidates are seriously pursued. Those caveats aside, some candidates may bear

investigation. The protein CCDC138 is notable because it was only very recently identified as a novel ciliary protein (Drew et al., 2017), and ciliogenesis has been implicated in the tumorigenesis and metastasis of breast cancer (Hassounah et al., 2017). Similarly, little is known about the protein NCKAP5L, but it is mutated with 5% frequency in melanoma (cBioPortal) and was recently shown to regulate microtubule assembly (Mori et al., 2015), a process of critical importance for cell migration. The proteins MYH9 and MYH10, myosins important for cell motility and chemotaxis, have not been studied in melanoma but are mutated in 4.3% and 4.5% of melanomas (cBioPortal). Further, MYH10 has been implicated in supporting tumorigenesis and metastasis in lung cancer cells, a process inhibited by mir-200 (Kim et al., 2015). Other proteins involved in cell motility were present in our mass spectrometry results, such as PLEC and SVIL, and bear further investigation for potential roles in supporting melanoma cell migration and invasion.

One protein in particular, Transmembrane glycoprotein Non-Metastatic Melanoma Protein B (GPNMB), is also of interest. GPNMB is a MITF-regulated gene (Loftus et al., 2009) named for its presence in non-metastatic samples, but as a regulator of wound repair may actually be tumor promoting by enhancing migration and invasion (Taya and Hammes, 2017). Silencing GPNMB downregulates melanocyte specific genes Tyrosinase and DCT (Zhang et al., 2012), and GPNMB is upregulated upon treatment with MAPK inhibitors (Rose et al., 2016), consistent with its appearance in Vemurafenib treated WM1799 cells (Table 3.3). If this protein is regulated by AKT2, it could be mediating the AKT2-dependent suppression of melanocyte genes that we observe during BRAF inhibition (Figure 3.5). Future work should validate GPNMB as an AKT-specific

target and investigate if overexpression of GPNMB rescues the AKT2-induced suppression of melanocyte-specific genes.

Another protein, titin (TNN), is seemingly out of place in melanoma cells, given its role as a regulator of cardiac muscle structure and contraction (Linke and Hamdani, 2014). However, the PI3K pathway has been shown to regulate titin function (Krüger et al., 2008) and titin has been previously identified in melanoma samples (Pföhler et al., 2007). Furthermore, it is mutated at a staggering frequency of nearly 60% in melanoma samples (cBioPortal), yet there are very few studies investigating titin function in melanoma. While a particular role in melanoma is unclear, future studies should first validate titin as an AKT-specific target, and then investigate whether titin promotes cell migration and invasion in melanoma cells, perhaps in an AKT-dependent manner.

In addition, there are several substrates identified in a previous phospho-proteomic screen of AKT isoform-specific substrates (Sanidas et al., 2014) that may have relevance to our studies. AKT2 preferentially phosphorylates both the Metastasis Suppressor Protein-1 (MTSS1), a metastasis driver in some melanomas (Mertz et al., 2014), and the protein AHNAK (Sussman et al., 2001), whose expression is strongly downregulated and correlated with poor prognosis in metastatic melanoma (Sheppard et al., 2016). Notably AHNAK, in addition to TCOF1, a protein identified in our mass spectrometry screen, were both implicated as markers of melanoma EVMM (Lugassy and Barnhill, 2011). Whether these proteins actively aid in AKT2-mediated metastasis by facilitating EVMM should be directly tested in future work.

Elucidating and validating further AKT-specific substrates is of high priority, as they could function as molecular connections between AKT and other key mediators of

tumor progression that may play a role in modulating cell migration and invasion in our system. In addition, understanding the substrates and key pathways utilized by AKT isoforms to promote different stages of the metastatic process could drastically expand our arsenal of actionable therapeutic targets.

6.2 AKT1 promotes BRAF mutant melanoma initiation and tumor progression

6.2.1 AKT1 promotes melanoma cell proliferation *in vitro* and *in vivo*

Because the role of AKT1 in supporting cellular proliferation and survival is well known in a variety of tumor types, it was not altogether surprising to observe that AKT1 KD inhibited cell proliferation in a variety of human melanoma cell lines (Figure 4.1). We did not observe any overt defects in cell survival or a complete cell-cycle arrest when AKT1 was inhibited, and this may be partially explained by our KD efficiency, which was not greater than 50% in any cell line (Figure 3.2).

Despite this, we also observed that tumor growth was inhibited when AKT1 was knocked down *in vivo* by the introduction of doxycycline chow once tumors were palpable (Figure 4.3). Interestingly, tumors were only transiently inhibited, and an analysis of protein levels at endpoint show that AKT1 is not knocked down, despite sustained administration of doxycycline chow. This result has several interpretations. First, it is possible that WM1799 cells silenced the shRNA hairpin or found an alternate AKT1 reactivation mechanism. If this is the case, it may also explain the results we observe in soft agar, in which there was a non-significant trend toward a reduction in size; some colonies may have escaped KD inhibition after prolonged incubation with doxycycline (Figure 4.2). Another interpretation is that a subpopulation of cells escaped initial puromycin selection during stable cell line generation, and suppression of AKT1

reduced growth or enhanced cell death enough to favor selection of a non-puromycin resistant cell population that lacks shAKT1. This could be tested by growing the cells in the presence of puromycin, to test for the presence of resistance. However, future studies may be advanced either by using additional doxycycline inducible hairpins with enhanced KD efficiency, or by gene deletion.

To circumvent the problem of knockdown avoidance and further study the role of AKT1 in cell proliferation, we used CRISPR/Cas9 to irreversibly delete AKT1 from human melanoma cells. Our results showed that in contrast to KD studies, neither cell proliferation nor anchorage independent growth were markedly affected by AKT1 loss *in vitro*, and there was only a delay in tumor growth that was eventually overcome, despite AKT1 deletion (Figure 4.4). This may suggest that an inducible hairpin system is advantageous in allowing for acute observations of transient effects not visible after long term selection for AKT1 depletion. We went on to investigate the dynamics of AKT1 deletion immediately after gene editing in more detail. We observed that AKT1 protein levels persisted in early passage cells, in contrast to AKT2 or AKT3 protein levels (Figure 4.6). This result could be interpreted in several ways. First, the chosen guide RNAs may be less efficient or ineffective at initiating a DNA double-strand break, or there was double strand break repair that prolonged AKT1 genetic integrity. This is unlikely given that three individual guide RNAs to AKT1 showed similar results, and all produced AKT1 KO cells after several passages in culture. Another, perhaps simultaneous possibility, is that compensatory “re-wiring” to maintain proliferative integrity and tolerate AKT1 loss is occurring within the cell. For example, WM1799 cells that grow effectively in the absence of AKT1 may be selected for within a mass culture,

and therefore we could not observe an overt proliferative defect when AKT1 was deleted over time. This is plausible, given that the MAPK pathway is hyperactivated in our human melanoma cells, and supports cell proliferation and survival by regulating some of the same downstream substrates as the PI3K/AKT pathway (Castellano and Downward, 2011). However, any potential mechanism of re-wiring likely requires extracellular growth signals or support from neighboring cells, since cells infected with AKT1 guide RNAs that were single cell sorted showed an absence of AKT1 KO colonies (Figure 4.7). An alternate approach may be to single-cell sort from a bulk population of cells with enhanced AKT1 depletion, and subsequently screen for AKT1 KO colonies to determine if AKT1 is indeed required for clonal growth.

6.2.2 AKT1 promotes $BRAF^{V600E}$ murine melanoma initiation

An analysis of Akt protein and phosphorylation in murine cell lines derived from BRAF mutant melanoma prone mice showed ubiquitous Akt1 phosphorylation, in contrast to Akt2 phosphorylation, which was not readily detectable (Figure 4.8). This observation that spontaneous mouse melanomas and a panel of human melanoma cell lines display differential Akt isoform phosphorylation strongly suggested that Akt isoforms may have non-redundant functions in melanomagenesis, and moreover that Akt1 was important for the formation of spontaneous tumors.

Additionally, in our murine model, we observed an increase in Akt2 Ser474 phosphorylation in individual lung metastases relative to cultured melanoma cells (Figure 4.8), arguing that in contrast to melanoma initiation, aspects of the metastatic process may be regulated by Akt2. Murine SM1-750 cells are derived from a primary melanoma, without prior selection for metastatic potential, and an Akt2-mediated pathway was not

the sole route to metastatic success, as some lesions still lacked detectable Akt2 phosphorylation. Despite this, increased Akt2 activity could provide a selective advantage to tumor cells extravasating from the circulation following tail vein injection, given our finding that Akt2 positively impacts expression of EMT genes (Figure 3.5). Future studies could utilize this murine melanoma model to further study the role of Akt2 in promoting a metastatic program.

The compelling observation that tumors from $BRAF^{V600E}$; $Arf^{-/-}$ mice have ubiquitous Akt1 phosphorylation make this genetic background ideal for evaluating the consequence of germline ablation of Akt1 to melanoma initiation. We crossed $Akt1^{-/-}$, $Akt2^{-/-}$, or $Akt3^{-/-}$ mice onto the melanoma prone $BRAF^{V600E}$; $Arf^{-/-}$ background, and our results suggest that Akt1 is important for melanoma initiation. Mice with Akt1 KO lived significantly longer than $BRAF^{V600E}$; $Arf^{-/-}$ control mice (Figure 4.9), but due to technical limitations, we were unable to calculate the percent melanomas. This determination was previously made by detecting human transgenic BRAF at higher levels in melanoma relative to other tumor types (Goel et al., 2009) such as sarcoma. However, melanomas in our mice did not harbor high expression of oncogenic $BRAF^{V600E}$ (data not shown), likely because overcoming OIS is tumor promoting but requires BRAF suppression, which is also mediated by Akt (Kennedy et al., 2011; Vredeveld et al., 2012) Specifically, the spectrum of tumors occurring in $BRAF^{V600E}$; $Arf^{-/-}$ mice is not limited to melanoma; Arf loss facilitates lymphoma and sarcoma development (Luo et al., 2013), and $BRAF^{V600E}$ can induce benign Schwann cell nerve sheath tumors (Luo et al., 2015). Further, Akt inhibition may enhance schwannoma development by affecting schwannian differentiation (Luo et al., 2015). This may increase overall tumor penetrance but

suppress melanoma development; future work must use additional markers that can differentiate schwann cells from melanocytes and establish tumor identity with more accuracy.

6.2.3 UV irradiation shifts the tumor spectrum toward melanoma

In order to circumvent the difficulty of determining the percent de novo melanomas in our $BRAF^{V600E}$; $Arf^{-/-}$ mice, we took advantage of the ability of *in vivo* UV-irradiation to shift the spectrum of tumors towards melanoma. In this way, we were able to observe how Akt isoform depletion affects melanoma penetrance. While this work is still ongoing and we have not fully examined the effect of Akt1 depletion on UV-induced tumors to date, results from Akt2 and Akt3 isoform loss in melanoma prone mice show that surprisingly, Akt3 loss extends survival of mice following UV-irradiation, while Akt2 does not (Figure 4.10). These results may be partially explained when considering the role of melanocyte stem cells and inflammation in UV-irradiated skin. First, during the process of UVB-irradiation, melanocyte stem cells are activated to leave the niche by an inflammation-dependent process involving the chromatin remodeling factor HMGA2 (Moon et al., 2017). Interestingly, an analysis of migrating melanoma cells positive for the melanocyte stem cell marker CD271 implicated both HMGA2 and AKT3 in this process (Radke et al., 2017). Together these results suggest that Akt3 loss may limit migration of melanocyte stem cells following UVB irradiation, suppressing UV-induced melanoma development. Analyzing $BRAF^{V600E}$; $Arf^{-/-}$; $Akt3^{-/-}$ murine melanoma cell migration following UVB-irradiation should be the focus of future studies, to determine if Akt3 loss reduces melanoma migration under these conditions and if this is a tumor-suppressive mechanism. While our study focused on $BRAF^{V600E}$-driven

disease, Akt3 is highly amplified in tumors that lack BRAF mutations (Akbani et al., 2015). Interestingly, these tumors tend to be chronically sun-damaged (CSD), in comparison to non-CSD melanomas which overwhelmingly display $BRAF^{V600E}$ driver mutations (Shain and Bastian, 2016). It is possible that the role of Akt3 in UV-induced melanoma is independent of BRAF and may be of particular importance in BRAF WT melanomas, which currently have the least therapeutic options. Further elucidating the role of Akt3 in UV-dependent melanoma development could reveal important new mechanisms critical for targeting the treatment refractory subclass of Triple WT melanoma.

6.3 Tumor targeted and combination therapies for improved delivery and efficacy of AKT and other kinase inhibitors *in vivo*

6.3.1 Adaptation of a murine melanoma cell line for syngeneic tumor studies

The ability to form tumors with reproducible efficiency in syngeneic mice was of critical importance for testing immune-modulatory compounds *in vivo*. Initially, the SM1 cell line did not grow with 100% penetrance in our C57BL6/H mice and it was necessary to additionally passage the cell line *in vivo* (Figure 5.1). While this approach increased tumor take, it is possible that immune evasion was enhanced by this process, resulting in a more aggressive and refractory cell line. Changes in cell signaling were observed in previous immunoblots, in which phosphorylation of Akt1 was greatly enhanced in passaged SM1-750 cells compared to the parental SM1 cell line (Figure 4.8). Selecting for increased aggressiveness may be a drawback when demonstrating therapeutic efficacy, but in contrast, any potential therapies that do show an effect in this model may have even greater utility in other, less aggressive melanomas.

6.3.2 Small molecule AKT inhibition and the FAP-activated AKT inhibitor ARI-5173

Because small molecule AKT-isoform specific inhibition is not yet a clinically viable approach, we chose to investigate if FAP-targeting to the tumor microenvironment could enhance the specificity of tumor targeting of pan-AKT inhibitor MK-2206 and limit off-target effects. Preliminary results suggested that not only did MK-2206 inhibit Akt phosphorylation and induce PARP cleavage in the SM1-750 murine melanoma cell line (Figure 5.2), but mice bearing SM1-750 subcutaneous tumors had FAP serine protease activity, suggesting an FAP-targeted prodrug of MK-2206 may have efficacy (Figure 5.4). Initial testing for FAP activity performed by the Bachovchin lab did not concurrently compare FAP activity to control tissues, and we retroactively compared our results to published standards of FAP activity in different murine tissues (Keane et al., 2013) to surmise that the FAP activity in our murine tumors was likely sufficient to activate a prodrug. Because the FAP activity within individual tumors varied as much as three-fold (Figure 5.4), the possibility that heterogeneous FAP activity may limit the efficacy of FAP-activatable therapies is a current concern.

Nonetheless, the toxicity of MK-2206 was so severe in our mice that sustained dosing regimens capable of halting tumor growth were impossible (Figure 5.3), and since we were able to show that the FAP-activatable ARI-5173 was preferentially converted to active MK-2206 in tumor tissue compared to the plasma (Figure 5.4), we initiated a dosing regimen with ARI-5173. Unfortunately, because synthesis of ARI-5173 is time-consuming and costly, we had limited amounts of ARI-5173 and therefore a restricted dosing regimen that consisted of just two low dose administrations of ARI-5173 or MK-2206 compared to vehicle control. Despite this, we observed a small initial anti-tumor

response in ARI-5173 treated mice, compared to MK-2206 or vehicle treatment (Figure 5.5). While no long term or statistically significant tumor reduction was achieved, this experiment was a proof-of-concept, showing that the approach of delivering an inactive prodrug may have efficacy at the site of the tumor, and future studies are warranted to investigate the anti-tumor effects of ARI-5173, or other FAP-activatable prodrugs in melanoma.

Additionally, assessing FAP activity in tumor samples, especially in responder versus non-responder mice, should be a priority to determine whether there is a threshold value for ARI-5173 efficacy in SM1-750 tumors. For example, graphs showing percent tumor growth inhibition of individual mice indicate that just 2/4 mice had strong initial responses to ARI-5173 (Figure 5.5), and this could be due to intrinsically higher FAP activity. Interestingly, one mouse also demonstrated up to 10% weight loss, a side effect of MK-2206 that was unexpected if ARI-5173 was targeted to the tumor and systemic effects were limited. The same mouse also had the most robust tumor inhibitory response to ARI-5173, and therefore it is possible that higher circulating FAP outside the tumor microenvironment, such as in the plasma, resulted in premature cleavage of the prodrug and subsequent off-target toxicity. Future studies should initiate a more sustained dosing regimen in combination with systematic evaluation of FAP activity in tumoral and non-tumoral tissues to fully assess the value of ARI-5173 as anti-melanoma therapy.

6.3.3 Utilization of serine protease inhibition for enhanced efficacy of BRAF inhibition in murine melanoma tumors

The observation that SM1-750 murine tumors expressed FAP was additionally leveraged to determine if serine protease inhibition, especially in combination with

BRAF inhibition, would have enhanced efficacy against established murine tumors. The first inhibitor we tested was the pan-DASH inhibitor ARI-4175. We observed that while ARI-4175 alone moderately limited tumor growth (Figure 5.6), that effect was significantly enhanced by co-treatment with the BRAF inhibitor Vemurafenib (Figure 5.7). In fact, ARI-4175 synergized with BRAF inhibition and was superior to Vemurafenib treatment alone.

The main side-effect of ARI-4175 administration was severe weight loss (Figure 5.7). This was unsurprising, given that a previous generation of this inhibitor, PT-100, interfered with glycemic regulation (Kieffer et al., 1995) and similar compounds are approved in Europe for the treatment of type 2 diabetes (Traynor, 2009). Furthermore, FAP regulates key metabolic substrates involved in energy maintenance, and its inhibition has been proposed to treat type 2 diabetes (Coppage et al., 2016). To limit the effects of weight loss, a two-day drug holiday successfully resulted in near-complete weight-loss recovery, and weight gain occurred after dosing was concluded (Figure 5.7). However, mice weighing more than 25g were a pre-requisite in the study design, and this could represent a potential limitation for future studies utilizing ARI-4175.

Because ARI-4175 is known to utilize immune-mediated mechanisms for its anti-tumor activity (Adams et al., 2004; Donahue et al., 2014; Duncan et al., 2013), we wanted to determine if the immune system was required for the synergistic activity in combination with Vemurafenib treatment in our model. Unfortunately, despite published reports that ARI-4175 is well-tolerated in immune-incompetent $Rag1^{-/-}$ mice (Donahue et al., 2014), we observed extreme acute and fatal toxicity across a variety of immune-deficient murine strains, including $Rag2^{-/-}$, NOD/SCID (not shown), and TCRα KO mice

(Figure 5.8). This limited our ability to test the above hypothesis that the immune system was a necessary component for Vemurafenib synergy. However, these effects shed light on the specific mechanism of action of ARI-4175, since TCRα KO mice are selectively devoid of only CD4 and CD8 T-cells (Mombaerts et al., 1992). In previous studies, ARI-4175 upregulated CD4 T-cell populations and sensitized tumor cells to T-cell mediated killing (Duncan et al., 2013). It is unclear how this mechanism would result in acute toxicity to immune-deficient animals, and as mentioned, ARI-4175 showed no toxicity in $Rag1^{-/-}$ mice (Duncan et al., 2013). While $Rag1^{-/-}$ and $Rag2^{-/-}$ mice are functionally similar in that they both lack mature B-cells and T-cells, one major difference between our study and Duncan et al is the genetic background of the mice; our $Rag2^{-/-}$ mice are maintained on a BL6 background, while the $Rag1^{-/-}$ mice are derived from the 129 strain. It is possible that the 129 strain has immunogenic or other strain-specific differences that contribute to improved tolerance. Future studies could utilize the 129 $Rag1^{-/-}$ mice to test whether the immune system is required for ARI-4175 synergy with Vemurafenib.

As an additional method to circumvent toxicities observed in non-immune mice, we tested a next-generation compound, ARI-4268, which was reportedly less toxic but had similar anti-tumor efficacy to ARI-4175 (unpublished data). Our initial tests confirmed that ARI-4268 was not toxic to $Rag2^{-/-}$ or TCRα KO mice (not shown), but also showed that the anti-tumor efficacy of ARI-4268 was diminished (Figure 5.9A) in comparison to ARI-4175. However, ARI-4268 induced dose-dependent weight loss, similar to the phenotype of ARI-4175 treatment (Figure 5.9B). This unfortunate side-effect limited the dosing regimen such that mice treated with high dose ARI-4268 were moribund after two weeks. Despite the greatly reduced anti-tumor effects *in vivo*, it may

still be worth investigating whether ARI-4268 has the potential to synergize with Vemurafenib treatment, and in this case, a lower dose may be given to ameliorate adverse weight loss. If no synergy is observed, further investigating the differences between ARI-4175 and ARI-4268 may shed light on the mechanism of both the synergy and anti-tumor activity of these compounds.

6.4 Conclusions and Future Directions

The work presented herein provides an investigation into the PI3K/AKT pathway in BRAF mutant melanoma, focused on examining differential roles for the AKT isoforms and exploring novel therapeutic options. Chapter 3 presented evidence that the AKT2 isoform played a critical role in melanoma metastasis, specifically by inhibiting seeding of the metastatic niche. This may be partly achieved through modulation of an EMT-like process, and a novel link between AKT2 and melanocyte specific factors may additionally support melanoma cell metastasis. Further elucidation of how AKT2 modulates these melanocyte-specific TF's could reveal a previously unknown melanocyte-specific role for the PI3K/AKT pathway and inform how future exploitation of this pathway could be tailored for melanoma-specific inhibition. It was also demonstrated that AKT2 functioned in melanoma metabolism through the regulation of glycolysis and by supporting the hypoxia response through HIF1α induction or stabilization. These AKT2-dependent phenotypes have not been described in melanoma and interrogating the mechanistic consequences could reveal novel drug targets. Lastly in this chapter, we performed an investigatory search for novel AKT-phospho-substrates and revealed proteins involved in cell motility, EVMM, and mitotic spindle function that may be involved in supporting melanoma metastasis. Validation and testing of candidate

substrates may elucidate both novel and melanoma-specific drug targets that could inhibit aspects of the metastatic process, a critical unmet need in melanoma.

Chapter 4 was largely focused on the more well-studied AKT1 isoform, revealing that AKT1 supports melanoma cell proliferation and tumor initiation. We used a combination of shRNA, *in vitro* gene editing, and *in vivo* genetic ablation to establish that while AKT1 inhibition limits cell proliferation, melanoma cells demonstrate a high degree of plasticity and may acclimatize to AKT1 loss to support continued cell proliferation in the absence of AKT1. Since a majority of AKT inhibitors target the AKT1 isoform with enhanced selectivity, understanding the mechanisms that support this potential "re-wiring" may help understand adaptive resistance to targeted therapy, the major barrier to successful treatment.

Furthermore, we show that loss of the Akt2 isoform has no effect on survival of melanoma prone mice, or the incidence of UV-irradiation induced melanoma. However, Akt2 phosphorylation was elevated in metastatic lesions compared to their cultured counterparts, suggesting that Akt2 may also support the metastatic process in this murine melanoma model. Using this model to further dissect the role of Akt2 in metastasis could have useful implications; an analysis of the lungs from $BRAF^{V600E}$; $Arf^{-/-}$; $Akt2^{-/-}$ mice for spontaneous metastases would indicate if Akt2 is required for metastasis in $BRAF^{V600E}$ melanoma. Similarly, assessing the intrinsic metastatic ability in syngeneic cell lines that lack Akt2 compared to their fully Akt2-competent counterparts is an immediate future goal.

Lastly, we found that unexpectedly, loss of Akt3 protects from UV-irradiation induced melanoma. Because Akt3 was the first of the isoforms to be specifically

implicated in melanoma progression (Stahl et al., 2004), many studies have focused on the role of Akt3 in melanoma promotion, and our work highlights a previously unrecognized role for Akt3 in UV-induced disease. Elucidating the mechanism whereby Akt3 supports UV-induced melanoma progression could have important implications for treatment options, especially when considering CSD versus non-CSD melanomas.

Chapter 5 examined a variety of small molecule therapeutics for their efficacy in syngeneic murine melanoma tumors. AKT inhibition was targeted to the tumor microenvironment using the tumor-associated antigen and serine protease FAP. The proteolytic activity of FAP was harnessed to deliver an AKT-inhibiting prodrug, cleaved by FAP selectively within the tumor microenvironment to deliver a cytotoxic payload. This novel approach to AKT inhibition showed acute efficacy, with promising and selective tumor inhibition. Future studies optimizing dose and treatment regimens are necessary to establish how this tumor-targeted AKT-inhibitor can be leveraged for anti-melanoma therapy.

We also demonstrated that inhibition of serine proteases could be an effective strategy against murine melanoma tumors. The pan-serine protease inhibitor ARI-4175 inhibited SM1-750 murine tumor growth but was most effective in combination with the BRAF inhibitor Vemurafenib. Future studies will investigate the mechanism of Vemurafenib/ARI-4175 synergy, which is hypothesized to include the immune system. It may also be beneficial to determine if the next-generation compound ARI-4268 also has synergistic activity with BRAF inhibitors, in an effort to expand the potential arsenal of actionable combination therapies.

Taken together, these studies provide the groundwork for discovery of selective, novel, therapeutic approaches to melanoma treatment leveraging the AKT pathway. Metastasis, the overwhelming arbiter of cancer mortality, remains one of the least understood biological processes with the fewest therapeutic options. This work reveals that AKT2 plays a substantial role in this process and provides many possible avenues for follow up and future research.

Chapter 7. Bibliography

Acosta, A.M., and Kadkol, S.S. (2016). Mitogen-Activated Protein Kinase Signaling Pathway in Cutaneous Melanoma: An Updated Review. Archives of pathology & laboratory medicine *140*, 1290-1296.

ACS (2017). Cancer Facts and Figures: 2017, A.C. Society, ed. (Atlanta, Ga).

Adams, S., Miller, G.T., Jesson, M.I., Watanabe, T., Jones, B., and Wallner, B.P. (2004). PT-100, a small molecule dipeptidyl peptidase inhibitor, has potent antitumor effects and augments antibody-mediated cytotoxicity via a novel immune mechanism. Cancer research *64*, 5471-5480.

Adler, N.R., Haydon, A., McLean, C.A., Kelly, J.W., and Mar, V.J. (2017). Metastatic pathways in patients with cutaneous melanoma. Pigment cell & melanoma research *30*, 13-27.

Akbani, R., Akdemir, K.C., Aksoy, B.A., Albert, M., Ally, A., Amin, S.B., Arachchi, H., Arora, A., Auman, J.T., Ayala, B., *et al.* (2015). Genomic Classification of Cutaneous Melanoma. Cell *161*, 1681-1696.

Alonso, S.R., Tracey, L., Ortiz, P., Perez-Gomez, B., Palacios, J., Pollan, M., Linares, J., Serrano, S., Saez-Castillo, A.I., Sanchez, L., *et al.* (2007). A High-Throughput Study in Melanoma Identifies Epithelial-Mesenchymal Transition as a Major Determinant of Metastasis. Cancer research *67*, 3450-3460.

Arozarena, I., and Wellbrock, C. (2017). Targeting invasive properties of melanoma cells. The FEBS journal.

Ascierto, P.A., McArthur, G.A., Dréno, B., Atkinson, V., Liszkay, G., Di Giacomo, A.M., Mandalà, M., Demidov, L., Stroyakovskiy, D., Thomas, L., *et al.* (2016). Cobimetinib combined with vemurafenib in advanced BRAF(V600)-mutant melanoma (coBRIM): updated efficacy results from a randomised, double-blind, phase 3 trial. The Lancet Oncology *17*, 1248-1260.

Bald, T., Quast, T., Landsberg, J., Rogava, M., Glodde, N., Lopez-Ramos, D., Kohlmeyer, J., Riesenberg, S., van den Boorn-Konijnenberg, D., Hömig-Hölzel, C., *et al.* (2014). Ultraviolet-radiation-induced inflammation promotes angiotropism and metastasis in melanoma. Nature *507*, 109-113.

Barazia, A., Li, J., Kim, K., Shabrani, N., and Cho, J. (2015). Combination therapy of hydroxyurea and an AKT2 inhibitor has beneficial effects on acute vaso-occlusive events in sickle cell disease mice. Blood.

Beg, M., Abdullah, N., Thowfeik, F.S., Altorki, N.K., and McGraw, T.E. (2017). Distinct Akt phosphorylation states are required for insulin regulated Glut4 and Glut1-mediated glucose uptake. eLife *6*.

Bonvin, E., Falletta, P., Shaw, H., Delmas, V., and Goding, C. (2012). A phosphatidylinositol 3-kinase-Pax3 axis regulates Brn-2 expression in melanoma. Molecular and cellular biology *32*, 4674-4683.

Brastianos, P.K., Carter, S.L., Santagata, S., Cahill, D.P., Taylor-Weiner, A., Jones, R.T., Van Allen, E.M., Lawrence, M.S., Horowitz, P.M., Cibulskis, K., *et al.* (2015). Genomic Characterization of Brain Metastases Reveals Branched Evolution and Potential Therapeutic Targets. Cancer discovery *5*, 1164-1177.

Brennen, W.N., Isaacs, J.T., and Denmeade, S.R. (2012). Rationale behind targeting fibroblast activation protein-expressing carcinoma-associated fibroblasts as a novel chemotherapeutic strategy. Molecular cancer therapeutics *11*, 257-266.

Brennen, W.N., Rosen, D.M., Chaux, A., Netto, G.J., Isaacs, J.T., and Denmeade, S.R. (2014). Pharmacokinetics and toxicology of a fibroblast activation protein (FAP)-activated prodrug in murine xenograft models of human cancer. The Prostate *74*, 1308-1319.

Brognard, J., Sierecki, E., Gao, T., and Newton, A.C. (2007). PHLPP and a second isoform, PHLPP2, differentially attenuate the amplitude of Akt signaling by regulating distinct Akt isoforms. Molecular cell *25*, 917-931.

Caramel, J., Papadogeorgakis, E., Hill, L., Browne, G., Richard, G., Wierinckx, A., Saldanha, G., Osborne, J., Hutchinson, P., Tse, G., *et al.* (2013). A switch in the expression of embryonic EMT-inducers drives the development of malignant melanoma. Cancer cell *24*, 466-480.

Carpten, J.D., Faber, A.L., Horn, C., Donoho, G.P., Briggs, S.L., Robbins, C.M., Hostetter, G., Boguslawski, S., Moses, T.Y., Savage, S., *et al.* (2007). A transforming mutation in the pleckstrin homology domain of AKT1 in cancer. Nature *448*, 439-444.

Castellano, E., and Downward, J. (2011). RAS Interaction with PI3K: More Than Just Another Effector Pathway. Genes & cancer *2*, 261-274.

Chang, C.-Y.Y., Pasolli, H.A., Giannopoulou, E.G., Guasch, G., Gronostajski, R.M., Elemento, O., and Fuchs, E. (2013). NFIB is a governor of epithelial-melanocyte stem cell behaviour in a shared niche. Nature *495*, 98-102.

Chapman, P.B., Hauschild, A., Robert, C., Haanen, J.B., Ascierto, P., Larkin, J., Dummer, R., Garbe, C., Testori, A., Maio, M., *et al.* (2011). Improved survival with vemurafenib in melanoma with BRAF V600E mutation. The New England journal of medicine *364*, 2507-2516.

Chen, G., Chakravarti, N., Aardalen, K., Lazar, A.J., Tetzlaff, M., Wubberhorst, B., Kim, S.-B.B., Kopetz, S., Ledoux, A., Nanda, V.G., *et al.* (2014). Molecular Profiling of Patient-Matched Brain and Extracranial Melanoma Metastases Implicates the

PI3K Pathway as a Therapeutic Target. Clinical cancer research : an official journal of the American Association for Cancer Research.

Chen, M., Xiang, R., Wen, Y., Xu, G., Wang, C., Luo, S., Yin, T., Wei, X., Shao, B., Liu, N., *et al.* (2015). A whole-cell tumor vaccine modified to express fibroblast activation protein induces antitumor immunity against both tumor cells and cancer-associated fibroblasts. Scientific reports *5*, 14421.

Cheng, G.Z., Chan, J., Wang, Q., Zhang, W., Sun, C.D., and Wang, L.-H.H. (2007). Twist transcriptionally up-regulates AKT2 in breast cancer cells leading to increased migration, invasion, and resistance to paclitaxel. Cancer research *67*, 1979-1987.

Chin, Y., Yoshida, T., Marusyk, A., Beck, A., Polyak, K., and Toker, A. (2014a). Targeting Akt3 signaling in triple-negative breast cancer. Cancer research *74*, 964-973.

Chin, Y.R., and Toker, A. (2009). Function of Akt/PKB signaling to cell motility, invasion and the tumor stroma in cancer. Cellular signalling *21*, 470-476.

Chin, Y.R., Yuan, X., Balk, S.P., and Toker, A. (2014b). PTEN-deficient tumors depend on AKT2 for maintenance and survival. Cancer discovery *4*, 942-955.

Cho, H., Mu, J., Kim, J.K., Thorvaldsen, J.L., Chu, Q., Crenshaw, E.B., Kaestner, K.H., Bartolomei, M.S., Shulman, G.I., and Birnbaum, M.J. (2001a). Insulin resistance and a diabetes mellitus-like syndrome in mice lacking the protein kinase Akt2 (PKB beta). Science (New York, NY) *292*, 1728-1731.

Cho, H., Thorvaldsen, J.L., Chu, Q., Feng, F., and Birnbaum, M.J. (2001b). Akt1/PKBalpha is required for normal growth but dispensable for maintenance of glucose homeostasis in mice. The Journal of biological chemistry *276*, 38349-38352.

Cho, J.H., Robinson, J.P., Arave, R.A., Burnett, W.J., Kircher, D.A., Chen, G., Davies, M.A., Grossmann, A.H., VanBrocklin, M.W., McMahon, M., *et al.* (2015). AKT1 Activation Promotes Development of Melanoma Metastases. Cell reports *13*, 898-905.

Colanesi, S., Taylor, K.L., Temperley, N.D., Lundegaard, P.R., Liu, D., North, T.E., Ishizaki, H., Kelsh, R.N., and Patton, E.E. (2012). Small molecule screening identifies targetable zebrafish pigmentation pathways. Pigment cell & melanoma research *25*, 131-143.

Coppage, A.L., Heard, K.R., DiMare, M.T., Liu, Y., Wu, W., Lai, J.H., and Bachovchin, W.W. (2016). Human FGF-21 Is a Substrate of Fibroblast Activation Protein. PLoS ONE *11*.

Cui, Y., Lin, J., Zuo, J., Zhang, L., Dong, Y., Hu, G., Luo, C., Chen, J., and Lu, Y. (2015). AKT2-knockdown suppressed viability with enhanced apoptosis, and attenuated chemoresistance to temozolomide of human glioblastoma cells in vitro and in vivo. OncoTargets and therapy *8*, 1681-1690.

Cui, Y., Wang, Q., Wang, J., Dong, Y., Luo, C., Hu, G., and Lu, Y. (2012). Knockdown of AKT2 expression by RNA interference inhibits proliferation, enhances apoptosis, and increases chemosensitivity to the anticancer drug VM-26 in U87 glioma cells. Brain research *1469*, 1-9.

Dai, D.L., Martinka, M., and Li, G. (2005). Prognostic significance of activated Akt expression in melanoma: a clinicopathologic study of 292 cases. J Clin Oncol *23*, 1473-1482.

Damsky, W., Curley, D., Santhanakrishnan, M., Rosenbaum, L., Platt, J., Gould Rothberg, B., Taketo, M., Dankort, D., Rimm, D., McMahon, M., *et al.* (2011). β-catenin signaling controls metastasis in Braf-activated Pten-deficient melanomas. Cancer cell *20*, 741-754.

Damsky, W.E., Theodosakis, N., and Bosenberg, M. (2014). Melanoma metastasis: new concepts and evolving paradigms. Oncogene *33*, 2413-2422.

Dankort, D., Curley, D.P., Cartlidge, R.A., Nelson, B., Karnezis, A.N., Damsky, W.E., You, M.J., DePinho, R.A., McMahon, M., and Bosenberg, M. (2009). Braf(V600E) cooperates with Pten loss to induce metastatic melanoma. Nature genetics *41*, 544-552.

Davies, H., Bignell, G.R., Cox, C., Stephens, P., Edkins, S., Clegg, S., Teague, J., Woffendin, H., Garnett, M.J., Bottomley, W., *et al.* (2002). Mutations of the BRAF gene in human cancer. Nature *417*, 949-954.

Davies, M.A., Stemke-Hale, K., Lin, E., Tellez, C., Deng, W., Gopal, Y.N., Woodman, S.E., Calderone, T.C., Ju, Z., Lazar, A.J., *et al.* (2009). Integrated Molecular and Clinical Analysis of AKT Activation in Metastatic Melanoma. Clinical cancer research : an official journal of the American Association for Cancer Research *15*, 7538-7546.

Davies, M.A., Stemke-Hale, K., Tellez, C., Calderone, T.L., Deng, W., Prieto, V.G., Lazar, A.J., Gershenwald, J.E., and Mills, G.B. (2008). A novel AKT3 mutation in melanoma tumours and cell lines. British Journal of Cancer *99*, 1265-1268.

Delmas, V., Beermann, F., Martinozzi, S., Carreira, S., Ackermann, J., Kumasaka, M., Denat, L., Goodall, J., Luciani, F., Viros, A., *et al.* (2007). Beta-catenin induces immortalization of melanocytes by suppressing p16INK4a expression and cooperates with N-Ras in melanoma development. Genes & development *21*, 2923-2935.

Denecker, G., Vandamme, N., Akay, O., Koludrovic, D., Taminau, J., Lemeire, K., Gheldof, A., Craene, D.B., Gele, V.M., Brochez, L., *et al.* (2014). Identification of a ZEB2-MITF-ZEB1 transcriptional network that controls melanogenesis and melanoma progression. Cell death and differentiation *21*, 1250-1261.

Deuker, M.M., Marsh Durban, V., Phillips, W.A., and McMahon, M. (2015). PI3'-kinase inhibition forestalls the onset of MEK1/2 inhibitor resistance in BRAF-mutated melanoma. Cancer discovery *5*, 143-153.

Dhomen, N., Reis-Filho, J., da Rocha Dias, S., Hayward, R., Savage, K., Delmas, V., Larue, L., Pritchard, C., and Marais, R. (2009). Oncogenic Braf induces melanocyte senescence and melanoma in mice. Cancer cell *15*, 294-303.

Dillon, R.L., and Muller, W.J. (2010). Distinct biological roles for the akt family in mammary tumor progression. Cancer research *70*, 4260-4264.

Donahue, R.N., Duncan, B.B., Fry, T.J., Jones, B., Bachovchin, W.W., Kiritsy, C.P., Lai, J.H., Wu, W., Zhao, P., Liu, Y., *et al.* (2014). A pan inhibitor of DASH family enzymes induces immunogenic modulation and sensitizes murine and human carcinoma cells to antigen-specific cytotoxic T lymphocyte killing: implications for combination therapy with cancer vaccines. Vaccine *32*, 3223-3231.

Drew, K., Lee, C., Huizar, R.L., Tu, F., Borgeson, B., McWhite, C.D., Ma, Y., Wallingford, J.B., and Marcotte, E.M. (2017). Integration of over 9,000 mass spectrometry experiments builds a global map of human protein complexes. Molecular systems biology *13*, 932.

Dror, S., Sander, L., Schwartz, H., Sheinboim, D., Barzilai, A., Dishon, Y., Apcher, S., Golan, T., Greenberger, S., Barshack, I., *et al.* (2016). Melanoma miRNA trafficking controls tumour primary niche formation. Nature cell biology *18*, 1006-1017.

Dummler, B., Tschopp, O., Hynx, D., Yang, Z.Z., Dirnhofer, S., and Hemmings, B.A. (2006). Life with a Single Isoform of Akt: Mice Lacking Akt2 and Akt3 Are Viable but Display Impaired Glucose Homeostasis and Growth Deficiencies. Molecular and cellular biology *26*, 8042-8051.

Duncan, B.B., Highfill, S.L., Qin, H., Bouchkouj, N., Larabee, S., Zhao, P., Woznica, I., Liu, Y., Li, Y., and Wu, W. (2013). A pan-inhibitor of DASH family enzymes induces immune-mediated regression of murine sarcoma and is a potent adjuvant to dendritic cell vaccination and adoptive T-cell therapy. Journal of immunotherapy (Hagerstown, Md: 1997) *36*.

Einarsdottir, B.O., Bagge, R., Bhadury, J., Jespersen, H., Mattsson, J., Nilsson, L.M., Truvé, K., López, M., Naredi, P., and Nilsson, O. (2014). Melanoma patient-derived xenografts accurately model the disease and develop fast enough to guide treatment decisions. Oncotarget *5*, 9609.

Fane, M.E., Chhabra, Y., Hollingsworth, D.E., Simmons, J.L., Spoerri, L., Oh, T.G., Chauhan, J., Chin, T., Harris, L., Harvey, T.J., *et al.* (2017). NFIB Mediates BRN2 Driven Melanoma Cell Migration and Invasion Through Regulation of EZH2 and MITF. EBioMedicine.

Farooq, A., and Zhou, M.-M.M. (2004). Structure and regulation of MAPK phosphatases. Cellular signalling *16*, 769-779.

Fecher, L.A., Amaravadi, R.K., and Flaherty, K.T. (2008). The MAPK pathway in melanoma. Current opinion in oncology *20*, 183-189.

Fecher, L.A., Cummings, S.D., Keefe, M.J., and Alani, R.M. (2007). Toward a molecular classification of melanoma. Journal of clinical oncology : official journal of the American Society of Clinical Oncology *25*, 1606-1620.

Fedorenko, I.V., Abel, E.V., Koomen, J.M., Fang, B., Wood, E.R., Chen, Y.A., Fisher, K.J., Iyengar, S., Dahlman, K.B., and Wargo, J.A. (2015). Fibronectin induction abrogates the BRAF inhibitor response of BRAF V600E/PTEN-null melanoma cells. Oncogene.

Fell, G.L., Robinson, K.C., Mao, J., Woolf, C.J., and Fisher, D.E. (2014). Skin β-Endorphin Mediates Addiction to UV Light. Cell *157*, 1527-1534.

Fenouille, N., Tichet, M., Dufies, M., Pottier, A., Mogha, A., Soo, J., Rocchi, S., Mallavialle, A., Galibert, M.-D., Khammari, A., *et al.* (2012). The epithelial-mesenchymal transition (EMT) regulatory factor SLUG (SNAI2) is a downstream target of SPARC and AKT in promoting melanoma cell invasion. PLoS ONE *7*.

Fischer, G.M., Vashisht Gopal, Y.N., McQuade, J.L., Peng, W., DeBerardinis, R.J., and Davies, M.A. (2017). Metabolic strategies of melanoma cells: Mechanisms, interactions with the tumor microenvironment, and therapeutic implications. Pigment cell & melanoma research.

Fruman, D.A., Chiu, H., Hopkins, B.D., Bagrodia, S., Cantley, L.C., and Abraham, R.T. (2017). The PI3K Pathway in Human Disease. Cell *170*, 605-635.

Garibyan, L., and Fisher, D.E. (2010). How sunlight causes melanoma. Current oncology reports *12*, 319-326.

Garraway, L., Widlund, H., Rubin, M., Getz, G., Berger, A., Ramaswamy, S., Beroukhim, R., Milner, D., Granter, S., Du, J., *et al.* (2005). Integrative genomic analyses identify MITF as a lineage survival oncogene amplified in malignant melanoma. Nature *436*, 117-122.

Giantonio, B.J., Derry, C., McAleer, C., McPhillips, J.J., and O'Dwyer, P.J. (2004). Phase I and pharmacokinetic study of the cytotoxic ether lipid ilmofosine administered by weekly two-hour infusion in patients with advanced solid tumors. Clinical

cancer research : an official journal of the American Association for Cancer Research *10*, 1282-1288.

Goel, V., Ibrahim, N., Jiang, G., Singhal, M., Fee, S., Flotte, T., Westmoreland, S., Haluska, F., and Hinds, P. (2009). Melanocytic nevus-like hyperplasia and melanoma in transgenic BRAFV600E mice. Oncogene *28*, 2289-2298.

Golan, T., Messer, A.R., Amitai-Lange, A., Melamed, Z.e., Ohana, R., Bell, R.E., Kapitansky, O., Lerman, G., Greenberger, S., Khaled, M., *et al.* (2015). Interactions of Melanoma Cells with Distal Keratinocytes Trigger Metastasis via Notch Signaling Inhibition of MITF. Molecular cell *59*, 664-676.

Gonzalez, E., and McGraw, T.E. (2009). The Akt kinases: isoform specificity in metabolism and cancer. Cell cycle (Georgetown, Tex) *8*, 2502-2508.

Govindarajan, B., Sligh, J., Vincent, B., Li, M., Canter, J., Nickoloff, B., Rodenburg, R., Smeitink, J., Oberley, L., Zhang, Y., *et al.* (2007). Overexpression of Akt converts radial growth melanoma to vertical growth melanoma. The Journal of clinical investigation *117*, 719-729.

Gray-Schopfer, V., Wellbrock, C., and Marais, R. (2007). Melanoma biology and new targeted therapy. Nature *445*, 851-857.

Haarberg, H.E., and Smalley, K.S. (2014). Resistance to Raf inhibition in cancer. Drug discovery today Technologies *11*, 27-32.

Haluska, F.G., Tsao, H., Wu, H., Haluska, F.S., Lazar, A., and Goel, V. (2006). Genetic alterations in signaling pathways in melanoma. Clinical cancer research : an official journal of the American Association for Cancer Research *12*.

Hanahan, D., and Weinberg, R. (2011). Hallmarks of cancer: the next generation. Cell *144*, 646-674.

Hanahan, D., and Weinberg, R.A. (2000). The hallmarks of cancer. Cell *100*, 57-70.

Haq, R., Fisher, D.E., and Widlund, H.R. (2014). Molecular pathways: BRAF induces bioenergetic adaptation by attenuating oxidative phosphorylation. Clinical cancer research : an official journal of the American Association for Cancer Research *20*, 2257-2263.

Haq, R., Shoag, J., Andreu-Perez, P., Yokoyama, S., Edelman, H., Rowe, G.C., Frederick, D.T., Hurley, A.D., Nellore, A., Kung, A.L., *et al.* (2013). Oncogenic BRAF regulates oxidative metabolism via PGC1α and MITF. Cancer cell *23*, 302-315.

Hassounah, N.B., Nunez, M., Fordyce, C., Roe, D., Nagle, R., Bunch, T., and McDermott, K.M. (2017). Inhibition of Ciliogenesis Promotes Hedgehog

Signaling, Tumorigenesis, and Metastasis in Breast Cancer. Molecular cancer research : MCR *15*, 1421-1430.

Hauschild, A., Grob, J.-J.J., Demidov, L.V., Jouary, T., Gutzmer, R., Millward, M., Rutkowski, P., Blank, C.U., Miller, W.H., Kaempgen, E., *et al.* (2012). Dabrafenib in BRAF-mutated metastatic melanoma: a multicentre, open-label, phase 3 randomised controlled trial. Lancet (London, England) *380*, 358-365.

Hayward, N.K., Wilmott, J.S., Waddell, N., Johansson, P.A., Field, M.A., Nones, K., Patch, A.-M.M., Kakavand, H., Alexandrov, L.B., Burke, H., *et al.* (2017). Whole-genome landscapes of major melanoma subtypes. Nature.

Hirai, H., Sootome, H., Nakatsuru, Y., Miyama, K., Taguchi, S., Tsujioka, K., Ueno, Y., Hatch, H., Majumder, P.K., Pan, B.-S.S., *et al.* (2010). MK-2206, an allosteric Akt inhibitor, enhances antitumor efficacy by standard chemotherapeutic agents or molecular targeted drugs in vitro and in vivo. Molecular cancer therapeutics *9*, 1956-1967.

Hodis, E., Watson, I.R., Kryukov, G.V., Arold, S.T., Imielinski, M., Theurillat, J.-P.P., Nickerson, E., Auclair, D., Li, L., Place, C., *et al.* (2012). A landscape of driver mutations in melanoma. Cell *150*, 251-263.

Honardoost, M., and Rad, S.M.A.H.M.A.H. (2017). Triangle of AKT2, miRNA, and Tumorigenesis in Different Cancers. Applied biochemistry and biotechnology.

Hsiao, J.J., and Fisher, D.E. (2014). The roles of microphthalmia-associated transcription factor and pigmentation in melanoma. Archives of biochemistry and biophysics *563*, 28-34.

Huang, F.W., Hodis, E., Xu, M.J., Kryukov, G.V., Chin, L., and Garraway, L.A. (2013). Highly recurrent TERT promoter mutations in human melanoma. Science (New York, NY) *339*, 957-959.

Huber, M.A., Kraut, N., Park, J.E., Schubert, R.D., Rettig, W.J., Peter, R.U., and Garin-Chesa, P. (2003). Fibroblast activation protein: differential expression and serine protease activity in reactive stromal fibroblasts of melanocytic skin tumors. The Journal of investigative dermatology *120*, 182-188.

Hugo, W., Shi, H., Sun, L., Piva, M., Song, C., Kong, X., Moriceau, G., Hong, A., Dahlman, K.B., Johnson, D.B., *et al.* (2015). Non-genomic and Immune Evolution of Melanoma Acquiring MAPKi Resistance. Cell *162*, 1271-1285.

Ibrahim, N., and Haluska, F. (2009). Molecular pathogenesis of cutaneous melanocytic neoplasms. Annual review of pathology *4*, 551-579.

Idilli, A.I., Precazzini, F., Mione, M.C., and Anelli, V. (2017). Zebrafish in Translational Cancer Research: Insight into Leukemia, Melanoma, Glioma and Endocrine Tumor Biology. Genes *8*.

Iliopoulos, D., Polytarchou, C., Hatziapostolou, M., Kottakis, F., Maroulakou, I.G., Struhl, K., and Tsichlis, P.N. (2009). MicroRNAs differentially regulated by Akt isoforms control EMT and stem cell renewal in cancer cells. Science signaling *2*.

Irie, H.Y., Pearline, R.V., Grueneberg, D., and of cell …, H.-M. (2005). Distinct roles of Akt1 and Akt2 in regulating cell migration and epithelial–mesenchymal transition. The Journal of cell ….

Jansen, V.M., Mayer, I.A., and Arteaga, C.L. (2016). Is There a Future for AKT Inhibitors in the Treatment of Cancer? Clinical Cancer Research *22*, 2599-2601.

Jenkins, R.W., Barbie, D.A., and Flaherty, K.T. (2018). Mechanisms of resistance to immune checkpoint inhibitors. British Journal of Cancer *118*, 9-16.

Jensen, P.J., Gunter, L.B., and Carayannopoulos, M.O. (2010). Akt2 modulates glucose availability and downstream apoptotic pathways during development. The Journal of biological chemistry *285*, 17673-17680.

Joseph, E.W., Pratilas, C.A., Poulikakos, P.I., Tadi, M., Wang, W., Taylor, B.S., Halilovic, E., Persaud, Y., Xing, F., Viale, A., *et al.* (2010). The RAF inhibitor PLX4032 inhibits ERK signaling and tumor cell proliferation in a V600E BRAF-selective manner. Proceedings of the National Academy of Sciences of the United States of America *107*, 14903-14908.

Kalluri, R., and Weinberg, R.A. (2009). The basics of epithelial-mesenchymal transition. The Journal of clinical investigation *119*, 1420-1428.

Kaufman, C.K., Mosimann, C., Fan, Z.P., Yang, S., Thomas, A.J., Ablain, J., Tan, J.L., Fogley, R.D., van Rooijen, E., Hagedorn, E.J., *et al.* (2016). A zebrafish melanoma model reveals emergence of neural crest identity during melanoma initiation. Science (New York, NY) *351*.

Keane, F.M., Yao, T.-W.W., Seelk, S., Gall, M.G., Chowdhury, S., Poplawski, S.E., Lai, J.H., Li, Y., Wu, W., Farrell, P., *et al.* (2013). Quantitation of fibroblast activation protein (FAP)-specific protease activity in mouse, baboon and human fluids and organs. FEBS open bio *4*, 43-54.

Kennedy, A.L., Morton, J.P., Manoharan, I., Nelson, D.M., Jamieson, N.B., Pawlikowski, J.S., McBryan, T., Doyle, B., McKay, C., Oien, K.A., *et al.* (2011). Activation of the PIK3CA/AKT pathway suppresses senescence induced by an activated RAS oncogene to promote tumorigenesis. Molecular cell *42*, 36-49.

Kieffer, T.J., McIntosh, C.H., and Pederson, R.A. (1995). Degradation of glucose-dependent insulinotropic polypeptide and truncated glucagon-like peptide 1 in vitro and in vivo by dipeptidyl peptidase IV. Endocrinology *136*, 3585-3596.

Kim, J.S., Kurie, J.M., and Ahn, Y.-H.H. (2015). BMP4 depletion by miR-200 inhibits tumorigenesis and metastasis of lung adenocarcinoma cells. Molecular cancer *14*, 173.

Koch, A., Lang, S.A., Wild, P.J., Gantner, S., Mahli, A., Spanier, G., Berneburg, M., Müller, M., Bosserhoff, A.K., and Hellerbrand, C. (2015). Glucose transporter isoform 1 expression enhances metastasis of malignant melanoma cells. Oncotarget *6*, 32748-32760.

Koelblinger, P., Thuerigen, O., and Dummer, R. (2018). Development of encorafenib for BRAF-mutated advanced melanoma. Current opinion in oncology.

Konieczkowski, D.J., Johannessen, C.M., Abudayyeh, O., Kim, J.W., Cooper, Z.A., Piris, A., Frederick, D.T., Barzily-Rokni, M., Straussman, R., Haq, R., *et al.* (2014). A melanoma cell state distinction influences sensitivity to MAPK pathway inhibitors. Cancer discovery *4*, 816-827.

Koya, R.C., Mok, S., Otte, N., Blacketor, K.J., Comin-Anduix, B., Tumeh, P.C., Minasyan, A., Graham, N.A., Graeber, T.G., Chodon, T., *et al.* (2012). BRAF inhibitor vemurafenib improves the antitumor activity of adoptive cell immunotherapy. Cancer research *72*, 3928-3937.

Kraman, M., Bambrough, P.J., Arnold, J.N., Roberts, E.W., Magiera, L., Jones, J.O., Gopinathan, A., Tuveson, D.A., and Fearon, D.T. (2010). Suppression of antitumor immunity by stromal cells expressing fibroblast activation protein-alpha. Science (New York, NY) *330*, 827-830.

Krepler, C., Sproesser, K., Brafford, P., Beqiri, M., Garman, B., Xiao, M., Shannan, B., Watters, A., Perego, M., Zhang, G., *et al.* (2017). A Comprehensive Patient-Derived Xenograft Collection Representing the Heterogeneity of Melanoma. Cell reports *21*, 1953-1967.

Krüger, M., Sachse, C., Zimmermann, W.H., Eschenhagen, T., Klede, S., and Linke, W.A. (2008). Thyroid hormone regulates developmental titin isoform transitions via the phosphatidylinositol-3-kinase/ AKT pathway. Circulation research *102*, 439-447.

Kwong, L.N., and Davies, M.A. (2013). Navigating the therapeutic complexity of PI3K pathway inhibition in melanoma. In Navigating the therapeutic complexity of PI3K pathway inhibition in melanoma (AACR).

Lambert, A.W., Pattabiraman, D.R., and Weinberg, R.A. (2017). Emerging Biological Principles of Metastasis. Cell *168*, 670-691.

Land, S.C., and Tee, A.R. (2007). Hypoxia-inducible factor 1α is regulated by the mammalian target of rapamycin (mTOR) via an mTOR signaling motif. Journal of Biological Chemistry.

Landsberg, J., Tueting, T., Barnhill, R.L., and Lugassy, C. (2016). The role of neutrophilic inflammation, angiotropism, and pericytic mimicry in melanoma progression and metastasis. Journal of Investigative Dermatology *136*, 372-377.

Larribère, L., and Utikal, J. (2016). Multiple roles of NF1 in the melanocyte lineage. Pigment cell & melanoma research *29*, 417-425.

Lassen, A., Atefi, M., Robert, L., Wong, D.J., Cerniglia, M., Comin-Anduix, B., and Ribas, A. (2014). Effects of AKT inhibitor therapy in response and resistance to BRAF inhibition in melanoma. Molecular cancer *13*, 83.

Lawrence, M.S., Stojanov, P., Polak, P., Kryukov, G.V., Cibulskis, K., Sivachenko, A., Carter, S.L., Stewart, C., Mermel, C.H., Roberts, S.A., *et al.* (2013). Mutational heterogeneity in cancer and the search for new cancer-associated genes. Nature *499*, 214-218.

Lee, J., Fassnacht, M., Nair, S., Boczkowski, D., and Gilboa, E. (2005). Tumor immunotherapy targeting fibroblast activation protein, a product expressed in tumor-associated fibroblasts. Cancer research *65*, 11156-11163.

Levy, C., Khaled, M., and Fisher, D.E. (2006). MITF: master regulator of melanocyte development and melanoma oncogene. Trends in molecular medicine *12*, 406-414.

Li, F.Z., Dhillon, A.S., Anderson, R.L., McArthur, G., and Ferrao, P.T. (2015). Phenotype switching in melanoma: implications for progression and therapy. Frontiers in oncology *5*, 31.

Li, X., Monks, B., Ge, Q., and Birnbaum, M.J. (2007). Akt/PKB regulates hepatic metabolism by directly inhibiting PGC-1alpha transcription coactivator. Nature *447*, 1012-1016.

Lindsley, C.W., Zhao, Z., Leister, W.H., Robinson, R.G., Barnett, S.F., Defeo-Jones, D., Jones, R.E., Hartman, G.D., Huff, J.R., Huber, H.E., *et al.* (2005). Allosteric Akt (PKB) inhibitors: discovery and SAR of isozyme selective inhibitors. Bioorganic & medicinal chemistry letters *15*, 761-764.

Linke, W.A., and Hamdani, N. (2014). Gigantic business: titin properties and function through thick and thin. Circulation research *114*, 1052-1068.

Lister, J., Capper, A., Zeng, Z., Mathers, M., Richardson, J., Paranthaman, K., Jackson, I., and Patton, E. (2014). A conditional zebrafish MITF mutation reveals MITF levels are critical for melanoma promotion vs. regression in vivo. The Journal of investigative dermatology *134*, 133-140.

Liu, F., Qi, L., Liu, B., Liu, J., Zhang, H., Che, D., Cao, J., Shen, J., Geng, J., Bi, Y., *et al.* (2015). Fibroblast activation protein overexpression and clinical implications in solid tumors: a meta-analysis. PLoS ONE *10*.

Liu, L.-L.L., Lu, S.-X.X., Li, M., Li, L.-Z.Z., Fu, J., Hu, W., Yang, Y.-Z.Z., Luo, R.-Z.Z., Zhang, C.Z., and Yun, J.-P.P. (2014). FoxD3-regulated microRNA-137 suppresses tumour growth and metastasis in human hepatocellular carcinoma by targeting AKT2. Oncotarget *5*, 5113-5124.

Liu, S., Tetzlaff, M.T., Wang, T., Chen, X., Yang, R., Kumar, S.M., Vultur, A., Li, P., Martin, J.S., Herlyn, M., *et al.* (2017a). Hypoxia-activated prodrug enhances therapeutic effect of sunitinib in melanoma. Oncotarget *8*, 115140-115152.

Liu, Y., Zhu, S.-T., Wang, X., Deng, J., Li, W.-H., Zhang, P., and Liu, B.-S. (2017b). MiR-200c regulates tumor growth and chemosensitivity to cisplatin in osteosarcoma by targeting AKT2. Scientific reports *7*.

Lo, J.A., and Fisher, D.E. (2014). The melanoma revolution: from UV carcinogenesis to a new era in therapeutics. Science (New York, NY) *346*, 945-949.

Locasale, J.W. (2013). Serine, glycine and one-carbon units: cancer metabolism in full circle. Nature reviews Cancer *13*, 572-583.

Loftus, S.K., Antonellis, A., Matera, I., Renaud, G., Baxter, L.L., Reid, D., Wolfsberg, T.G., Chen, Y., Wang, C., Program, N., *et al.* (2009). Gpnmb is a melanoblast-expressed, MITF-dependent gene. Pigment cell & melanoma research *22*, 99-110.

Long, G.V., Stroyakovskiy, D., Gogas, H., Levchenko, E., de Braud, F., Larkin, J., Garbe, C., Jouary, T., Hauschild, A., Grob, J.-J.J., *et al.* (2015). Dabrafenib and trametinib versus dabrafenib and placebo for Val600 BRAF-mutant melanoma: a multicentre, double-blind, phase 3 randomised controlled trial. Lancet (London, England) *386*, 444-451.

Lugassy, C., and Barnhill, R. (2011). Gene expression profiling of human angiotropic primary melanoma: selection of 15 differentially expressed genes potentially involved in extravascular migratory …. European journal of Cancer *47*, 1267-1275.

Lugassy, C., and Barnhill, R.L. (2007). Angiotropic melanoma and extravascular migratory metastasis: a review. Advances in anatomic pathology *14*, 195-201.

Lugassy, L., van den Oord, J. J., Winnepenninckx - V. (2011). Gene expression profiling of human angiotropic primary melanoma: selection of 15 differentially expressed genes potentially involved in extravascular migratory …. European journal of Cancer.

Luke, J.J., Flaherty, K.T., Ribas, A., and Long, G.V. (2017). Targeted agents and immunotherapies: optimizing outcomes in melanoma. Nature Reviews Clinical Oncology *14*, 463-482.

Luo, C., Lim, J.-H.H., Lee, Y., Granter, S.R., Thomas, A., Vazquez, F., Widlund, H.R., and Puigserver, P. (2016). A PGC1α-mediated transcriptional axis suppresses melanoma metastasis. Nature *537*, 422-426.

Luo, C., Pietruska, J.R., Sheng, J., Bronson, R.T., Hu, M.G., Cui, R., and Hinds, P.W. (2015). Expression of oncogenic BRAF(V600E) in melanocytes induces Schwannian differentiation in vivo. Pigment cell & melanoma research.

Luo, C., Sheng, J., Hu, M.G., Haluska, F.G., Cui, R., Xu, Z., Tsichlis, P.N., Hu, G.F., and Hinds, P.W. (2013). Loss of ARF sensitizes transgenic BRAFV600E mice to UV-induced melanoma via suppression of XPC. Cancer Res *73*, 4337-4348.

Majmundar, A.J., Wong, W.J., and Simon, M.C. (2010). Hypoxia-inducible factors and the response to hypoxic stress. Molecular cell *40*, 294-309.

Manning, B.D., and Cantley, L.C. (2007). AKT/PKB signaling: navigating downstream. Cell *129*, 1261-1274.

Manning, B.D., and Toker, A. (2017). AKT/PKB Signaling: Navigating the Network. Cell *169*, 381-405.

Maroulakou, I., Oemler, W., Naber, S., and Tsichlis, P. (2007). Akt1 ablation inhibits, whereas Akt2 ablation accelerates, the development of mammary adenocarcinomas in mouse mammary tumor virus (MMTV)-ErbB2/neu and MMTV-polyoma middle T transgenic mice. Cancer research *67*, 167-177.

Marsh Durban, V., Deuker, M., Bosenberg, M., Phillips, W., and McMahon, M. (2013). Differential AKT dependency displayed by mouse models of BRAFV600E-initiated melanoma. The Journal of clinical investigation.

Meacham, C.E., and Morrison, S.J. (2013). Tumour heterogeneity and cancer cell plasticity. Nature *501*, 328-337.

Medalie, N., and Ackerman, A.B. (2004). Sentinel node biopsy has no benefit for patients whose primary cutaneous melanoma has metastasized to a lymph node and therefore should be abandoned now. British Journal of Dermatology *151*, 298-307.

Melnik, B.C. (2015). MiR-21: an environmental driver of malignant melanoma? Journal of translational medicine *13*, 202.

Mercer, K., Giblett, S., Green, S., Lloyd, D., Dias, S., Plumb, M., Marais, R., and Pritchard, C. (2005). Expression of endogenous oncogenic V600EB-raf induces proliferation and developmental defects in mice and transformation of primary fibroblasts. Cancer research *65*, 11493-11500.

Mertz, K.D., Pathria, G., Wagner, C., Saarikangas, J., Sboner, A., Romanov, J., Gschaider, M., Lenz, F., Neumann, F., Schreiner, W., *et al.* (2014). MTSS1 is a

metastasis driver in a subset of human melanomas. Nature communications *5*, 3465.

Michaloglou, C., Vredeveld, L.C., Soengas, M.S., Denoyelle, C., Kuilman, T., van der Horst, C.M.A.M., Majoor, D.M.M., Shay, J.W., Mooi, W.J., and Peeper, D.S. (2005). BRAFE600-associated senescence-like cell cycle arrest of human naevi. Nature *436*, 720-724.

Miller, A.J., and Mihm, M.C. (2006). Melanoma. The New England journal of medicine *355*, 51-65.

Mobley, A., Braeuer, R., Kamiya, T., Shoshan, E., and Bar-Eli, M. (2012). Driving transcriptional regulators in melanoma metastasis. Cancer metastasis reviews *31*, 621-632.

Molina, D.M., Grewal, S., and Bardwell, L. (2005). Characterization of an ERK-binding domain in microphthalmia-associated transcription factor and differential inhibition of ERK2-mediated substrate phosphorylation. The Journal of biological chemistry *280*, 42051-42060.

Mombaerts, P., Clarke, A.R., Rudnicki, M.A., Iacomini, J., Itohara, S., Lafaille, J.J., Wang, L., Ichikawa, Y., Jaenisch, R., and Hooper, M.L. (1992). Mutations in T-cell antigen receptor genes alpha and beta block thymocyte development at different stages. Nature *360*, 225-231.

Mooi, W.J., and Peeper, D.S. (2006). Oncogene-induced cell senescence--halting on the road to cancer. The New England journal of medicine *355*, 1037-1046.

Moon, H., Donahue, L.R., Choi, E., Scumpia, P.O., Lowry, W.E., Grenier, J.K., Zhu, J., and White, A.C. (2017). Melanocyte Stem Cell Activation and Translocation Initiate Cutaneous Melanoma in Response to UV Exposure. Cell stem cell *21*, 665-678000000.

Mori, Y., Inoue, Y., Tanaka, S., Doda, S., Yamanaka, S., Fukuchi, H., and Terada, Y. (2015). Cep169, a Novel Microtubule Plus-End-Tracking Centrosomal Protein, Binds to CDK5RAP2 and Regulates Microtubule Stability. PLoS ONE *10*.

Moy, A.P., Duncan, L.M., and Investigation, K.-S. (2017). Lymphatic invasion and angiotropism in primary cutaneous melanoma. Laboratory Investigation.

Murtas, D., Maxia, C., Diana, A., Pilloni, L., Corda, C., Minerba, L., Tomei, S., Piras, F., Ferreli, C., and Perra, M.T. (2017). Role of epithelial-mesenchymal transition involved molecules in the progression of cutaneous melanoma. Histochemistry and cell biology *148*, 639-649.

Nakamura, M., and Tokura, Y. (2011). Epithelial-mesenchymal transition in the skin. Journal of dermatological science *61*, 7-13.

Neben, C.L., Lo, M., Jura, N., and Klein, O.D. (2017). Feedback regulation of RTK signaling in development. Developmental biology.

Niessner, H., Forschner, A., Klumpp, B., Honegger, J.B.B., Witte, M., Bornemann, A., Dummer, R., Adam, A., Bauer, J., Tabatabai, G., *et al.* (2013). Targeting hyperactivation of the AKT survival pathway to overcome therapy resistance of melanoma brain metastases. Cancer medicine *2*, 76-85.

Niessner, H., Schmitz, J., Tabatabai, G., Schmid, A.M., Calaminus, C., Sinnberg, T., Weide, B., Eigentler, T.K., Garbe, C., Schittek, B., *et al.* (2016). PI3K Pathway Inhibition Achieves Potent Antitumor Activity in Melanoma Brain Metastases In Vitro and In Vivo. Clinical Cancer Research *22*, 5818-5828.

Nitulescu, G., Margina, D., Juzenas, P., Peng, Q., Olaru, O., Saloustros, E., Fenga, C., Spandidos, D.A., Libra, S., and Tsatsakis, A.M. (2015). Akt inhibitors in cancer treatment: The long journey from drug discovery to clinical use (Review). International Journal of Oncology *48*, 869-885.

Nogueira, C., Kim, K.H.H., Sung, H., Paraiso, K.H., Dannenberg, J.H.H., Bosenberg, M., Chin, L., and Kim, M. (2010). Cooperative interactions of PTEN deficiency and RAS activation in melanoma metastasis. Oncogene *29*, 6222-6232.

Noonan, F.P., Recio, J.A., Takayama, H., Duray, P., Anver, M.R., Rush, W.L., De Fabo, E.C., and Merlino, G. (2001). Neonatal sunburn and melanoma in mice. Nature *413*, 271-272.

Okkenhaug, K., Graupera, M., and Vanhaesebroeck, B. (2016). Targeting PI3K in Cancer: Impact on Tumor Cells, Their Protective Stroma, Angiogenesis, and Immunotherapy. Cancer discovery *6*, 1090-1105.

Okondo, M.C., Johnson, D.C., Sridharan, R., Go, E.B., Chui, A.J., Wang, M.S., Poplawski, S.E., Wu, W., Liu, Y., Lai, J.H., *et al.* (2017). DPP8 and DPP9 inhibition induces pro-caspase-1-dependent monocyte and macrophage pyroptosis. Nature chemical biology *13*, 46-53.

Okondo, M.C., Rao, S.D., Taabazuing, C.Y., Chui, A.J., Poplawski, S.E., Johnson, D.C., and Bachovchin, D.A. (2018). Inhibition of Dpp8/9 Activates the Nlrp1b Inflammasome. Cell chemical biology.

Paraiso, K.H., Xiang, Y., Rebecca, V.W., Abel, E.V., Chen, Y.A., Munko, A.C., Wood, E., Fedorenko, I.V., Sondak, V.K., Anderson, A.R., *et al.* (2011). PTEN loss confers BRAF inhibitor resistance to melanoma cells through the suppression of BIM expression. Cancer research *71*, 2750-2760.

Pardoll, D.M. (2012). The blockade of immune checkpoints in cancer immunotherapy. Nature reviews Cancer *12*, 252-264.

Patton, E.E., Widlund, H.R., Kutok, J.L., Kopani, K.R., Amatruda, J.F., Murphey, R.D., Berghmans, S., Mayhall, E.A., Traver, D., Fletcher, C.D., *et al.* (2005). BRAF mutations are sufficient to promote nevi formation and cooperate with p53 in the genesis of melanoma. Current biology : CB *15*, 249-254.

Pearlman, R.L., Montes de Oca, M.K., Pal, H.C., and Afaq, F. (2017). Potential therapeutic targets of epithelial-mesenchymal transition in melanoma. Cancer letters *391*, 125-140.

Pérez-Guijarro, E., Day, C.-P.P., Merlino, G., and Zaidi, M.R. (2017). Genetically engineered mouse models of melanoma. Cancer *123*, 2089-2103.

Perna, D., Karreth, F.A., Rust, A.G., Perez-Mancera, P.A., Rashid, M., Iorio, F., Alifrangis, C., Arends, M.J., Bosenberg, M.W., Bollag, G., *et al.* (2015). BRAF inhibitor resistance mediated by the AKT pathway in an oncogenic BRAF mouse melanoma model. Proceedings of the National Academy of Sciences of the United States of America *112*, 45.

Pföhler, C., Preuss, K.-D.D., Tilgen, W., Stark, A., Regitz, E., Fadle, N., and Pfreundschuh, M. (2007). Mitofilin and titin as target antigens in melanoma-associated retinopathy. International journal of cancer *120*, 788-795.

Pollock, P.M., Harper, U.L., Hansen, K.S., Yudt, L.M., Stark, M., Robbins, C.M., Moses, T.Y., Hostetter, G., Wagner, U., and Kakareka, J. (2003). High frequency of BRAF mutations in nevi. Nature genetics *33*, 19-20.

Polytarchou, C., Iliopoulos, D., Hatziapostolou, M., Kottakis, F., Maroulakou, I., Struhl, K., and Tsichlis, P. (2011). Akt2 regulates all Akt isoforms and promotes resistance to hypoxia through induction of miR-21 upon oxygen deprivation. Cancer research *71*, 4720-4731.

Poulikakos, P.I., Persaud, Y., Janakiraman, M., Kong, X., Ng, C., Moriceau, G., Shi, H., Atefi, M., Titz, B., Gabay, M.T., *et al.* (2011). RAF inhibitor resistance is mediated by dimerization of aberrantly spliced BRAF(V600E). Nature *480*, 387-390.

Pratilas, C.A., Taylor, B.S., Ye, Q., Viale, A., Sander, C., Solit, D.B., and Rosen, N. (2009). V600EBRAF is associated with disabled feedback inhibition of RAF–MEK signaling and elevated transcriptional output of the pathway. Proceedings of the National Academy of Sciences *106*.

Qiao, M., Sheng, S., and Pardee, A.B. (2008). Metastasis and AKT activation. Cell cycle (Georgetown, Tex) *7*, 2991-2996.

Quail, D.F., and Joyce, J.A. (2013). Microenvironmental regulation of tumor progression and metastasis. Nature Medicine *19*.

Quelle, D.E., Zindy, F., Ashmun, R.A., and Sherr, C.J. (1995). Alternative reading frames of the INK4a tumor suppressor gene encode two unrelated proteins capable of inducing cell cycle arrest. Cell *83*, 993-1000.

Quintana, E., Shackleton, M., Foster, H., Fullen, D., Sabel, M., Johnson, T., and Morrison, S. (2010). Phenotypic heterogeneity among tumorigenic melanoma cells from patients that is reversible and not hierarchically organized. Cancer cell *18*, 510-523.

Quintana, E., Shackleton, M., Sabel, M., Fullen, D., Johnson, T., and Morrison, S. (2008). Efficient tumour formation by single human melanoma cells. Nature *456*, 593-598.

Radke, J., Roßner, F., and Redmer, T. (2017). CD271 determines migratory properties of melanoma cells. Scientific reports *7*, 9834.

Rajakulendran, T., Sahmi, M., Lefrançois, M., Sicheri, F., and Therrien, M. (2009). A dimerization-dependent mechanism drives RAF catalytic activation. Nature *461*, 542-545.

Ratnikov, B.I., Scott, D.A., Osterman, A.L., Smith, J.W., and Ronai, Z.e.A. (2017). Metabolic rewiring in melanoma. Oncogene *36*, 147.

Reddy, B.Y., Miller, D.M., and Tsao, H. (2017). Somatic driver mutations in melanoma. Cancer *123*, 2104-2117.

Robey, R.B., and Hay, N. (2009). Is Akt the "Warburg kinase"?-Akt-energy metabolism interactions and oncogenesis. Seminars in cancer biology *19*, 25-31.

Roesch, A., Fukunaga-Kalabis, M., Schmidt, E., Zabierowski, S., Brafford, P., Vultur, A., Basu, D., Gimotty, P., Vogt, T., and Herlyn, M. (2010). A temporarily distinct subpopulation of slow-cycling melanoma cells is required for continuous tumor growth. Cell *141*, 583-594.

Rose, A.A., Annis, M.G., Frederick, D.T., Biondini, M., Dong, Z., Kwong, L., Chin, L., Keler, T., Hawthorne, T., Watson, I.R., *et al.* (2016). MAPK Pathway Inhibitors Sensitize BRAF-Mutant Melanoma to an Antibody-Drug Conjugate Targeting GPNMB. Clinical cancer research : an official journal of the American Association for Cancer Research *22*, 6088-6098.

Rychahou, P.G., Kang, J., Gulhati, P., Doan, H.Q., Chen, L.A., Xiao, S.-Y.Y., Chung, D.H., and Evers, B.M. (2008). Akt2 overexpression plays a critical role in the establishment of colorectal cancer metastasis. Proceedings of the National Academy of Sciences of the United States of America *105*, 20315-20320.

Sanidas, I., Polytarchou, C., Hatziapostolou, M., Ezell, S.A., Kottakis, F., Hu, L., Guo, A., Xie, J., Comb, M.J., Iliopoulos, D., *et al.* (2014). Phosphoproteomics screen

reveals akt isoform-specific signals linking RNA processing to lung cancer. Molecular cell *53*, 577-590.

Schadendorf, D., Fisher, D.E., Garbe, C., Gershenwald, J.E., Grob, J.-J.J., Halpern, A., Herlyn, M., Marchetti, M.A., McArthur, G., Ribas, A., *et al.* (2015). Melanoma. Nature reviews Disease primers *1*, 15003.

Schlegel, N.C., von Planta, A., Widmer, D.S., Dummer, R., and Christofori, G. (2015). PI3K signalling is required for a TGFβ-induced epithelial-mesenchymal-like transition (EMT-like) in human melanoma cells. Experimental dermatology *24*, 22-28.

Schroeder, A., Heller, D.A., Winslow, M.M., Dahlman, J.E., Pratt, G.W., Langer, R., Jacks, T., and Anderson, D.G. (2011). Treating metastatic cancer with nanotechnology. Nature reviews Cancer *12*, 39-50.

Shain, A.H., and Bastian, B.C. (2016). From melanocytes to melanomas. Nature reviews Cancer *16*, 345-358.

Shain, H.A., Yeh, I., Kovalyshyn, I., Sriharan, A., Talevich, E., Gagnon, A., Dummer, R., North, J., Pincus, L., Ruben, B., *et al.* (2015). The Genetic Evolution of Melanoma from Precursor Lesions. The New England journal of medicine *373*, 1926-1936.

Shalem, O., Sanjana, N.E., Hartenian, E., Shi, X., Scott, D.A., Mikkelsen, T.S., Heckl, D., Ebert, B.L., Root, D.E., Doench, J.G., *et al.* (2014). Genome-scale CRISPR-Cas9 knockout screening in human cells. Science (New York, NY) *343*, 84-87.

Sharpless, N.E., Bardeesy, N., Lee, K.H., Carrasco, D., Castrillon, D.H., Aguirre, A.J., Wu, E.A., Horner, J.W., and DePinho, R.A. (2001). Loss of p16Ink4a with retention of p19Arf predisposes mice to tumorigenesis. Nature *413*, 86-91.

Sheng, L., He, P., Yang, X., Zhou, M., and Feng, Q. (2015). miR-612 negatively regulates colorectal cancer growth and metastasis by targeting AKT2. Cell death & disease *6*.

Sheppard, H.M., Feisst, V., Chen, J., Print, C., and Dunbar, P.R. (2016). AHNAK is downregulated in melanoma, predicts poor outcome, and may be required for the expression of functional cadherin-1. Melanoma research *26*, 108-116.

Shi, H., Hong, A., Kong, X., Koya, R., Song, C., Moriceau, G., Hugo, W., Yu, C., Ng, C., Chodon, T., *et al.* (2014). A novel AKT1 mutant amplifies an adaptive melanoma response to BRAF inhibition. Cancer discovery *4*, 69-79.

Shi, H., Hugo, W., Kong, X., Hong, A., Koya, R.C., Moriceau, G., Chodon, T., Guo, R., Johnson, D.B., Dahlman, K.B., *et al.* (2013). Acquired resistance and clonal evolution in melanoma during BRAF inhibitor therapy. Cancer discovery *4*, 80-93.

Siegel, R.L., Miller, K.D., and Jemal, A. (2017). Cancer Statistics, 2017. CA: a cancer journal for clinicians *67*, 7-30.

Song, L.-B.B., Li, J., Liao, W.-T.T., Feng, Y., Yu, C.-P.P., Hu, L.-J.J., Kong, Q.-L.L., Xu, L.-H.H., Zhang, X., Liu, W.-L.L., *et al.* (2009). The polycomb group protein Bmi-1 represses the tumor suppressor PTEN and induces epithelial-mesenchymal transition in human nasopharyngeal epithelial cells. The Journal of clinical investigation *119*, 3626-3636.

Stahl, J., Sharma, A., Cheung, M., Zimmerman, M., Cheng, J., Bosenberg, M., Kester, M., Sandirasegarane, L., and Robertson, G. (2004). Deregulated Akt3 activity promotes development of malignant melanoma. Cancer research *64*, 7002-7010.

Stoletov, K., Kato, H., Zardouzian, E., Kelber, J., Yang, J., Shattil, S., and Klemke, R. (2010). Visualizing extravasation dynamics of metastatic tumor cells. Journal of cell science *123*, 2332-2341.

Sussman, J., Stokoe, D., Ossina, N., and Shtivelman, E. (2001). Protein kinase B phosphorylates AHNAK and regulates its subcellular localization. The Journal of cell biology *154*, 1019-1030.

Taya, M., and Hammes, S.R. (2017). Glycoprotein Non-Metastatic Melanoma Protein B (GPNMB) and Cancer: A Novel Potential Therapeutic Target. Steroids.

Toker, A., and Marmiroli, S. (2014). Signaling specificity in the Akt pathway in biology and disease. Advances in biological regulation *55*, 28-38.

Traynor, K. (2009). FDA approves saxagliptin for type 2 diabetes. FDA approves saxagliptin for type 2 diabetes.

Tsai, J., Lee, J.T., Wang, W., Zhang, J., Cho, H., Mamo, S., Bremer, R., Gillette, S., Kong, J., Haass, N.K., *et al.* (2008). Discovery of a selective inhibitor of oncogenic B-Raf kinase with potent antimelanoma activity. Proceedings of the National Academy of Sciences of the United States of America *105*, 3041-3046.

Van Es, S.L., Colman, M., Thompson, J.F., McCarthy, S.W., and Scolyer, R.A. (2008). Angiotropism is an independent predictor of local recurrence and in-transit metastasis in primary cutaneous melanoma. The American journal of surgical pathology *32*, 1396-1403.

Vandamme, N., and Berx, G. (2014). Melanoma cells revive an embryonic transcriptional network to dictate phenotypic heterogeneity. Frontiers in oncology *4*, 352.

von der Crone, S., Deppe, C., Barthel, A., Sasson, S., Joost, H.G., and Schürmann, A. (2000). Glucose deprivation induces Akt-dependent synthesis and incorporation of GLUT1, but not of GLUT4, into the plasma membrane of 3T3-L1 adipocytes. European journal of cell biology *79*, 943-949.

Vredeveld, L.C., Possik, P.A., Smit, M.A., Meissl, K., Michaloglou, C., Horlings, H.M., Ajouaou, A., Kortman, P.C., Dankort, D., McMahon, M., *et al.* (2012). Abrogation of BRAFV600E-induced senescence by PI3K pathway activation contributes to melanomagenesis. Genes Dev *26*, 1055-1069.

Walsh, M.P., Duncan, B., Larabee, S., Krauss, A., Davis, J.P., Cui, Y., Kim, S.Y., Guimond, M., Bachovchin, W., and Fry, T.J. (2013). Val-boroPro accelerates T cell priming via modulation of dendritic cell trafficking resulting in complete regression of established murine tumors. PLoS ONE *8*.

Wang, H., Quah, S.Y., Dong, J.M., Manser, E., Tang, J.P., and Zeng, Q. (2007). PRL-3 down-regulates PTEN expression and signals through PI3K to promote epithelial-mesenchymal transition. Cancer research *67*, 2922-2926.

Weber, C.K., Slupsky, J.R., Kalmes, H.A., and Rapp, U.R. (2001). Active Ras induces heterodimerization of cRaf and BRaf. Cancer research *61*, 3595-3598.

Weisner, J., Gontla, R., van der Westhuizen, L., Oeck, S., Ketzer, J., Janning, P., Richters, A., Mühlenberg, T., Fang, Z., Taher, A., *et al.* (2015). Covalent-Allosteric Kinase Inhibitors. Angewandte Chemie (International ed in English) *54*, 10313-10316.

Wellbrock, C., and Marais, R. (2005). Elevated expression of MITF counteracts B-RAF–stimulated melanocyte and melanoma cell proliferation. The Journal of cell biology *170*, 703-708.

Westphal, D., Glitza Oliva, I.C., and Niessner, H. (2017). Molecular insights into melanoma brain metastases. Cancer *123*, 2163-2175.

Whitehurst, A.W., Bodemann, B.O., Cardenas, J., Ferguson, D., Girard, L., Peyton, M., Minna, J.D., Michnoff, C., Hao, W., Roth, M.G., *et al.* (2007). Synthetic lethal screen identification of chemosensitizer loci in cancer cells. Nature *446*, 815-819.

Whitehurst, A.W., Xie, Y., Purinton, S.C., Cappell, K.M., Swanik, J.T., Larson, B., Girard, L., Schorge, J.O., and White, M.A. (2010). Tumor antigen acrosin binding protein normalizes mitotic spindle function to promote cancer cell proliferation. Cancer research *70*, 7652-7661.

Wiederschain, D., Wee, S., Chen, L., Loo, A., Yang, G., Huang, A., Chen, Y., Caponigro, G., Yao, Y.-M.M., Lengauer, C., *et al.* (2009). Single-vector inducible lentiviral RNAi system for oncology target validation. Cell cycle (Georgetown, Tex) *8*, 498-504.

Wu, D., and Yotnda, P. (2011). Induction and Testing of Hypoxia in Cell Culture. Journal of Visualized Experiments.

Wu, M., Hemesath, T.J., Takemoto, C.M., Horstmann, M.A., Wells, A.G., Price, E.R., Fisher, D.Z., and Fisher, D.E. (2000). c-Kit triggers dual phosphorylations, which

couple activation and degradation of the essential melanocyte factor Mi. Genes & development *14*, 301-312.

Wu, W.-I.I., Voegtli, W.C., Sturgis, H.L., Dizon, F.P., Vigers, G.P., and Brandhuber, B.J. (2010). Crystal structure of human AKT1 with an allosteric inhibitor reveals a new mode of kinase inhibition. PLoS ONE *5*.

Xing, F., Persaud, Y., Pratilas, C.A., Taylor, B.S., Janakiraman, M., She, Q.B., Gallardo, H., Liu, C., Merghoub, T., Hefter, B., *et al.* (2011). Concurrent loss of the PTEN and RB1 tumor suppressors attenuates RAF dependence in melanomas harboring V600EBRAF. Oncogene *31*, 446-457.

Yan, S., Holdeess, B.M., Zhongze, L.I., Seidel, G.D., Gui, J., Fisher, J.L., and Estoff, M.S. (2016). Epithelial–Mesenchymal Expression Phenotype of Primary Melanoma and Matched Metastases and Relationship with Overall Survival. Anticancer Research *36*, 6449-6456.

Yu, Y., Dai, M., Lu, A., Yu, E., and Merlino, G. (2018). PHLPP1 mediates melanoma metastasis suppression through repressing AKT2 activation. Oncogene.

Zhang, B., Gu, F., She, C., Guo, H., Li, W., Niu, R., Fu, L., Zhang, N., and Ma, Y. (2009). Reduction of Akt2 inhibits migration and invasion of glioma cells. International journal of cancer Journal international du cancer *125*, 585-595.

Zhang, P., Liu, W., Zhu, C., Yuan, X., Li, D., Gu, W., Ma, H., Xie, X., and Gao, T. (2012). Silencing of GPNMB by siRNA inhibits the formation of melanosomes in melanocytes in a MITF-independent fashion. PLoS ONE *7*.

Zhou, G.-L., Tucker, D.F., Bae, S., Bhatheja, K., Birnbaum, M.J., and Field, J. (2006). Opposing Roles for Akt1 and Akt2 in Rac/Pak Signaling and Cell Migration. Journal of Biological Chemistry *281*, 36443-36453.

Zhou, L., Yang, K., Dunaway, S., Abdel-Malek, Z., Andl, T., Kadekaro, A.L., and Zhang, Y. (2017). Suppression of MAPK signaling in BRAF-activated PTEN-deficient melanoma by blocking β-catenin signaling in cancer-associated fibroblasts. Pigment cell & melanoma research.